

Regulating Mitotic Fidelity and Susceptibility to Cell Death:

Non-Canonical Functions of Two Kinases

by

Chao-Chieh Lin

University Program in Genetics and Genomics
Duke University

Date: _____

Approved:

Jen-Tsan Chi, Supervisor

Donald Fox, Chair

Tso-Pang Yao

James Alvarez

Beth Sullivan

Dissertation submitted in partial fulfillment of
the requirements for the degree of Doctor of Philosophy
in the University Program in Genetics and Genomics
in the Graduate School of Duke University

2018

ABSTRACT

Regulating Mitotic Fidelity and Susceptibility to Cell Death:

Non-Canonical Functions of Two Kinases

by

Chao-Chieh Lin

University Program in Genetics and Genomics

Duke University

Date: _____

Approved:

Jen-Tsan Chi, Supervisor

Donald Fox, Chair

Tso-Pang Yao

James Alvarez

Beth Sullivan

An abstract of a dissertation submitted in partial
fulfillment of the requirements for the degree of Doctor of Philosophy
in the University Program in Genetics and Genomics
in the Graduate School of Duke University

2018

Copyright by
Chao-Chieh Lin
2018

Abstract

In this dissertation, I will present two studies on the non-canonical mechanisms of the how two kinases in the oncogenesis of cancer cells. In the first study, we investigate the role of CoA synthase (COASY) in the regulation of the protein acetylation and precise timing of mitotic progression. In the second study, we will investigate the dysregulation of the necrosis kinase RIPK3 in the recurrent breast tumor cells which may play an unexpected role in the tumor recurrence.

The first study focuses on the COASY in regulating acetylation during mitosis. Successful mitosis is critical for the faithful inheritance of genetic materials during cell division of both normal and tumor cells. Dysregulated mitosis play a critical role in the oncogenesis process and many cancer therapeutics target the mitosis processes. The faithful execution and precise timing mitosis depends on the temporal regulation of protein phosphorylation and timely ubiquitin-mediated degradation. Compared with the phosphorylation and ubiquitination, the regulatory role of protein acetylation during mitosis is relatively unknown. Here we present evidence that TPX2 acetylation, controlled by the stage-specific COASY and acetyltransferase CBP, constitutes a novel mechanism that ensures faithful mitosis. Since COASY is only known as the CoA synthetase responsible for the de novo synthesis of Coenzyme A, the regulatory role of COASY in the CBP-mediated TPX2 acetylation during mitosis is unexpected. Such non-

canonical function of COASY is revealed by the phenotypic effects of its knockdown that triggers prolonged mitosis and multinucleation. Acetylome analysis reveals that COASY inactivation leads to hyper-acetylation of a subset of proteins associated with mitosis, including CBP and an Aurora A kinase activator, TPX2. We found that TPX2 is hyper-acetylated under COASY knockdown, which rendered TPX2 accumulation by resistant to ubiquitination. Further experiments confirmed that the direct interaction of COASY and CBP regulates CBP-mediated TPX2 acetylation. We therefore propose a regulatory mechanism that a transient CBP-mediated TPX2 acetylation is associated with TPX2 accumulation and Aurora A activation during early mitosis. The recruitment of COASY inhibits CBP-mediated TPX2 acetylation, promoting TPX2 degradation for mitotic exit. Remarkably, pharmacological and genetic inactivation of CBP effectively rescued the mitotic defects caused by COASY knockdown. We also found that PPAT domain on COASY is in responsible for the inhibitory effect of COASY on CBP. Together, our findings uncover a novel mitotic regulation wherein COASY and CBP coordinate an acetylation network to enforce productive mitosis.

In the second study, we identify the unexpected upregulation and potential role of RIPK3 in the recurrence of breast cancers after oncogenic withdrawal in a mouse model of breast cancer recurrence. Tumor recurrence is responsible for most of the mortality in breast cancer. Since the recurrent tumor cells are usually incurable and unresponsive to

most of the treatments. We have previously reported that triple negative breast cancer cells are cystine addicted mediated by epithelial-mesenchymal transition. Here we report that recurrent tumor cells, when compared with primary tumor cells, are also more sensitive to cystine deprivation. RNA expression profiling identifies a much higher expression of RIPK3 mRNA in recurrent cells. RIPK3 is previously known to mediate canonical necrosis program and silenced in the tumors as part of death-avoiding program during oncogenesis. Therefore, the dramatic re-expression of RIPK3 in the recurrent tumor is unexpected. Further functional studies indicate that the exaggerated RIPK3 contributes to the cystine addiction and erastin sensitivity of recurrent tumor cells. Unexpectedly, we found that RIPK3 expression is crucial for the rapid cell proliferation and “invasive” phenotypes in the tumor sphere of recurrent tumor cells. Thus, the collateral vulnerability can be a potential therapeutic target for recurrent tumor specific treatment. We are still actively investigating the molecular mechanism for the recurrent cells taking advantage of high RIPK3 expression for these recurrent-specific phenotypes via non-canonical mechanisms.

Contents

Abstract	iv
List of Tables.....	x
1. Introduction.....	1
1.1 The role of protein modifications in regulation mitotic timing	3
1.1.1 Phosphorylation	3
1.1.2 Ubiquitination.....	4
1.1.3 Acetylation	6
1.2 The function of CBP and HBO1 complex.....	7
1.2.1 CBP	7
1.2.2 HBO1 complex.....	8
1.3 The role of CoA synthase in the de novo synthesis of Coenzyme A	9
1.4 Clinical challenges of recurrent breast cancers	11
1.5 Murine models of recurrent breast cancers	12
1.6 Cystine addiction of breast cancer cells.....	14
1.7 RIPK3 kinase determines programmed necrosis	15
2. CoA Synthase Regulates Mitotic Fidelity via CBP-Mediated Acetylation	16
2.1 Introduction.....	16
2.2 Materials and Methods	17
2.2.1 Cell culture and plasmid	17
2.2.2 SiRNA and drug treatments	18

2.2.3 Measurement of CoA and Acetyl-CoA	19
2.2.4 Live-cell imaging	19
2.2.5 Immunofluorescence microscopy	20
2.2.6 Acetylome analysis.....	20
2.2.7 Parallel-reaction monitoring (PRM).....	21
2.2.8 Western blots and immunoprecipitation	21
2.2.9 Quantitative real-time PCR.....	23
2.2.10 In vitro CBP activity assay	23
2.2.11 Statistical analysis.....	24
2.3 Results	24
2.3.1 COASY knockdown induced mitotic defects.....	24
2.3.2 COASY knockdown increases acetylation of specific proteins.....	30
2.3.3 TPX2 is a downstream effector of COASY during mitosis.....	35
2.3.4 CBP acetylates and stabilizes TPX2 protein.....	46
2.3.5 COASY inhibits CBP-mediated TPX2 acetylation	57
2.3.6 The PPAT domain regulates TPX2 protein stability.....	65
2.3.7 Low COASY expression is associated with chemo-resistance and poor outcome in tumor expression datasets	74
3. RIP3 upregulation of the recurrent breast cancers lead to collateral vulnerability	78
3.1 Introduction.....	78
3.2 Materials and Methods.....	79
3.2.1 Cell culture	79

3.2.2 ShRNA and lentivirus infections.....	79
3.2.3 Western blots.....	80
3.2.4 Quantitative real-time PCR.....	80
3.2.5 Immunofluorescence microscopy	81
3.3 Results	81
3.3.1 Recurrent breast tumor cells are unique addicted to exogenous cystine	81
3.3.2 Differential expression of RIPK3 in the recurrent tumor cells and tumors	87
3.3.3 RIPK3 over-expression contribute to the recurrent-specific cystine addiction	91
3.3.4 Functional role of exaggerated RIPK3 in the mitosis of recurrent tumor cells.	95
4. Discussion and Future directions	99
4.1 COASY-CBP-TPX2 ensures faithful mitosis	99
4.2 Inhibition of CoA biosynthesis does not alter global acetylation pattern	101
4.3 Implications of more potential hits in the hyper-acetylated protein network.....	103
4.4 The potential regulatory mechanism of PPAT domain on CBP	105
4.5 High RIPK3 expression in recurrent tumor cells determines its sensitivity to programmed necrosis.	106
4.6 Implication of high RIPK3 expression in recurrent tumor cells	107
4.7 Potential role of RIPK3 in altering overall expression pattern.....	108
5. Conclusions.....	110
References	114
Biography	130

List of Tables

Figure 1 COASY knockdown decreased cell numbers, CoA, acetyl-CoA and increased multi-nucleation.	27
Figure 2 COASY knockdown induced prolonged mitosis and cytokinesis failure.....	30
Figure 3 COASY knockdown leads to hyper-acetylation of a subset of proteins.....	32
Figure 4 COASY knockdown leads to hyper-acetylation of a protein network.	34
Figure 5 TPX2 are hyperacetylated on three lysine residues under COASY silencing.....	37
Figure 6 PRM chromatogram of the native acetylated TPX2 peptides	39
Figure 7 COASY knockdown decreased TPX2 ubiquitination in HEK-293T cells.	40
Figure 8 TPX2 protein expression level and acetylation on TPX2 regulated the percentage of COASY-dependent multinucleation and extended mitosis.....	42
Figure 9 Western blot for validating the expression of indicated proteins.	43
Figure 10 COASY knockdown triggered increased Aurora A Thr 288 phosphorylation and extended mitosis by the elevation of TPX2.....	44
Figure 11 COASY silencing triggered aberrant localization of TPX2 and phosphor-Aurora A.	46
Figure 12 CBP acetylates TPX2 protein.....	49
Figure 13 CBP increased the half-life of TPX2.	51
Figure 14 CBP increased TPX2 acetylation on three lysine residues involving in TPX2 protein degradation.	53
Figure 15 Inhibition of CBP rescued the aberrant upregulation of TPX2 and multinucleation.	55
Figure 16 CBP is a physiological regulator of the TPX2 protein levels.	57

Figure 17 Validation of knockdown efficiency of COASY (a) and p300 (b) mRNA by real-time PCR. c p300 knockdown did not rescue the multinucleation caused by COASY knockdown.	57
Figure 18 Stage-specific physical association suggest direct interaction among COASY, CBP and TPX2.	59
Figure 19 Stage-specific physical association among COASY, CBP and TPX2.....	61
Figure 20 Mass spectrometry confirmed enrichment of COASY peptides when Flag-CBP was pulled down from HEK-293T cells overexpressing Flag-CBP and COASY cDNA...	62
Figure 21 COASY inhibited CBP-mediated TPX2 acetylation <i>in vitro</i>	65
Figure. 22 Both wild and R499C of COASY cDNAs rescued multinucleation.	67
Figure 23 PPAT domain rescued multinucleation and interacted with CBP.	69
Figure 24 Both COASY and PPAT, but not DPCK, promote the degradation of TPX2 protein.....	71
Figure 25 Silencing of enzymes upstream of COASY did not lead to TPX2 upregulation and multinucleation.....	73
Figure 26 Low COASY expression is associated with poor outcome.....	76
Figure 27 Schematic illustration of the COASY-CBP-TPX2 model.....	77
Figure 28 Mouse recurrent cells are more sensitive to Cystine deprivation	84
Figure 29 Mouse recurrent cells are more sensitive to Erastin treatment.....	86
Figure 30 Erastin-induced cell death was rescued by Nec-5 and Ferrostatin-1.....	87
Figure 31 Primary and recurrent cell lines are transcriptionally distinct.	89
Figure 32 RIPK3 was highly expressed in recurrent tumor cells.	91
Figure 33 RIPK3 over-expression contribute to the recurrent-specific cystine addiction.	93
Figure 34 MLKL phosphorylation by RIPK3 triggered erastin-induced cell death.	95

Figure 35 RIPK3 silencing increase mitotic defects in mouse recurrent cells..... 98

1. Introduction

Since the first kinase was identified to phosphorylate substrates using ATP in 1954(Krebs, 1983), approximately 518 putative kinases have been identified in human genome (Manning et al., 2002). These kinases mediate most of the cell signaling and biological processes through the modification of their substrates by phosphorylation at specific tyrosine, serine or threonine (Manning et al., 2002). Later studies found that many of the kinases are somatically mutated in human cancers and making them valuable druggable targets. By designing small molecule inhibitors to compete with ATP for the nucleotide binding sites, the activity of specific kinases can be inhibited for therapeutic purposes. Usually, the unique structure of each kinase allows specific protein substrates to reach the kinase domain for phosphorylation. However, cumulative studies over decades has revealed that many kinases also exert non-canonical roles independent of their enzymatic activities. One example to support this idea is from the studies of pseudokinases. Pseudokinases are first identified to possess the overall structure of a kinase, but lack the kinase activities because of mutations at the catalytic domains. It was considered as remnants of evolution with no biological function. However, many of the pseudokinases have been found to play important roles via non-enzymatic functions. For example, mixed lineage kinase domain like pseudokinase (MLKL) is crucial for the execution of programmed necrosis through the formation of membrane pore by their polymerization (Wang et al., 2014). Further

evidence to the non-catalytic roles of kinase is proposed by the findings that different approach to manipulate the same kinase has different biological outcome. Taking epidermal growth factor receptor (EGFR), a tyrosine kinase, as an example, the genetic knockout of EGFR was lethal to mice after birth (Miettinen et al., 1995). However, the enzymatic deficient mutant of EGFR in mice only led to minor defect (Lueteteke et al., 1994). These findings are further supported by the study in receptor-interacting serine/threonine-protein kinase 3 (RIPK3). Genetic knockout of RIPK3 led to healthy mice, while RIPK3 mutants at catalytic residues have led to perinatal lethality (Mandal et al., 2014). By extensive study of these mechanism, the non-canonical roles of kinase has been found to be involved in a wide variety of biological processes, including scaffolding, allosteric regulation or protein-DNA interactions(Kung and Jura, 2016).

In this dissertation, I present the non-canonical roles of two independent kinases: CoA synthase (COASY) and RIPK3. In the introductory chapter for the COASY studies, I will first discuss our current understanding of various protein modifications during cell cycle, then describe the role of acetylation in regulating mitotic fidelity and function of potential acetyltransferases involving mitotic regulation. I then introduce COASY, CoA biosynthesis pathway and the genetic diseases caused by this pathway. These findings have been reported in a recent publication (Lin et al., 2018). For the RIPK3 studies, I introduce the clinical challenge of recurrent breast cancers and murine model of tumor recurrence as an alternative method to study its molecular mechanism. I then introduce

cysteine deprivation as a novel approach to eliminate certain types of cancer cells and the role of RIPK3 in determining the programmed necrosis.

1.1 The role of protein modifications in regulation mitotic timing

The eukaryotic cell cycle is a highly regulated and orchestrated process. Mitosis is important because it allows for the successful division of the genetic materials into two identical copies in each of the daughter cells during development, tissue repairs and various biological processes. The temporal and spatial progression of mitosis is tightly regulated by the precise control of the levels and activities of mitotic proteins (Malumbres and Barbacid, 2009). Acetylation is a relatively understudied form of protein modification in mitosis. I will introduce these protein modification in details in the following paragraph.

1.1.1 Phosphorylation

The well-studied protein modifications regulating the mitotic fidelity is protein phosphorylation mediated by a family of kinases termed cyclin-dependent kinases (CDKs). CDKs interact with one or several cyclins to regulate stability, enzymatic activities and substrate specificity (Malumbres, 2014). For example, Cdk1 first interacts with cyclin A to catalyze phosphorylation on a subset of proteins and promote the transition to mitosis of G2 phase. Once entering mitosis, cyclin A is degraded and Cdk1

interact with cyclin B1, which allows Cdk1 to phosphorylate a different subset of proteins required for the execution of mitosis (Edgar and Lehner, 1996; Nigg, 1995).

Once entering mitosis, the microtubules are rearranged to form a bipolar spindle that functions to segregate a duplicate set of genetic materials into two daughter cells (Wittmann et al., 2001). During early mitosis, Targeting Protein for Xklp2 (TPX2) is one critical regulator of many aspects of the spindle assembly, including nucleating microtubules around chromosomes, targeting mitotic proteins to mitotic spindles and activating another crucial mitotic kinase, Aurora A kinase (Eyers and Maller, 2004; Kufer et al., 2002a; Stewart and Fang, 2005; Wittmann et al., 2000). Activated Aurora A then triggers a phosphorylation cascade that dictates the timing of mitotic spindle assembly and disassembly (Bayliss et al., 2003; Fu et al., 2007). Dysregulated Aurora A activation lead to aberrant mitosis and contribute to genomic instability and aneuploidies in cancer (Anand et al., 2003; Cheong et al., 2010; Storchova and Pellman, 2004). Therefore, the regulatory mechanisms that govern the degradation of TPX2, as well as cyclin B1, are crucial for the inactivation of Aurora A and Cdk1 and exit of mitosis. Here, we further discuss how TPX2 and cyclin B1 are degraded by ubiquitination.

1.1.2 Ubiquitination

In addition to phosphorylation, the cellular transitions between different phases of mitosis requires temporal and spatial control of protein degradation via poly-

ubiquitination. The catalysis of ubiquitination requires three major enzymes in APC/C: a ubiquitin activating enzyme (E1), a ubiquitin conjugating enzyme (E2) and ubiquitin ligase (E3)(Nakayama and Nakayama, 2006). Ubiquitin is first transferred to E1. E1 then transfers ubiquitin to E2. E3 binds to the selected targets and catalyzes the transfer of ubiquitin from E2 to the lysine residues on target proteins(Sivakumar and Gorbsky, 2015). Anaphase-Promoting Complex/Cyclosome (APC/C) is the most studied protein complex involving in degradation of these mitotic proteins at different stages of mitosis(Sivakumar and Gorbsky, 2015). APC/C is an E3 ubiquitin ligase catalyzing protein degradation by covalently labeling target proteins with ubiquitin to be degraded by 26S proteasome complex(Weissman, 2001). To facilitate APC/C to target the right mitotic proteins for degradation at different stages of mitosis, APC/C needs to recruit co-activator proteins to determine the substrate specificity to different substrates. APC/C first recruits CDC20 to degrade cyclin A to promote the end of G2 phase and initiation of mitosis. At metaphase APC/C-CDC20 starts to catalyze the ubiquitination of cyclin B1. During metaphase to anaphase transition, APC/C replaces CDC20 with CDH1 (CDC20 homologue 1) to initiate the ubiquitination and degradation of TPX2 as well as Aurora A kinase for proper mitotic exit (Stewart and Fang, 2005).

1.1.3 Acetylation

Compared with phosphorylation and ubiquitination, the role of acetylation in mitotic regulation is relatively un-appreciated. The most well-known regulatory role of acetylation during mitosis is that acetylation of SMC3 establish the cohesion and separation of sister chromatids (Beckouet et al., 2010). The acetylation on K106 of SMC3 during S phase by Eco1 acetyltransferase promotes the formation of a tripartite ring composed of Smc1, Smc3 and Scc1 to tether sister DNAs. At anaphase, SMC3 is deacetylated by Hos1 or HDAC8 to release sister chromatids to two daughter cells (Deardorff et al., 2012).

Another example of a mitotic protein regulated by acetylation is BuBR1. BuBR1 is a major component in spindle assembly checkpoint (SAC)(Bolanos-Garcia and Blundell, 2011). At prometaphase, BuBR1 recruits MAD2, CDC20 and BUB3 to form mitotic checkpoint complex (MCC) to inhibit APC/C before spindle alignment is ready. When spindles are properly aligned, SAC is then dissociated to release APC/C from inhibition. Activated APC/C turns on the separase activity to cleave Scc1 on tripartite ring. Sister chromatids are then release for the cells to enter the later stage of mitosis(Bolanos-Garcia and Blundell, 2011). Acetylation on BuBR1 has been found to activate checkpoint function by inhibiting APC/C at prometaphase(Choi et al., 2009). Once deacetylated, BuBR1 is degraded to release APC/C activity(Choi et al., 2009).

1.2 The function of CBP and HBO1 complex

Our current understanding of whether acetylation can serve as another layer of mitotic regulation is still in its infancy. Lysine acetylation on histone or non-histone proteins is catalyzed by histone acetyltransferases (HATs). Based on the catalytic mechanism, HATs can be categorized into four families, including CBP/P300, MYST/HBO1, Gcn5/PCAF and Rtt109 (Carrozza et al., 2003). In this dissertation, we have identified CBP and HBO1 as two potential acetyltransferases (figure 4, later) in regulating the execution of mitosis.

1.2.1 CBP

Reversible histone acetylation has been intensively studied as a key epigenetic mark. The abundance and distribution of histone acetylation plays a critical role in chromatin structure central to gene expression (Rice and Allis, 2001). CREB-binding protein (CBP) is one of the best characterized histone acetyltransferases. CBP was first identified by its association with CREB, a transcription factor, to regulate transcription (Iyer et al., 2004). Follow-up studies showed that CBP acts as a transcriptional co-activator by interacting with several transcription factors, including cJun, P53 and MyoD, and facilitates gene transcription by histone acetylation (Duyndam et al., 1999; Grossman, 2001; Puri et al., 1997). CBP also have non-genomic functions and

non-histone substrates (Dancy and Cole, 2015). Acetylation by CBP has been shown to stabilize multiple non-histone proteins (Ito et al., 2001; van der Heide and Smidt, 2005).

P300 is a paralog of CBP with high sequence homology (Roth et al., 2001). CBP and P300 share most of the targets with minor difference (Kalkhoven, 2004). However, homozygous deletion of either CBP or P300 led to embryonic lethality in mice (Tanaka et al., 2000; Yao et al., 1998). Mutations in either CBP or P300 cause Rubinstein–Taybi syndrome, characterized by mental and growth retardation (Roelfsema and Peters, 2007). These findings suggest that both CBP and P300 are indispensable. The minor difference of the target proteins between CBP and P300 also account of proper function and viability of the cells.

1.2.2 HBO1 complex

The initiation of DNA replication requires the binding of origin recognition complex (ORC) at S phase (DePamphilis, 2003). ORC then starts to recruit several subunits, including Cdc6/Cdc18, Cdt1, to form pre-replication complex for the bidirectional replication (DePamphilis, 2003). HBO1 was first identified as the largest subunit in ORC (Iizuka and Stillman, 1999). Follow-up studies showed that HBO1 promotes the recruitment of pre-replication complex and acetylation on histone H3 and H4 (Aggarwal and Calvi, 2004; Doyon et al., 2006; Iizuka et al., 2006; Iizuka and Stillman, 1999). Thus, acetylation of histone H3 and H4 by HBO1 might help open the

conformation and structure of chromatin to facilitate the recruitment of pre-replication complex.

HBO1 complex is composed of scaffold proteins JADE1/2/3, accessory proteins ING4/5, Eaf6 and acetyltransferase KAT7. The scaffold proteins provides the platform for the assembly of acetyltransferase with accessory proteins. By the assembly with different subtypes of scaffold proteins and accessory proteins, acetyltransferase KAT7 has different substrate preference and preferable acetylation sites on the same substrate(Avvakumov et al., 2012; Doyon et al., 2006; Foy et al., 2008; Lalonde et al., 2013; Saksouk et al., 2009). HBO1 complex is categorized as the MYST family by catalytic mechanism. Although several acetyltransferases of MYST family have been found to require lysine autophosphorylation for its acetyltransferase activity (Yuan et al., 2012), it is still unknown whether acetylation on the subunits of HBO1 complex can alter its substrate preference or acetyltransferase activity.

1.3 The role of CoA synthase in the de novo synthesis of Coenzyme A

Reversible acetylation is intimately linked to metabolism (Choudhary et al., 2014). This connection is thought, at least in part, bridged by acetyl-CoA, the common source of acetyl group for both lysine acetylation and metabolic flux. CoA biosynthetic pathway consists of multiple catalytic steps that convert pantothenate to CoA. First, the pantothenate is phosphorylated by pantothenate kinase, followed by the addition of

cystine, followed by decarboxylation to form 4'-phosphopantetheine. COASY catalyzes the last two steps of converting 4'-phosphopantetheine to CoA through its PPAT and DPCK domain to generate CoA. Mis-sense mutations in PANK2 and COASY can lead to neurodegeneration with brain iron accumulation in human (Dusi et al., 2014). Further study suggests that inhibition of pathothenate kinase can decrease the availability of CoA and lower the acetylation of specific subset of proteins (Siudeja et al., 2011). The biosynthesis of Coenzyme A (CoA) requires CoA synthase (COASY), a bifunctional metabolic enzyme catalyzing the last two steps of *de novo* Coenzyme A biosynthesis (Zhyvoloup et al., 2002). In human, the R499C mutation of COASY has been reported to disrupt COASY enzymatic activity, leading to neurodegeneration (Dusi et al., 2014). In *S. pombe* and *D. melanogaster*, CoA biosynthesis has been suggested to maintain DNA integrity and proper mitosis (Bosveld et al., 2008; Nakamura et al., 2012). However, whether COASY plays any role in the regulation of protein acetylation or how it affects mitosis remains unclear.

Next, I want to introduce the background of RIPK3 studies. I start with the current challenges of tumor recurrence and using the murine model as a surrogate for the investigation. Then, I introduce cystine deprivation as a promising approach to target specific tumor cells and role of RIPK3 in programmed necrosis induced by cystine deprivation.

1.4 Clinical challenges of recurrent breast cancers

Breast cancer is major cause of mortality in women(Jemal et al., 2011). Breast cancer is typically treated by the surgical resection of the primary tumor followed by some combinations of adjuvant radiation, chemotherapy, and hormonal therapy. However, although the 5-year survival rates of women suffering from breast cancer is ~90%(Siegel et al., 2013), about 5-10% of patients will develop recurrent breast cancer – either locally, regionally or at distant sites. The majority of occurrence happen within 2 to 5 years(Gupta and Massague, 2006; Karrison et al., 2000) but the relapse can also occur up to 25 years following completion of initial treatments(Esserman et al., 2011). Recurrent breast tumors are generally incurable, more aggressive and unresponsive to the treatments effective for primary tumors(Kimbung et al., 2015).

Several factors have shown to be associated with breast tumor recurrence and often used as prognostic factors, including the age primary tumor is diagnosed (Albain et al., 1994; Kollias et al., 1997), lymph node status, tumor size, histological grade(Carter et al., 1989; Chiang and Massague, 2008; Elston and Ellis, 1991), the status of estrogen receptor (ER), progesterone receptor (PR) and the expression of human epidermal growth factor receptor 2 (HER2)(Esserman et al., 2011; Goldhirsch et al., 2005; Slamon et al., 1987). However, the molecular mechanism underlying these associations remain largely unknown. Phenotypic differences between primary and recurrent tumors suggests that recurrent tumors may have distinct gene expression profile. While

extensive efforts have been focused on how the somatic mutations and oncogenic pathways contribute to primary breast, far less is known about the genes and oncogenic pathways that govern tumor recurrence following therapy. Tumor recurrence accounts for the majority of the cancer-associated death and the failure to prevent or treat recurrent tumors is the major impediment to improving survival of women with breast cancer. Therefore, better understanding of tumor recurrence mechanism could potentially provide effective and rational targeting to improve clinical outcomes.

1.5 Murine models of recurrent breast cancers

This paucity of information of recurrent breast cancers is due, in large part, to the limited availability of clinical samples from patients with tumor recurrence. In addition, there are also lack of appropriate animal models to replicate the biology of recurrent breast cancers (Boxer et al., 2004; D'Cruz et al., 2001; Gunther et al., 2003; Moody et al., 2005; Moody et al., 2002). To overcome this limitation, we have used a genetically engineered mouse (GEM) model of recurrent breast cancers based on the doxycycline-inducible system to generate mice, in which specific oncogenes can be conditionally expressed and withdrawn in the mammary gland (Boxer et al., 2004; D'Cruz et al., 2001; Gunther et al., 2003; Moody et al., 2005; Moody et al., 2002). MMTV-rtTA (MTB) mice with mammary gland-specific expression of rtTA are crossed to TetO-neu (TAN) mice to generate bi-transgenic mice, in which each oncogene is expressed or turned off in the

mammary gland in response to the administration or withdrawal of doxycycline. Administration of doxycycline to MTB/TAN mice in the drinking water leads to mammary adenocarcinomas with near complete penetrance within 2-10 months. Remarkably, oncogene withdrawal by removal of doxycycline from the drinking water leads to tumor regression. After the tumor regression, the recurrent tumors will eventually emerge in most mice. The recurrence of these GEM models bears significant similarities to human breast cancer recurrence in several important ways: (1) Tumor recurrence occurs over a long timeframe relative to the lifespan of the mouse, similar to the timing of recurrences in human breast cancer; (2) During the latency period between primary and recurrent tumor formation, residual tumor cells remain in the mouse, analogous to minimal residual disease in women with breast cancer; (3) The formation of recurrent tumors seems to be independent from the initial oncogene of the primary tumors, reminiscent of the finding that recurrences from Her2-amplified breast cancers have often lost Her2 amplification; (4) Recurrent breast cancer is often more aggressive than the initial primary tumor and may be resistant to therapies that were effective against the primary tumor. Presumably, these recurrent cells accumulate additional mutations or oncogenic properties to undergo oncogene-independent growth. Importantly, while the initial oncogenic event is driven by one oncogene (such as Her2), the additional mutations and oncogenic events in the recurrent tumors reflect many aspects of the disease heterogeneity and complex genetics of human recurrence breast

cancers. There are also significant similarities in molecular pathways and clinical courses between this GEM and human breast cancer recurrence.

1.6 Cystine addiction of breast cancer cells

Although cystine is not considered as an essential amino acid, deficiency of cystine has been associated with skeletal muscle function, body cell mass of cancer patients and immunological function with an increase in reactive oxygen species (Droge, 2005). Cystine is the precursor of glutathione (GSH), which is a crucial antioxidant to decrease reactive oxygen species (ROS) in cells (Lu, 2009). Therefore, depletion of GSH can increase the cellular level of ROS, activate tumor necrosis factor α (TNF α) pathway and lead to necrosis (Garcia-Ruiz and Fernandez-Checa, 2007). In the extracellular space, cysteine (L-Cys) typically exist as a dimeric form, called cystine (CSSC). We have previously demonstrated that cystine deprivation can sensitize certain cancer cell types, including renal cell carcinomas and triple-negative breast cancer cells (TNBC) (Tang et al., 2017; Tang et al., 2016), and lead to non-apoptotic cell death. In TNBC, epithelial-mesenchymal transition (EMT) determines the activation of TNF α -RIP1/3 pathway and sensitivity to necrosis (Tang et al., 2017). The cystine-deprived cell death occurs through the reciprocal amplification of the Src-p38-Noxa signaling and TNF α -RIP1/3-MLKL necrosis pathways, which culminate in MLKL oligomerization and programmed necrosis. Since the recurrence of tumor cells in the GEM are accompanied with EMT

(Moody et al., 2005), we hypothesize that recurrent tumor cells may be uniquely sensitive to cystine deprivation.

1.7 RIPK3 kinase determines programmed necrosis

RIPK3 (Receptor Interacting Serine/Threonine Kinase 3) is first appreciated as a critical protein for the programmed necrosis (Zhang et al., 2009) because RIPK3 phosphorylate MLKL (Mixed Lineage Kinase Domain Like Pseudokinase), resulting in the polymerization of MLKL as the canonical hallmark and executioner of necrosis (Wang et al., 2014). Necrosis can be blocked via inhibition of MLKL by its inhibitor NSA (Necrosulfonamide, NSA) (Sun et al., 2012). Wild-type RIPK3, but not catalytically inactive RIPK3 mutants, can reconstitute necrosis in RIPK3-deficient cells, indicating that the kinase activity of RIPK3 is critical. In the cancer biology, the conventional view is that RIPK3, similar to many components of apoptosis, is a tumor suppressor. Therefore, RIPK3 expression is often diminished in tumors compared with normal tissues (Karami-Tehrani et al., 2016). RIPK3 is usually silenced at the mRNA levels in cancer cells due to the promoter methylation (Geserick et al., 2015; Koo et al., 2015). Also, RIPK3 expression suppresses the development of AML (Hockendorf et al., 2016). Importantly, the expression of RIPK3 predicts cancer cells to various stimuli that trigger the necrosis cell death (Geserick et al., 2015; He et al., 2009; Koo et al., 2015).

2. CoA Synthase Regulates Mitotic Fidelity via CBP-Mediated Acetylation

This chapter was modified from a manuscript (CoA Synthase Regulates Mitotic Fidelity via CBP-Mediated Acetylation) published in *Nature Communications*:

1039 (2018). The authors were Chao-Chieh Lin, Mayumi Kitagawa, Xiaohu Tang, Ming-Hsin Hou, Jianli Wu, Dan Chen Qu, Vinayaka Srinivas, Xiaojing Liu, J. Will Thompson, Bernard Mathey-Prevot, Tso-Pang Yao, Sang Hyun Lee & Jen-Tsan Chi.

2.1 Introduction

In this chapter, we found that knockdown of COASY, metabolic enzyme involving in the CoA biosynthesis, can trigger mitotic defects. To identify the proteins in response for the mitotic defects, we performed acetylome analysis and found that CBP and TPX2 were hyperacetylated under COASY knockdown. By further mechanistic studies, we report the identification of COASY as a novel regulator of mitosis via its stage-specific interaction with CBP during mitosis to inhibit CBP acetyltransferase activity. We found that CBP acetylates and stabilized TPX2 to promote Aurora A activation during mitosis. Importantly, at later stage of mitosis, the physical binding of COASY to CBP interferes with CBP-mediated TPX2 acetylation, thereby promoting Aurora A inactivation and proper mitotic exit. Therefore, COASY knockdown led to persistent TPX2 protein levels and prolonged Aurora A activation, resulting in mitotic defects. These findings identify an important contribution of TPX2 acetylation, regulated

through the interaction of COASY and CBP, to proper regulation of mitotic progression and prevention of genome instability.

2.2 Materials and Methods

2.2.1 Cell culture and plasmid

MDA-MB-231 cells, A549 cells, PANC-1 cells and APRE-19 cells were obtained from Duke Cell Culture Facility (Durham, NC, USA). As suggested by Duke Cell Culture Facility. All four cell lines were cultured in Dulbecco's modified Eagle's medium (DMEM; GIBCO-11995) supplemented with 10% fetal bovine serum and 1 × antibiotics (penicillin, 10,000 UI/ml and streptomycin, 10,000 UI/ml). These cell lines have been validated to be *mycoplasma*-free and authenticated by STR DNA profiling before being frozen by the Duke Cell Culture Facility (Durham, NC, USA), and were maintained for fewer than 6 months. The cells were maintained in a humidified incubator at 37°C and 5% CO₂. For COASY-GFP expressing cells, COASY cDNA from pDONR223-COASY was cloned into pLenti CMV GFP DEST (736-1) using Gateway cloning following the manufacturer's protocol. PLX302-TPX2 was generated by transferring TPX2 cDNA from pENTR223-TPX2 to PLX302 using gateway cloning. Lentivirus was generated by transfecting HEK-293T cells with a 1: 0.1: 1 ratio of pMDG2: pVSVG: pLKO.1 with TransIT-LT1 transfection reagent (Mirus). COASY-GFP expressing cell line were generated by adding 250 µl virus to a 60mm dish of A549 cells with polybrene (8µg/ml).

pLenti CMV GFP DEST (736-1) was a gift from Eric Campeau (Addgene plasmid # 19732)(Campeau et al., 2009). PLX302 V5-N terminus domain (1-179), PLX302 V5-PPAT (180-350), PLX302 V5-DPCK (351-564) were generated by Gateway cloning. pDONR223-COASY was a gift from William Hahn & David Root (Addgene plasmid # 23660)(Johannessen et al., 2010). pcDNA3 β -FLAG-CBP-HA and pcDNA3 β -FLAG-CBP-LD-HA were gifts from Tso-Pang Yao (Addgene plasmid # 32908)(Zhao et al., 2005). pLX302 was a gift from David Root (Addgene plasmid # 25896)(Yang et al., 2011). pENTR223-TPX2 was a gift from The ORFeome Collaboration (DNASU). mEmerald-AuroraAKD-C-7 was a gift from Michael Davidson (Addgene plasmid # 54010).

2.2.2 SiRNA and drug treatments

SiRNA knockdown was performed using lipofectamine RNAiMAX (ThermoFisher) following the manufacturer's protocol. AllStars negative control siRNA (#1027281) was purchased from ThermoFisher. COASY siRNAs (D-006751-01, D-006751-02, D-006751-03), CBP siRNA (D-003477-18) and TPX2 siRNA (D-010571-04) were purchased from Dharmacon. To enrich the mitotic cells under COASY silencing, A549 cells were transfected by siRNA using lipofectamine RNAiMAX (Invitrogen) following the manufacturer's protocol. After 24 hours of incubation, the cells were treated with 2 mM of thymidine (T1895; Sigma) for 16 to 18 hours. After 2 hours of release in fresh media, the cells were treated with 100 ng/ml nocodazole (M1404; Sigma) for 16 hours.

The cells were then released and harvested by mitotic shake-off for further experiments. Colchicine (5 mM, SML0002; Sigma) was added to the media at the same time point nocodazole was treated. For ubiquitination assay, cells overexpressing TPX2-V5 were treated with MG132 (M7449, Sigma) for 6 hours. TPX2-V5 in the lysed samples were pulled down by V5 antibody (MA5-15253, ThermoFisher) and blotted with ubiquitin antibody (sc-8017, Santa Cruz).

2.2.3 Measurement of CoA and Acetyl-CoA

MDA-MB-231 cells were cultured in DMEM medium in 6-well plate. After 3 days of COASY siRNA knockdown, the metabolites were extracted as described previously (Liu et al., 2015). Cell extract was reconstituted into 30 μ l of 50 mM ammonium acetate, and 10 μ l was injected to LC-MS for acyl-CoA profiling analysis. LC-MS method was described previously⁵.

2.2.4 Live-cell imaging

H2B-mCherry was a gift from Robert Benezra (Addgene plasmid # 20972)(Nam and Benezra, 2009). A549 cells stably expressing H2B-mCherry were selected using G418 (800 μ g/ml) for 14 days. The cells were then silenced by COASY or control siRNAs. The phenotypes of extended mitosis and cytokinesis failure were assessed in living cells

using Olympus VivaView FL incubator microscope. The images of DIC and mCherry were taken every 6 min.

2.2.5 Immunofluorescence microscopy

For AF 488 Phalloidin (A12379, ThermoFisher), CBP and TPX2 staining, cells were washed once with PBS and fixed in 3.7% paraformaldehyde for 15 min, followed by permeabilization and blocking with 0.2% Triton X-100 and 2% BSA for 15 min. Primary antibodies were incubated with the cells for 1 hour. Transmitted light microscopy and immunofluorescence microscopy were performed using EVOS FL cell imaging system (ThermoFisher). The confocal microscope (SP8, Leica) was used to detect and capture the signal of CBP, TPX2 and COASY-GFP.

2.2.6 Acetylome analysis

Global proteomics analysis of differential acetylation was performed in a manner similar to previously described, with relatively minor modifications (Davies et al., 2016). Cell lysates were lysed in urea, digested with trypsin and enriched with pan anti-acetyl Lysine antibody. Enriched samples were analyzed by label-free liquid chromatography tandem mass spectrometry to determine the relative abundance of acetylated peptides between control and COASY knockdown condition. The raw data and spectrum files

can be downloaded at <ftp://massive.ucsd.edu/MSV000081937>. For full description of the methods, see the Supplementary Information.

2.2.7 Parallel-reaction monitoring (*PRM*)

Quantification of the native acetylated TPX2 peptides as a ratio to the stable-isotope internal standards was performed using PRM targeted mass spectrometry (Peterson et al., 2012). Using the combination of targeted mass spectrometry and synthetic stable isotope labeled peptides, site-specific quantification of acetylation can be performed with little to no ambiguity. Skyline software (<http://skyline.ms>) was utilized to export inclusion lists to the mass spectrometer and for quantitative data analysis. Samples were analyzed under the same LC conditions as described for discovery experiments, with the exception that a 60 minute LC-MS gradient was used. The mass spectrometer utilized was a QExactive HF (Thermo Scientific), with precursor isolation window of 2.0 m/z, maximum accumulation of 0.5 sec, target AGC of 1e6, and MS resolution of 60,000. The raw data and spectrum files can be downloaded at <https://goo.gl/hy2fQd>.

2.2.8 Western blots and immunoprecipitation

The cells were harvested and washed once with ice cold PBS, then resuspended in NP-40 buffer with Trichostatin A, protease and phosphatase inhibitors. The samples

were lysed by incubating in at 4°C with constant vortex for 30min, then spun down at 13000 rpm for 10 min at 4°C. Supernatant was transferred to new tube, and protein concentration was measured by the Pierce BCA protein assay kit (#23225, ThermoFisher). Between 15-40ug of protein was loaded on 8% SDS-PAGE gels, wet-transferred to PDVF membrane, blocked with 5% non-fat milk in 1xTBST, then incubated with primary antibodies overnight at 4°C. For immunoprecipitation, between 400-600 µg of protein lysate was incubated with 2 µg of primary antibody overnight at 4°C. Dynabeads protein G was then added and incubated for 2 hours. Beads were pulled down and boiled in 1x protein loading buffer for Western blots. Antibodies: v5 (1:1000, MA5-15253, ThermoFisher), Cyclin B1 (1:2000, 4135s, Cell Signaling), GAPDH (1:2000, sc-25778, Santa Cruz), alpha-tubulin (1:2000, T9026, Sigma-Aldrich), HA (1:2000, sc-805, Santa Cruz), TPX2 (1:1000, 12245, Cell Signaling), TPX2 (1:1000, sc-376812, Santa Cruz), Aurora A (1:1000, 610938, BD Biosciences), Phospho-Aurora A pThr288 (1:1000, MA5-14904, ThermoFisher), COASY (1:1000, sc-393812, Santa Cruz), CBP (1:1000, sc-369, Santa Cruz), CBP (1:1000, 7389s, Cell Signaling). Acetylated lysine (1:1000, ICP0380, Immunechem). Acetylated lysine (1:1000, 9441s, Cell Signaling).

2.2.9 Quantitative real-time PCR

Total RNA was extracted by the RNeasy Mini Kit (Qiagen) following the manufacturer's protocol. RNA was reverse transcribed to cDNA by the SuperScript II (Invitrogen) using random hexamers. Quantitative real-time PCR was performed using Power SYBR Green PCR Mix (Applied Biosystems) and StepOnePlus Real-time PCR system (Applied Biosystems) following the manufacturer's protocol. Beta-actin (reference gene) primers: sense, 5'-CAC TCTT CCA GCC TTC CTT C-3', antisense, 5'-GGA TGT CCA CGT CAC ACT TC-3'; COASY primers: sense, 5'-TGT GGC TGA GGG AAA GCG T-3', antisense, 5'-ACC TGG CGT TGG GTG ATA TG-3'; TPX2 primers: sense, 5'-ACT TCC GCA CAG ATG AGC G-3', antisense, 5'-GGA TGC TTT CGT AGT TCA GAT GT-3'; PANK1 primers: sense, 5'-CTG CCT TGA TAA CCC ATA CCC T-3', antisense, 5'-CTT GGA GTA CAC GGC TAG AAT G-3'; PANK2 primers: sense, 5'-AGG GGA CTA TGA GAG GTT TGG-3', antisense, 5'-GCA CAC ATT CTT GCT ATT GAG C-3'; PPCDC primers: sense, 5'-TGC CTC TTC TGG TGT CAA AGC-3', antisense, 5'-TGT TTG GCT CTC TCA GTT GTG A-3'. Reactions were performed in triplicate.

2.2.10 In vitro CBP activity assay

Recombinant COASY or equal amount of control BSA were first combined with CBP protein in HAT buffer (50 mM Tris-base, pH 8.0, 10 % glycerol, 0.1 mM EDTA and 1

mM dithiothreitol) and incubated at 30 °C for 30 min. Acetyl-CoA and recombinant TPX2 protein were then added to the reactions and incubated at 30 °C for 30 min. Proteins were resolved by 10% SDS-PAGE, and acetylation was detected by western blot using Acetyl lysine (1:1000, ICP0380, Immunechem). Recombinant proteins: CBP (03-189, Millipore), TPX2 (T40-30H-50, SignalChem).

2.2.11 Statistical analysis

Data represent the mean +/- the standard error of the mean. P-values were determined by a two-tailed Student's t-test or ANOVA test with Bonferroni post hoc tests in Excel or Graphpad. Error bars represent SEM, and significance between samples is denoted as *P < 0.05; **P < 0.01; and ***P < 0.001.

2.3 Results

2.3.1 COASY knockdown induced mitotic defects

In a genetic screen, we serendipitously identified that COASY knockdown reduced the viability of a triple negative breast cancer cell line (MDA-MB-231) (Fig. 1a, b). COASY is a metabolic enzyme required for the last two steps of *de novo* CoA biosynthesis (Zhyvoloup et al., 2002). Consistent with the role of COASY in CoA synthesis, we verified that COASY knockdown reduced the level of CoA and acetyl-CoA using LC-MS analysis (Fig. 1c, d). However, the acetyl-CoA/CoA ratio was not altered

(Fig. 1e). Surprisingly, we also found that COASY knockdown altered cell morphology into a flattened cobble-stone appearance (Fig. 1f) and a multinucleation phenotype (Fig. 1g). We found that COASY knockdown similarly triggered multinucleation in multiple cancer cell lines, including A549 (lung adenocarcinoma) (Fig. 1h), MDA-MB-231 (breast cancer) (Fig. 1i), PANC-1 (pancreatic cancer) (Fig. 1j) and non-cancerous cell line ARPE-19 (human retina) (Fig. 1k).

Figure. 1 COASY knockdown decreased cell numbers, CoA, acetyl-CoA and increased multi-nucleation. **a** COASY siRNAs reduced the levels of COASY protein. MDA-MB-231 cells were transfected with COASY siRNAs for 3 days before being lysed and analyzed by Western blots. **b** COASY knockdown reduced cell numbers of MDA-MB-231 cells. Indicated siRNAs were transfected to MDA-MB-231 cells (1500 cells/well) and the cell numbers were determined at indicated days. Two-way ANOVA: $p < 0.0001$. Bonferroni post hoc tests, $***p < 0.001$. $n = 3$ independent repeats. **c-e** COASY knockdown reduced the levels of CoA and acetyl-CoA. COASY knockdown did not alter the Acetyl-CoA/CoA ratio. The CoA and acetyl-CoA level of A549 cells as quantified by mass spectrometry. **f, g** COASY knockdown by siRNA in MDA-MB231 triggered cobble-stone morphological change (**f**) and multinucleation (**g**). MDA-MB-231 cells transfected with control or COASY siRNA for 72 hours were stained with DAPI (nuclei) and Alexa Fluor 488 phalloidin (F-actin). Scale bars, 50 μ m (**f**), 20 μ m (**g**). **h-k** The percentage of multi-

nucleated A549 cells (**h**) MDA-MB-231 (**i**) PANC-1 (**j**) and ARPE-19 (**k**) after transfection with control or two independent COASY siRNAs for 72 hours. For each sample, more than 150 cells were examined by immunofluorescence microscopy. * $p < 0.05$, ** $p < 0.01$, *** $p < 0.001$, two-tailed Student's t-test, $n=3$ independent repeats. Bars show standard error of the mean.

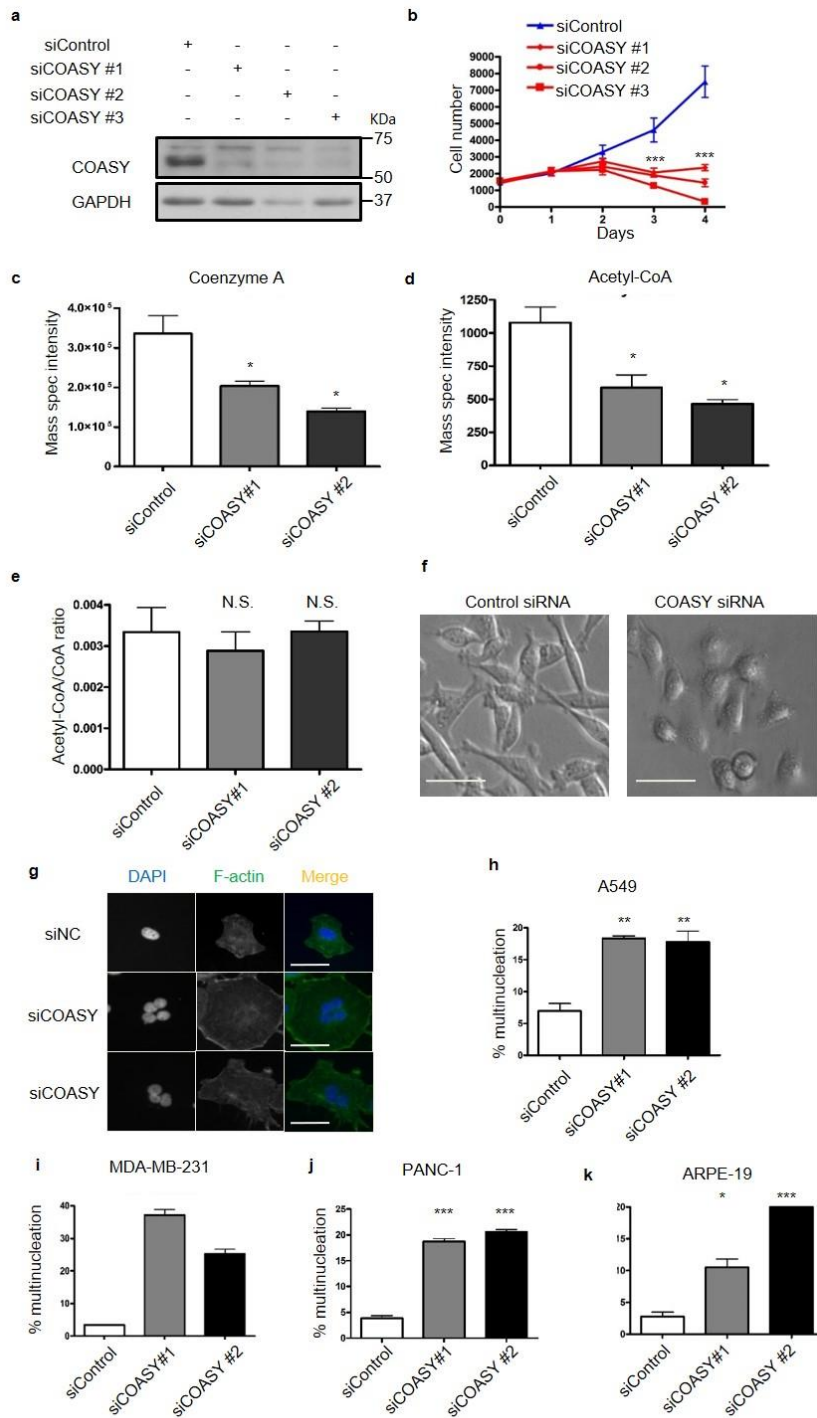


Figure. 1 COASY knockdown decreased cell numbers, CoA, acetyl-CoA and increased multi-nucleation.

Since multinucleation often results from aberrant mitotic progression (Vakifahmetoglu et al., 2008), we used a live cell imaging approach to determine how COASY knockdown affected the mitotic progression (Fig. 2a). We found that COASY knockdown extended mitosis from an average of 38 min to 162 min (Fig. 2a, b) and significantly increased the occurrence of cytokinesis failure from 2.3% to ~60% (Fig. 2c). To further confirm the extended mitosis, we synchronized A549 cells at the prometaphase using thymidine-nocodazole block. The expression of cyclin B1, a mitotic marker, was then examined after releasing the cells into fresh media (Fig. 2d). In control cells, cyclin B1 protein mostly disappeared 40 min after thymidine-nocodazole release indicating the normal duration of mitosis. In contrast, in COASY knockdown cells, cyclin B1 protein remained detectable up to ~160 min after release (Fig. 2d). Together, these results indicate that COASY knockdown prolonged mitosis and caused cytokinesis failure.

Figure. 2 COASY knockdown induced prolonged mitosis and cytokinesis failure. **a** Live cell time-lapse imaging showed that COASY knockdown extended mitosis and induced cytokinesis failure. A549 cells expressing histone 2B (H2B)-mCherry (nucleus marker) were transfected with control or COASY siRNA for 24 hours before live cell imaging. Scale bars, 10 μ m. **b** COASY knockdown increased the time in mitosis as determined by the time of nuclear envelope breakdown (NEBD) to anaphase onset (in minutes). For

each sample, more than 35 cells were examined by live cell imaging. **c** COASY knockdown increased percentage of cytokinesis failure during mitosis. For each sample, more than 35 cells were examined by live cell imaging. **d** Western blots shows that COASY knockdown extend the time of mitosis by using cyclin B1 expression as a mitotic marker. A549 cells were synchronized by thymidine-nocodazole block and released in fresh media. The samples were then harvested every 20 min and analyzed by Western blots. Bars show standard error of the mean. ** $p < 0.01$, *** $p < 0.001$, two-tailed Student's *t*-test, $n=3$ independent repeats.

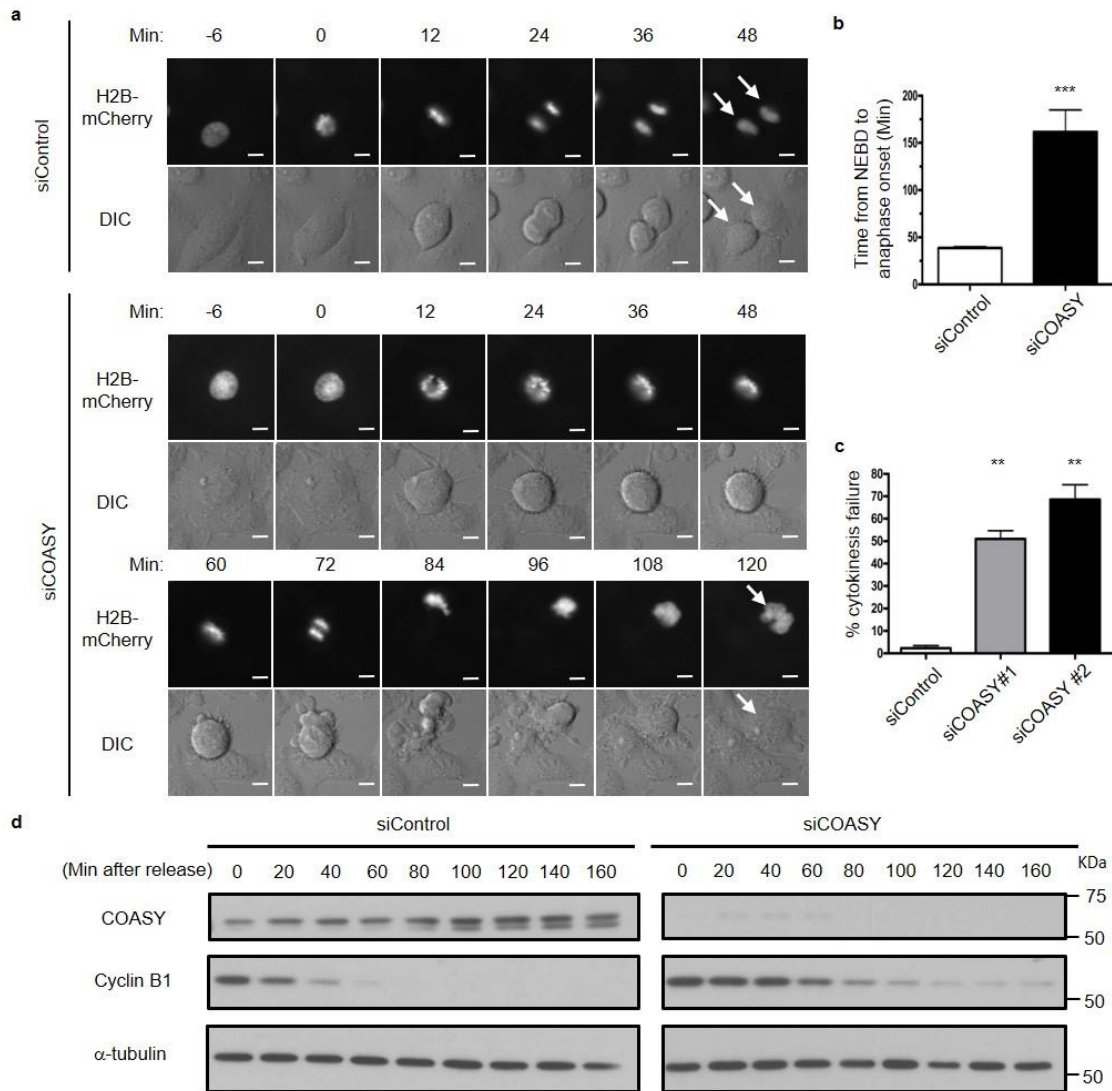


Figure. 2 COASY knockdown induced prolonged mitosis and cytokinesis failure.

2.3.2 COASY knockdown increases acetylation of specific proteins

Given that CoA is the main acetyl carrier for the reversible acetylation of lysine residues in proteins, we speculated that COASY knockdown would affect the acetylation of proteins, leading to mitotic defects. Therefore, we performed an acetylome analysis in synchronized A549 cells treated with control or COASY siRNAs. We

identified a total of 1074 acetylated peptides that belong to 504 proteins (1% false discovery rate (FDR)) (Fig. 3a, b). Two-tail Students t-test identified 119 differentially acetylated peptides (from 96 proteins) between the control and COASY-knockdown samples with a cut-off value of $p < 0.001$ (Fig. 3c). Although the lower acetyl-CoA level associated with COASY knockdown would logically predict reduced protein acetylation, to our surprise, we found that COASY knockdown increased the acetylation in 105 peptides (9.8%) of total acetylated peptides (1074 peptides) while only reduced the acetylation in 14 peptides (1.3%) of total acetylated peptides (Fig. 3b).

Figure. 3 COASY knockdown leads to hyper-acetylation of a subset of proteins. **a** Heatmap shows all the acetylated peptides ($n=1074$) across all samples transfected with siRNAs targeting Control or COASY. The color (yellow: induced, blue: repressed) indicates the normalized Zscore in Table S1. **b** Pie chart shows the percentage of hyperacetylated and hypoacetylated peptides by using a cut-off value of $p < 0.001$ in two-tail Students t-test. **c** Heatmap and hierarchical clustering of a subset of selected peptides whose levels have been significantly altered in A549 cells by COASY knockdown ($n=119$) $p < 0.001$ (two-tailed Student's t-test).

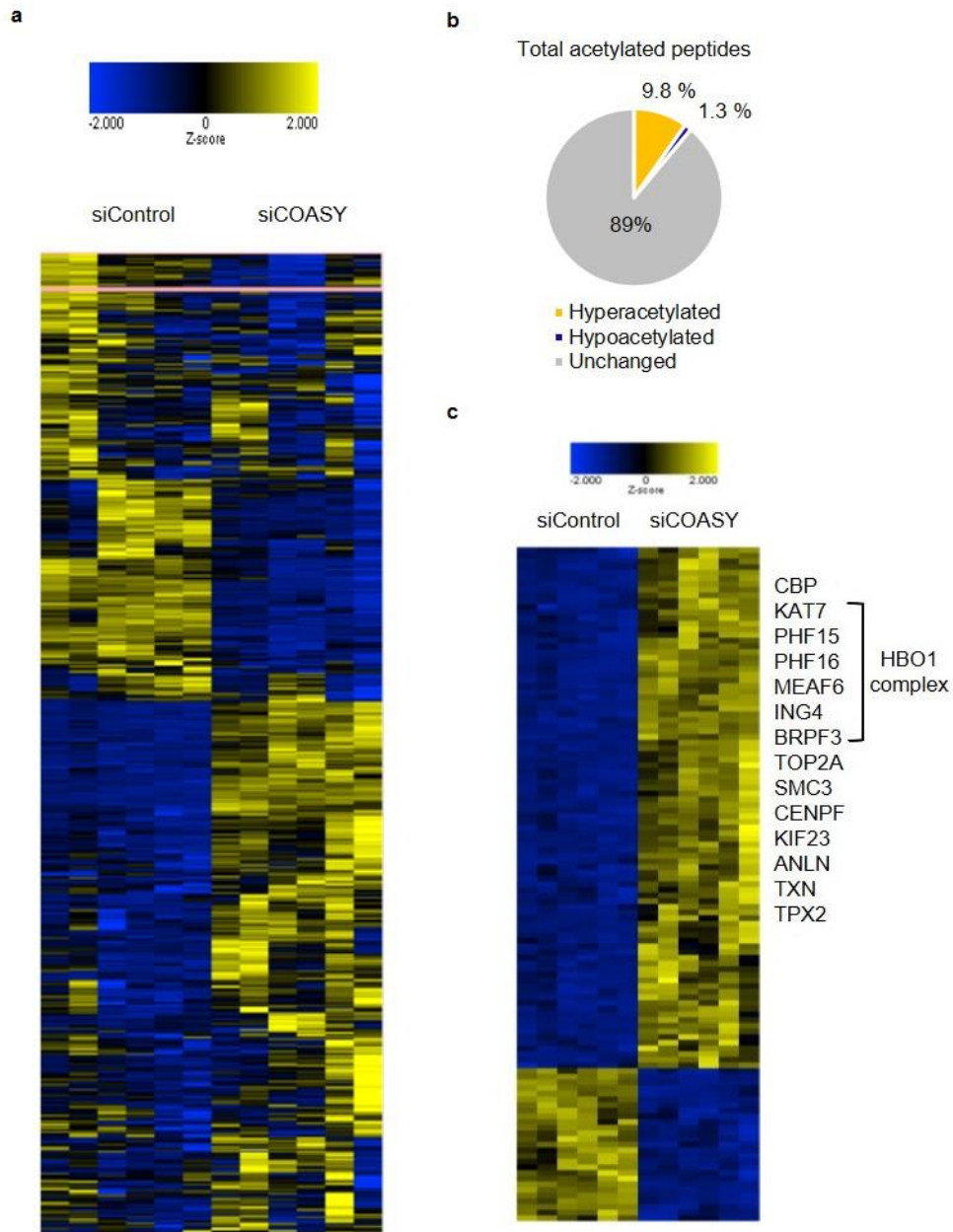
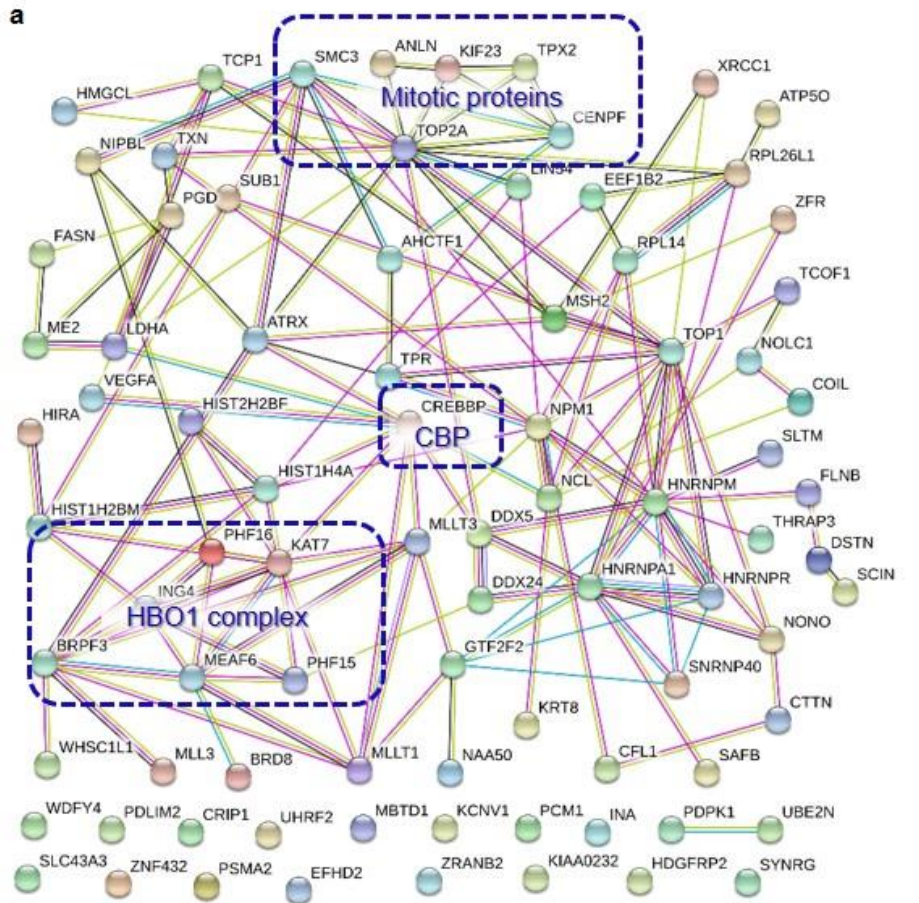


Figure. 3 COASY knockdown leads to hyper-acetylation of a subset of proteins

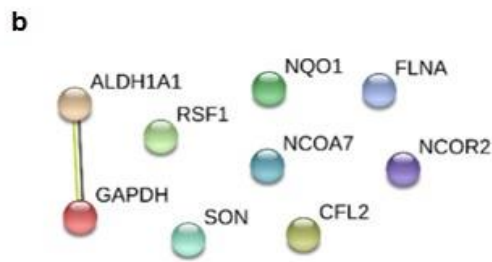
By analyzing the hyper- and hypo-acetylated proteins using STRING database (Szklarczyk et al., 2015), we found the hyperacetylated proteins form a strong protein

association network with significant amount of experimental determined interactions (Fig 4a). Interestingly, we found that CBP acetyltransferase is a prominent node with large number of connections with other hyperacetylated proteins, suggesting its potential importance in these hyperacetylated proteins. We also identified clusters of proteins involved in mitosis/cytokinesis, including TPX2, TOP2A, SMC3, CENPF, KIF23, ANLN and TXN. Of note, COASY knockdown led to the hyperacetylation of SMC3 K106, a modification previously implicated in regulating sister chromatid cohesion (Beckouet et al., 2010; Zhang et al., 2008). Moreover, many members of the HBO1 acetyltransferase complex, including KAT7, PHF15, PHF16, MEAF6, ING4 and BRPF3 , were found as a cluster (Avvakumov et al., 2012). In contrast, the hypoacetylated proteins showed only weak or no interaction (Fig. 4b).

Figure. 4 COASY knockdown leads to hyper-acetylation of a protein network. **a** Hypoacetylated proteins under COASY knockdown generated using STRING database. **b** Hypoacetylated proteins under COASY knockdown generated using STRING database.



— from curated databases — textmining — gene neighborhood
— experimentally determined — co-expression — protein homology



— textmining
— co-expression

Figure. 4 COASY knockdown leads to hyper-acetylation of a protein network.

2.3.3 TPX2 is a downstream effector of COASY during mitosis

Given the prominent mitotic phenotypes associated with COASY knockdown, we focus on the candidate proteins involved in mitosis. Among the hyperacetylated peptides, we found a notable 5-10 fold enrichment in three acetylated peptides (containing either K75, K476 or K582) of the TPX2 protein (Fig. 5a-d), a key co-activator of Aurora A kinase (Eyers and Maller, 2004; Kufer et al., 2002b). By comparing the TPX2 sequences among 15 different species, we found that K476 and K582, but not K75, were evolutionarily conserved (Fig. 5e). To validate the increased acetylation on TPX2 protein under COASY knockdown during mitosis, we enriched the mitotic population of A549 cells by thymidine-nocodazole block and mitotic shake-off. The levels of TPX2 protein (Fig. 5f), but not mRNA (Fig. 5g, h), were markedly higher in cells with COASY knockdown. TPX2 was then pulled down by TPX2 antibody and probed with a pan-acetylated lysine antibody. When normalized to the TPX2 protein levels, COASY knockdown indeed increased TPX2 acetylation (Fig. 5i).

Figure. 5 TPX2 are hyperacetylated on three lysine residues under COASY silencing. **a** COASY knockdown increased three acetylated peptides (K75, K476 and K582) of TPX2 as determined by acetylome analysis. **b-d** Acetylome analysis identified three potential acetylation residues on TPX2. MS/MS Spectra Images of TPX2 K75 (**b**) K476 (**c**) and K582 (**d**). **e** Two of the three potential acetylation sites of TPX2 are highly conserved among 15

different examined species. . **f** COASY knockdown increased TPX2 protein level in A549 cells. **g, h** COASY knockdown reduced COASY RNA (**g**), but did not alter TPX2 RNA expression (**h**). A549 cells transfected with siControl or siCOASY were enriched in mitosis by thymidine-nocodazole block. The levels of COASY and TPX2 transcripts were then determined by Real-Time PCR. **i** COASY knockdown increased the TPX2 acetylation in A549 cells. A549 cells enriched in early mitosis by thymidine-nocodazole block were transfected with control or COASY siRNA and probed with indicated antibodies The TPX2 in the cell lysates were then immunoprecipitated and blotted for pan-acetylated lysine antibody.

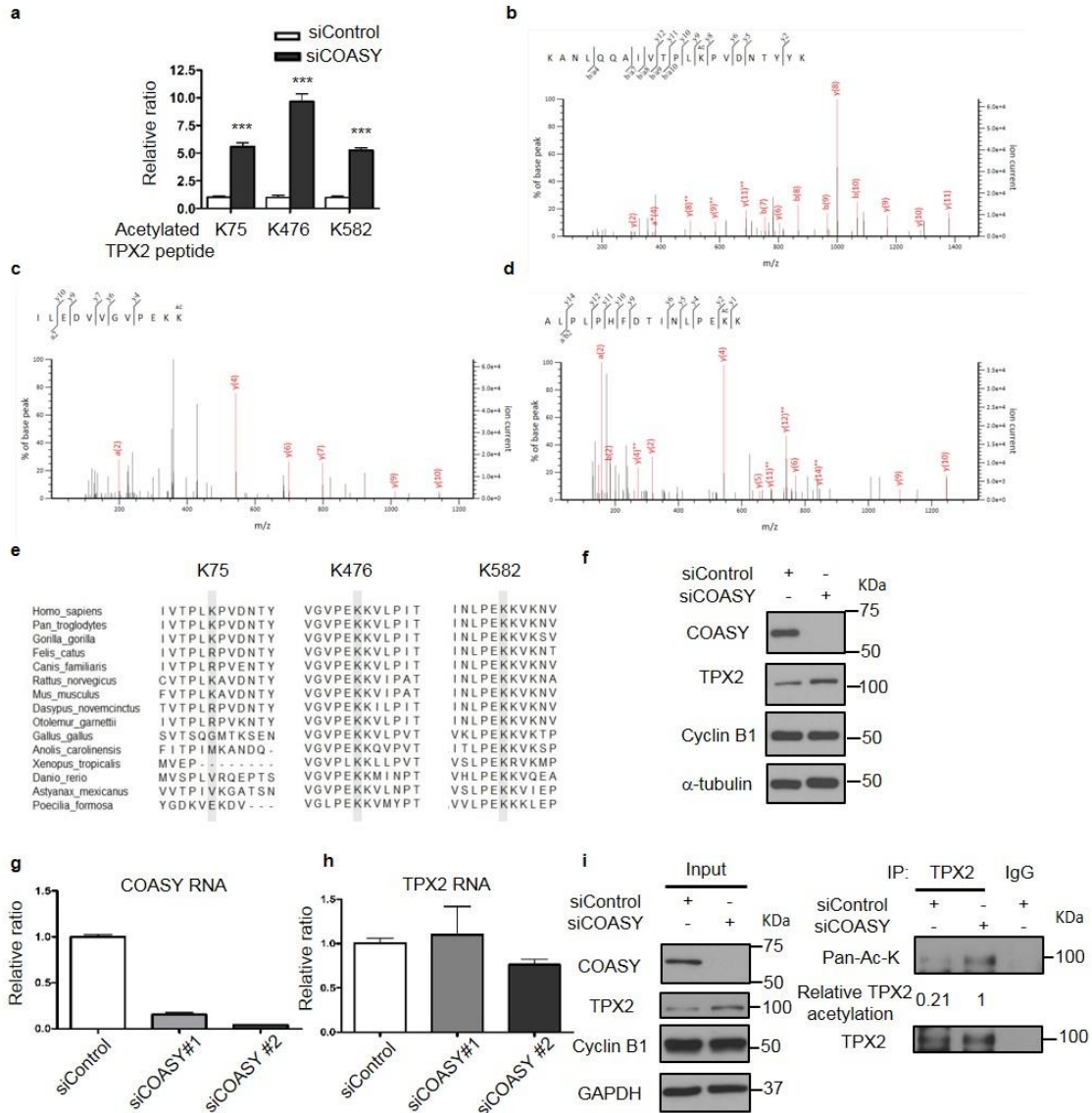


Figure. 5 TPX2 are hyperacetylated on three lysine residues under COASY silencing.

The increase in acetylation at K476 and K582 upon COASY knockdown were further validated and quantified in a site-specific manner by parallel-reaction monitoring (PRM)(Peterson et al., 2012) targeted mass spectrometry using synthetic heavy isotope peptides (Fig. 6g-l).

Figure 6 PRM chromatogram of the native acetylated TPX2 peptides including K476 (**a**) and K582 (**b**). **c, d** PRM Chromatogram of the stable-isotope internal standard acetylated TPX2 peptides including K476 (**c**) and K582 (**d**). **e, f** Quantification of acetylation of K476 (**e**) and K582 (**f**) on TPX2 using PRM. COASY knockdown increased the acetylation of both K476 and K582. Quantification of the native acetylated TPX2 peptides , calculated as a ratio to the stable-isotope internal standard peptide spiked prior to sample digestion and IP, was performed using PRM targeted mass spectrometry. n=3 for each group.

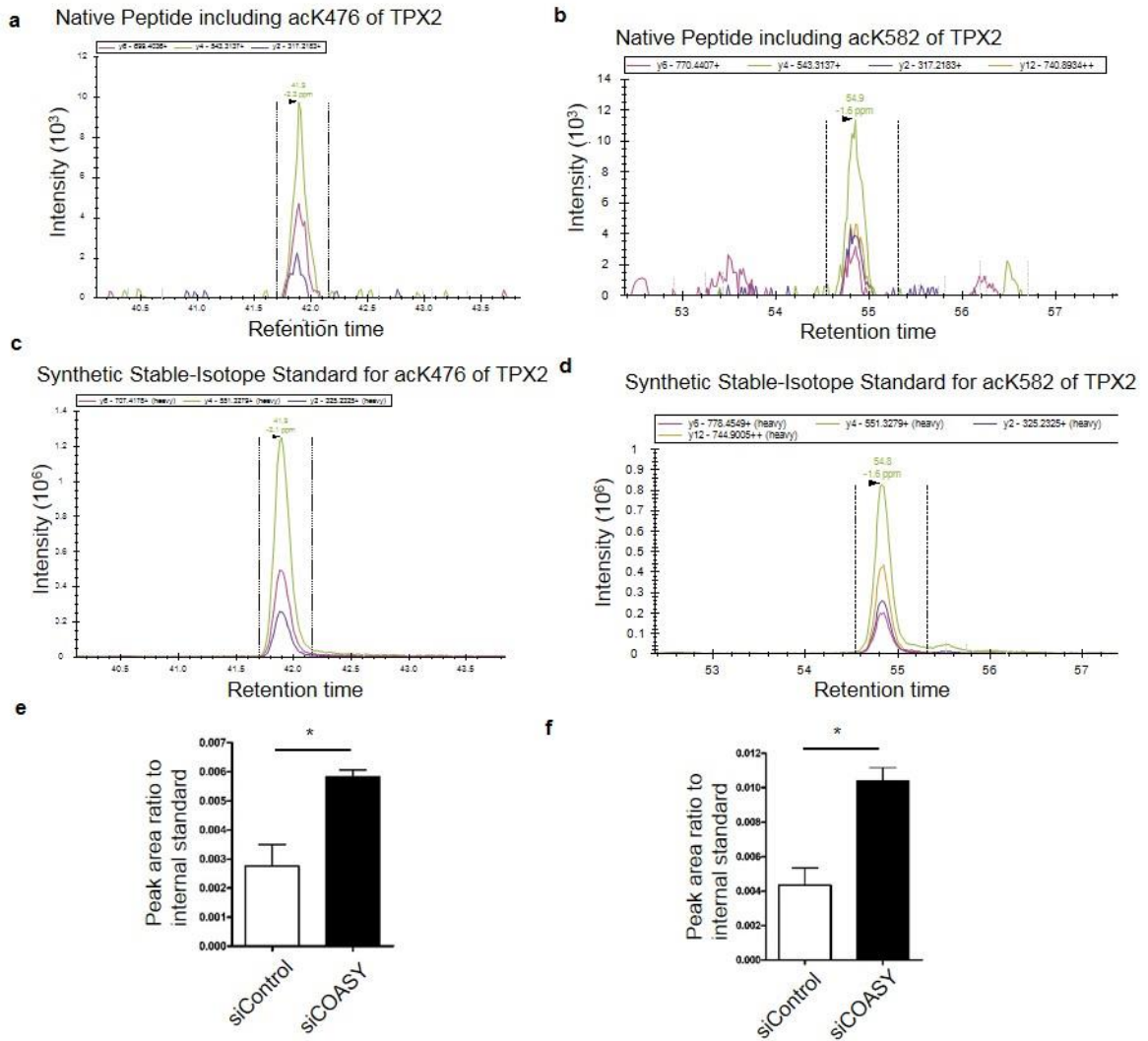


Figure 6 PRM chromatogram of the native acetylated TPX2 peptides

Since protein lysine acetylation could regulate protein stability by affecting protein ubiquitination via competing for similar sets of lysine residues (Caron et al., 2005), we investigated whether COASY knockdown affected TPX2 ubiquitination. We transfected V5-tagged TPX2 cDNA into HEK-293T cells treated with either control or

COASY siRNA. TPX2 was then immunoprecipitated by V5 antibody for Western blots. With MG132 treatment, a proteasome inhibitor, we found that the while COASY knockdown did not affect the general ubiquitination levels (Fig. 7, left panel), it markedly reduced TPX2 ubiquitination (Fig. 7, right panel). These findings suggest that the increased TPX2 acetylation induced by COASY knockdown may prevent TPX2 ubiquitination and increase its levels.

Figure 7 COASY knockdown decreased TPX2 ubiquitination in HEK-293T cells. HEK-293T cells were transfected with COASY siRNA and TPX2 cDNA. After MG132 treatment, TPX2 were immunoprecipitated and blotted for pan-ubiquitination antibody.

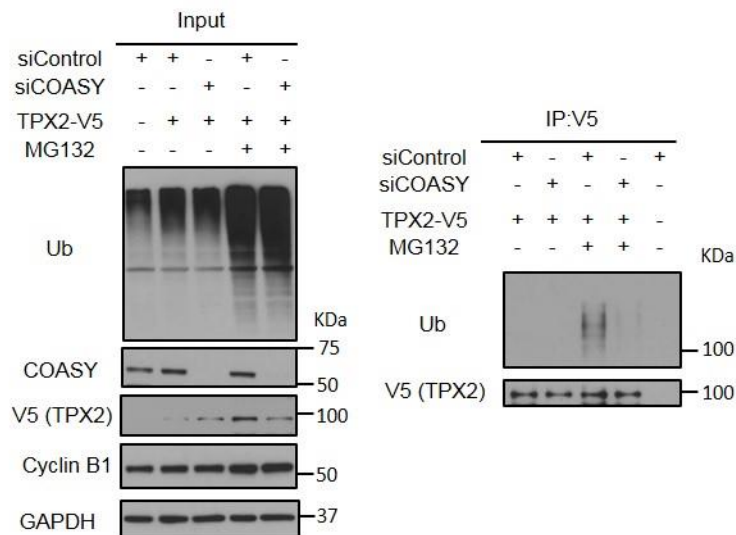


Figure 7 COASY knockdown decreased TPX2 ubiquitination in HEK-293T cells.

Since the induction and degradation of TPX2 is tightly regulated during the cell cycle to control mitotic spindle and Aurora A kinase activity (Neumayer et al., 2014), the aberrant mitosis phenotype in COASY knockdown might be contributed by dysregulated TPX2 protein level. Therefore, we knocked down the expression of TPX2 and COASY simultaneously. We found that the multinucleation (Fig. 8a, b) and extended mitosis phenotype (Fig. 9) induced by COASY knockdown was significantly suppressed by simultaneous knockdown of TPX2. Under the same experimental design, we further re-expressed siRNA-resistant wild-type TPX2, *acetylation-deficient* (3R) or *acetylation-mimicking* (3Q) TPX2 mutants cDNA at close to physiological level (Fig 9). We found that wild-type and *acetylation-mimicking* mutant TPX2 expression increased multinucleation and extended mitosis, while *acetylation-deficient* mutant significantly reduced these phenotypes (Fig. 8). These data indicated that the elevation and lysine acetylation of TPX2 protein contributes to the mitotic defects induced by COASY knockdown.

Figure 8 TPX2 protein expression level and acetylation on TPX2 regulated the percentage of COASY-dependent multinucleation and extended mitosis. **a** TPX2 knockdown rescued the multinucleation induced by COASY knockdown. Reintroducing wild type (WT), or acetylation-mimetic mutant (3Q), but not acetylation-deficient (3R), of siRNA-resistant TPX2 cDNA recapitulated multinucleation phenotype. **b** The

acetylated lysines on TPX2 regulated the percentage of COASY-dependent extended mitosis. TPX2 knockdown rescued the extended mitosis induced by COASY knockdown. Reintroducing wild type (WT), or acetylation-mimetic (3Q), but not acetylation-deficient (3R), mutant of siRNA-resistant TPX2 cDNA recapitulated extended mitosis phenotype.

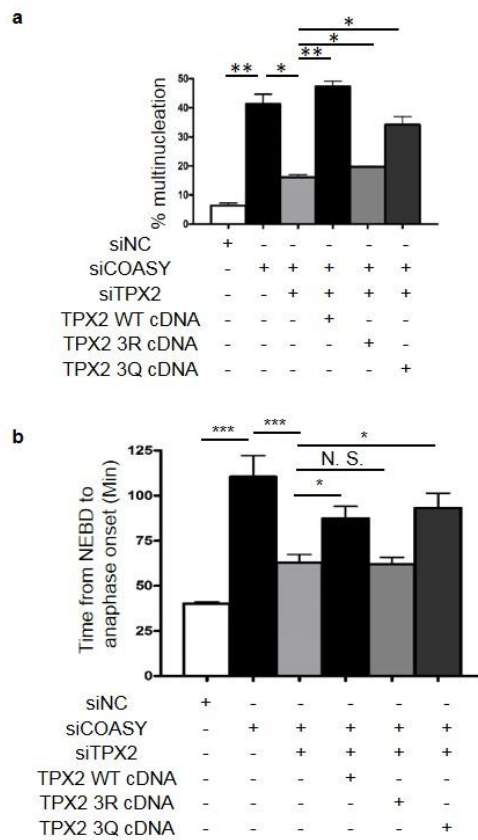


Figure 8 TPX2 protein expression level and acetylation on TPX2 regulated the percentage of COASY-dependent multinucleation and extended mitosis.

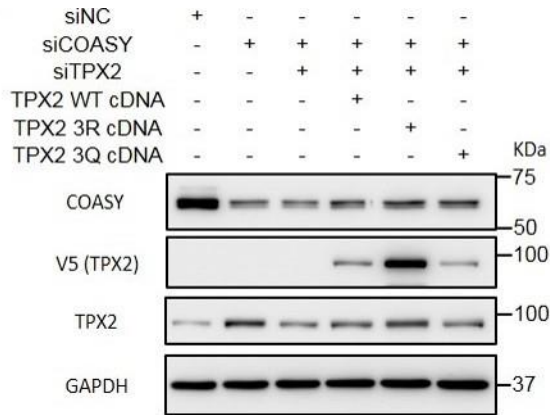


Figure 9 Western blot for validating the expression of indicated proteins.

Next, we determined the role of TPX2 mis-regulation in the mitotic defects induced by COASY knockdown. A549 cells transfected with control, COASY siRNA or COASY siRNA combined with TPX2 siRNA were synchronized by thymidine-nocodazole block and released. Samples were collected at different time points and used to evaluate the levels and activities of TPX2 and Aurora A kinase by Western blots (Fig. 10). In the control cells, TPX2 protein level increased sharply and reached a peak after 20 min that is accompanied by the autophosphorylation (Thr288) of Aurora A kinase. After 40 min, TPX2 protein level, Aurora A phosphorylation and Cyclin B1 all plummeted, indicating mitotic exit (Fig. 10, left panel). Remarkably, COASY knockdown enhanced TPX2 protein level and Aurora A phosphorylation in both amplitude and duration; the mitotic exit was significantly prolonged to ~120 min as indicated by the persistence of cyclin B1 (Fig. 10, middle panel). When TPX2 was suppressed to approximately

physiological level using siRNA (Fig. 10a, right panel), the prolonged mitosis induced by COASY knockdown was significantly rescued as indicated by the levels of cyclin B1 and Aurora A phosphorylation (Fig. 10, right panel).

Figure 10 COASY knockdown triggered increased Aurora A Thr288 phosphorylation and extended mitosis by the elevation of TPX2. A549 cells were synchronized by thymidine-nocodazole block and released in fresh media for the indicated time (in minutes). COASY knockdown increased TPX2 expression and delayed its decline during from 40 mins (control) to >160 mins. COASY knockdown also delayed the inactivation of Aurora A and degradation of cyclin B1, indicating extended mitosis. The extended mitosis caused by COASY knockdown can be abolished by simultaneous TPX2 knockdown.

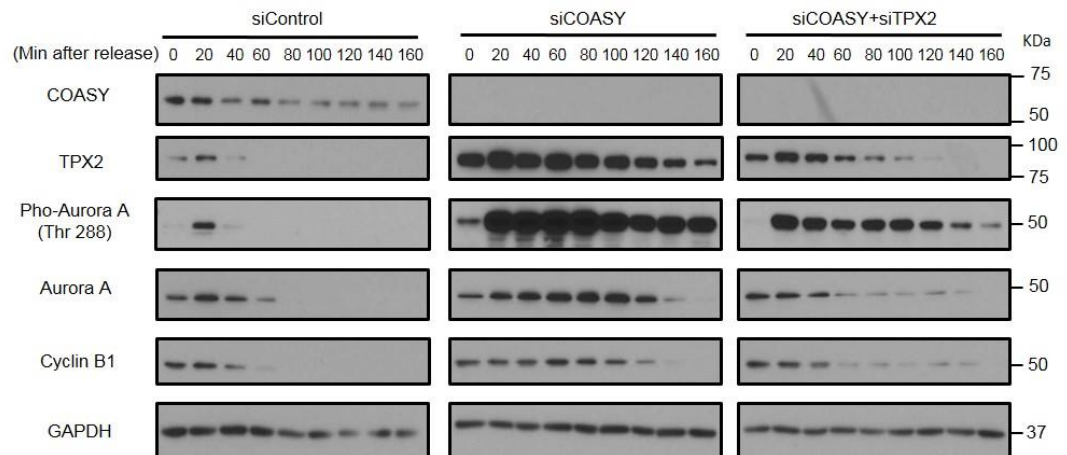


Figure 10 COASY knockdown triggered increased Aurora A Thr 288 phosphorylation and extended mitosis by the elevation of TPX2.

Since TPX2 level and Aurora A phosphorylation were upregulated under COASY knockdown (Fig. 10), we further examined the localization of these signals by confocal microscopy (Fig. 11a-c). Under COASY knockdown, we observed stronger and broader distribution of TPX2 proteins reaching from spindle poles to chromosomes during metaphase when comparing to the control (Fig. 11a). During metaphase, the stage Aurora A are both activated under both control and COASY knockdown, COASY knockdown did not dramatically change the signal of Aurora A phosphorylation (Fig. 11b). However, during interphase, Aurora A phosphorylation was much higher under COASY knockdown, indicating COASY can determine the precise activation of Aurora A at specific stages of cell cycle (Fig. 11c). Taken together, these results strongly suggested that TPX2 dysregulated by COASY knockdown contributed to the abnormal TPX2 distribution, Aurora A activation and prolonged mitosis.

Figure 11 COASY silencing triggered aberrant localization of TPX2 and phosphor-Aurora A. **a** During metaphase in A549 cells, TPX2 had high intensity in spindle poles under confocal microscopy. Upon COASY knockdown, more TPX2 signal was observed extending from spindle poles to chromosomes. **b** COASY knockdown did not alter Aurora A phosphorylation during metaphase. **c** COASY knockdown led to stronger Aurora A phosphorylation was observed in the nuclei during interphase. Scale bars, 10 mm.

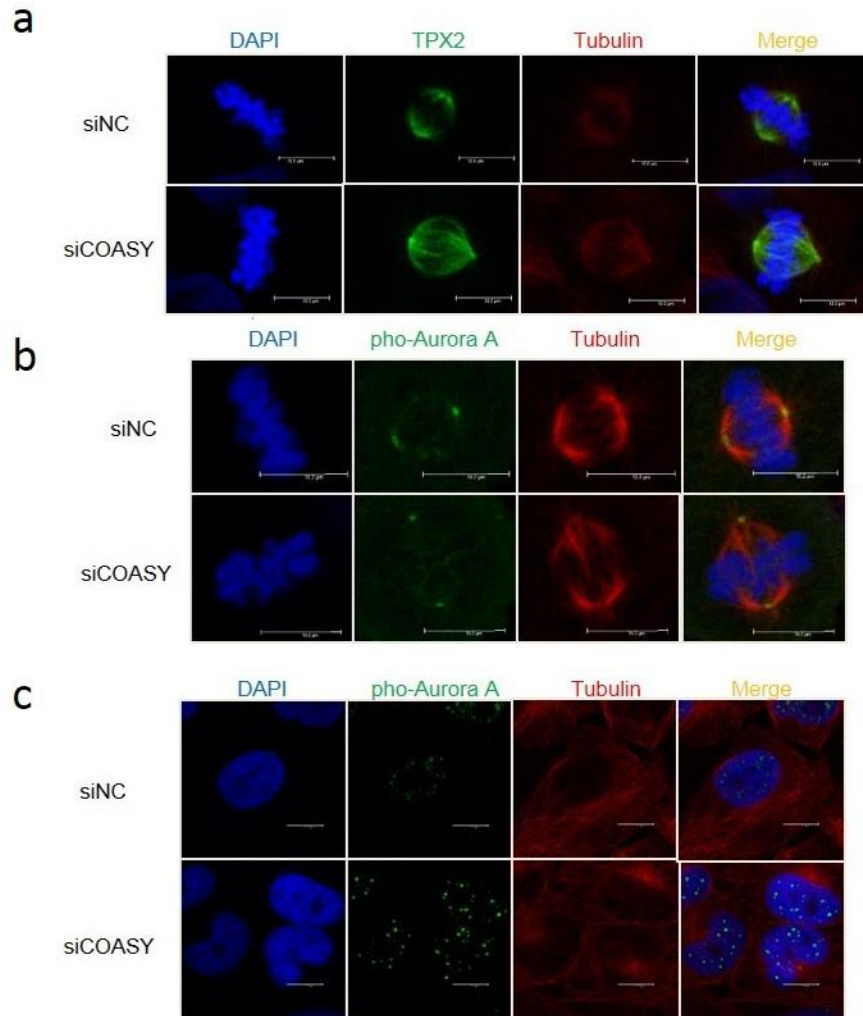


Figure. 11 COASY silencing triggered aberrant localization of TPX2 and phosphor-Aurora A.

2.3.4 CBP acetylates and stabilizes TPX2 protein

Next, we investigated how COASY knockdown increases TPX2 acetylation. In the COASY-dependent acetylome, we found that COASY knockdown increased the

acetylation of two over-lapping peptides that include K1762 of the acetyltransferase CBP (Fig. 12a-c). As autoacetylation on CBP is known to increase its acetyltransferase activity (Thompson et al., 2004) and CBP showed extensive interactions with other hyperacetylated proteins in our acetylome dataset (Fig. 4a), we hypothesized that CBP might be responsible for increased TPX2 acetylation and protein accumulation under COASY knockdown. To test this possibility, we first examined whether CBP forms a complex with TPX2. By using TPX2 antibody to pull down the endogenous TPX2 protein, we observed that endogenous CBP was co-immunoprecipitated independent of COASY (Fig. 12d). Next, we tested whether CBP acetylated TPX2. In HEK-293T cells, V5-tagged TPX2 was co-transfected with either wild type or a catalytic deficient mutant HA-CBP construct (Ito et al., 2002) (Fig. 12e). When co-transfected with wild type, but not catalytic mutant CBP, wild type CBP was co-immunoprecipitated with acetylated TPX2. (Fig. 12e). Similar results were also repeated in MDA-MB-231 cells (Fig. 12f).

Figure. 12 CBP acetylates TPX2 protein. **a** COASY knockdown increased two CBP acetylated peptides that cover K1762. **b, c** MS/MS Spectra Images of two peptides that include CBP K1762. **d** COASY knockdown did not alter the CBP-TPX2 interaction in A549 cells. A549 cells enriched in early mitosis by thymidine-nocodazole block were transfected with control or COASY siRNA and probed with indicated antibodies. The TPX2 in the cell lysates were then immunoprecipitated and blotted for CBP antibody. **e**

CBP acetylated TPX2 *in vivo* in MDA-MB-231 cells. HA-tagged CBP was cotransfected with V5 tagged TPX2 into HEK-293T cells. After 20 min of release from thymidine-nocodazole block, the V5 tagged TPX2 was then immunoprecipitated with V5 antibody and then probed with HA (CBP), acetylated lysine or V5 (TPX2). **f** CBP acetylated TPX2 *in vivo*. Wild type or catalytic deficient mutant of HA-tagged CBP was cotransfected with V5 tagged TPX2 into HEK-293T cells. After 20 min of release from thymidine-nocodazole block, the V5 tagged TPX2 was then immunoprecipitated with control (IgG) or V5 antibody (V5) and then probed with HA (CBP), acetylated lysine or V5 (TPX2). Wild type, but not catalytic deficient mutant, CBP increased TPX2 acetylation and levels.

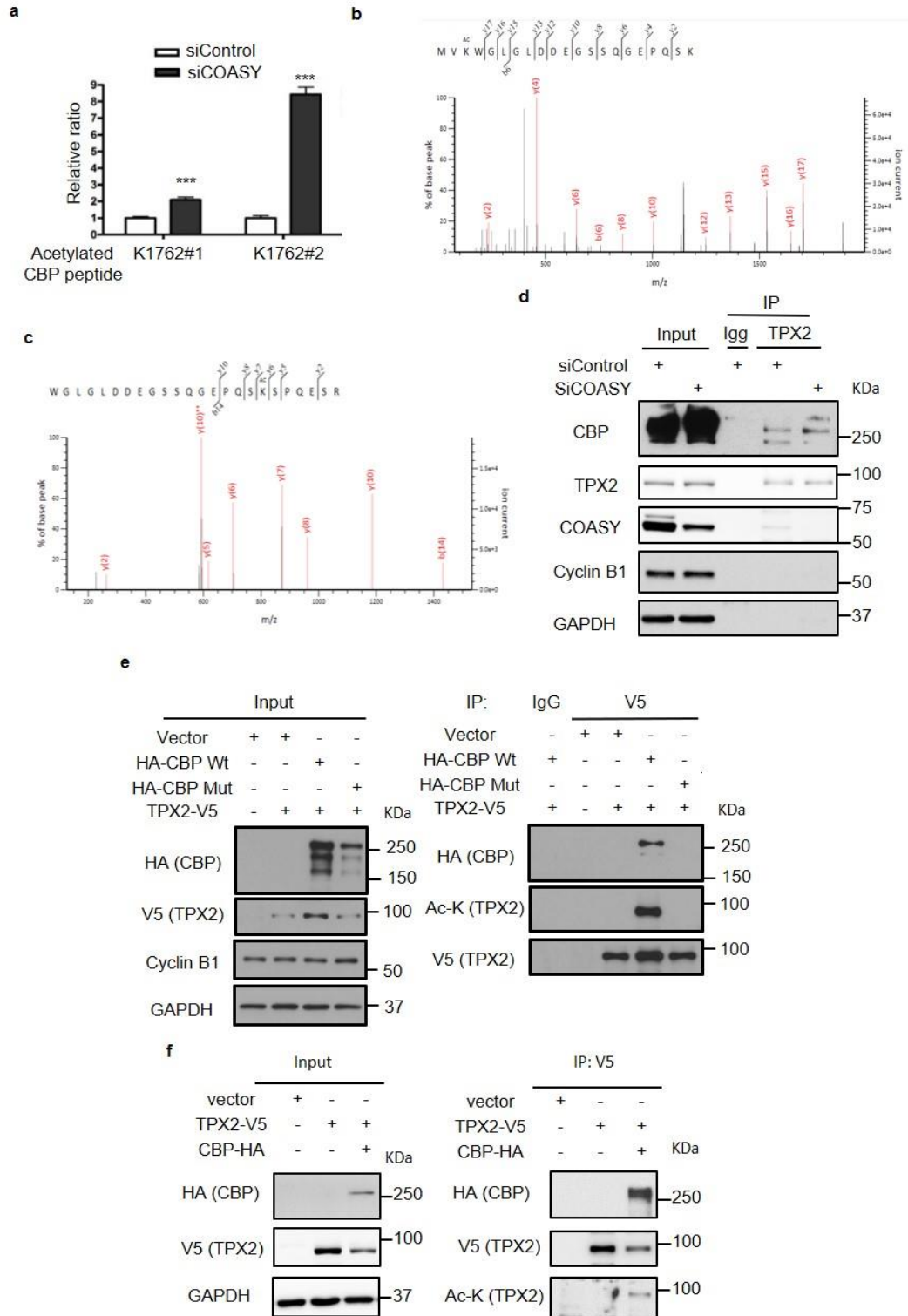


Figure. 12 CBP acetylates TPX2 protein.

Since TPX2 acetylation appears to be negatively correlated with its ubiquitination (Fig. 5i, 7), we tested whether CBP-mediated TPX2 acetylation contributes to the stabilization of TPX2. We co-transfected a V5-TPX2 construct with either wild type or catalytic deficient mutant CBP into HEK-293T cells and determined the half-life of V5-TPX2 protein in the presence of cycloheximide, an inhibitor of protein synthesis (Fig. 13a). When co-transfected with mutant CBP, the half-life of TPX2 protein was significantly decreased to approximately 3 hours compared with wild type CBP (Fig. 13a). Similar trends were also observed in A549 cells (Fig. 13b). These results indicated that the acetylation modification of TPX2 is CBP dependent and contributes to TPX2 protein accumulation.

Figure 13 CBP increased the half-life of TPX2. Wild type or catalytic deficient mutant of CBP was cotransfected with V5 tagged TPX2 into unsynchronized HEK-293T cells (a) or A549 cells (b). After 24 hours, the protein synthesis of the transfected cells was halted with 25 mg/ml cycloheximide and collected at the indicated times for Western blots. The TPX2 protein level at indicated time points was quantified by Image J software and normalized to β -tubulin protein level.

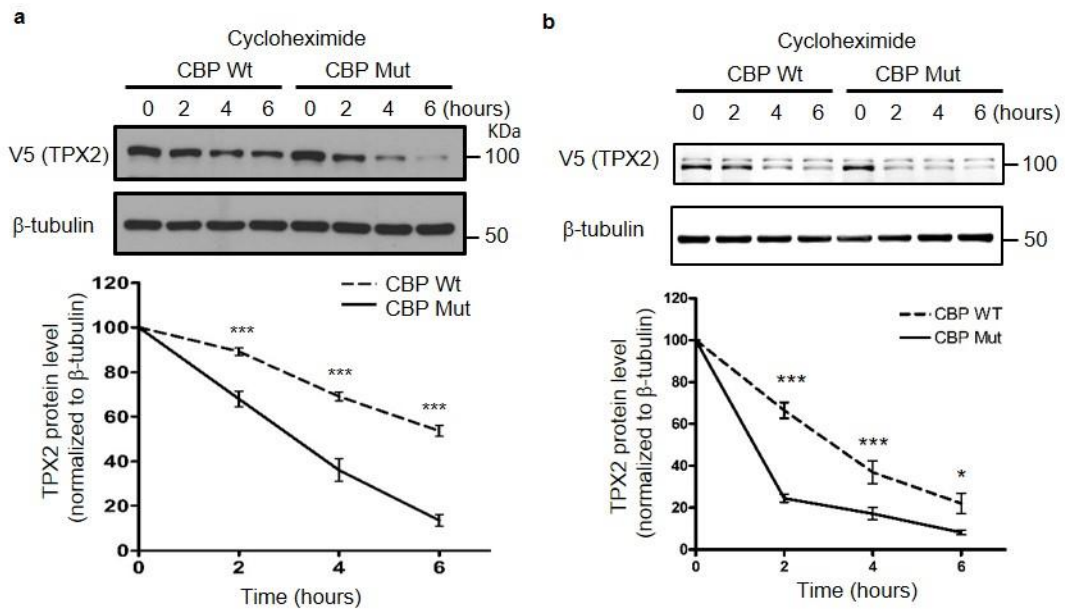


Figure 13 CBP increased the half-life of TPX2.

To further test whether TPX2 is acetylated by CBP on the three lysine residues (K75, K476 and K582) enriched in our COASY knockdown acetylome dataset (Fig. 3a and 5a), The V5 tagged TPX2 or TPX2-RRR (*acetylation-deficient mutant*) were co-transfected with HA-tagged CBP in HEK-293T cells. The V5-TPX2 protein was then pulled down by V5 antibody and detected using a pan-acetylated antibody. TPX2-RRR showed a ~90% reduction in acetylation, indicating the acetylation modification of K75, K476 and K582 are the main lysine residues on TPX2 that acetylated by CBP (Fig. 14a). To further confirm whether the three lysine residues affect TPX2 ubiquitination, we overexpressed V5-tagged TPX2 or TPX2-RRR under MG132 treatment. The TPX2 protein in cell lysates was pulled down by V5 antibody and detected using a pan-ubiquitination

antibody which detect a broad range of ubiquitylated TPX2 species from 100-160 KDa (Fig. 14b, c). We found a decrease in TPX2 ubiquitination in TPX2-RRR under both native (HEK-293T cells, Fig. 14b) and denaturing conditions (MDA-MB-231 cells, Supplementary Fig. 14c), indicating these three acetylation sites are crucial for TPX2 ubiquitination.

Figure 14 CBP increased TPX2 acetylation on three lysine residues involving in TPX2 protein degradation. **a** Wild-type and triple mutant TPX2 (RRR, K75R, K476R and K582R) were co-transfected with CBP cDNA in HEK-293T cells. When the TPX2 protein was pulled down by V5 tag, triple mutant of TPX2 showed ~91% decrease in normalized acetylation than wild-type TPX2. Two-way ANOVA: $p < 0.0001$. Bonferroni post hoc tests, $*p < 0.05$, $***p < 0.001$. $n = 4$ independent repeats. **b, c** Removal of the three potential acetylation residues on TPX2 decreased its ubiquitination. **b** HEK-293T cells transfected with wild-type or triple mutant TPX2 (RRR, K75R, K476R and K582R) were treated with MG132. TPX2 were then immunoprecipitated by V5 antibody and blotted for pan-ubiquitination antibody. **c** MDA-MB-231 cells co-transfected with HA tagged ubiquitin and wild-type or triple mutant TPX2 (RRR, K75R, K476R and K582R) were treated with MG132. After lysing cells in denaturing condition (1% SDS and boiling for 5 min), TPX2 were then immunoprecipitated by V5 antibody and blotted for ubiquitination by HA antibody. A broad range of ubiquitylated TPX2 species from 100-190 Kda.

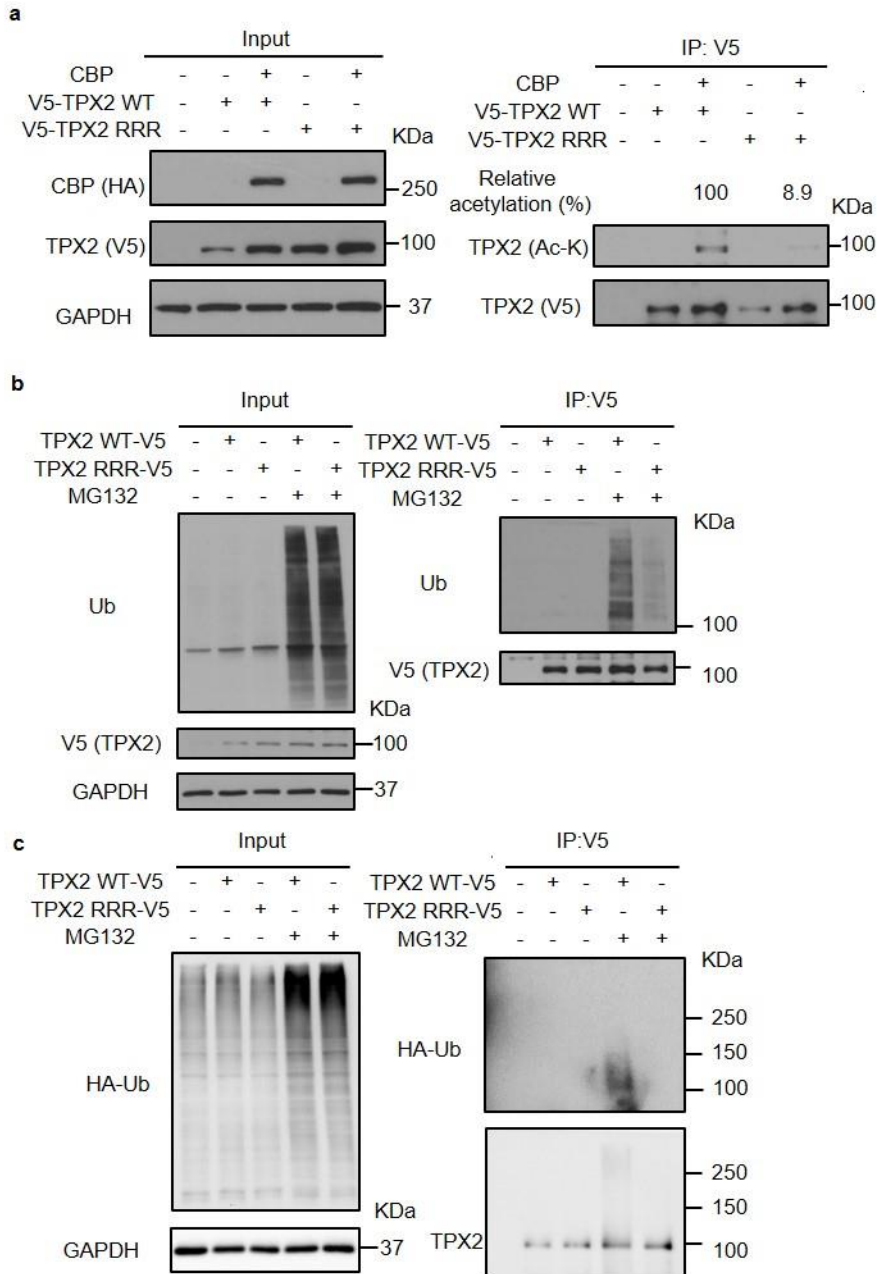


Figure 14 CBP increased TPX2 acetylation on three lysine residues involving in TPX2 protein degradation.

To directly assess the role of CBP in the TPX2 upregulation and multinucleation upon COASY knockdown, we inhibited CBP by either siRNA or a chemical inhibitor C646 (Fig. 15 a-d) (Bowers et al., 2010). Remarkably, inhibition of CBP by either method significantly rescued the aberrant upregulation of TPX2 and multinucleation phenotype in COASY knockdown cells (Fig. 15 a-d). Therefore, CBP contributed to both TPX2 upregulation and the multinucleation in COASY knockdown scenario.

Figure 15 Inhibition of CBP rescued the aberrant upregulation of TPX2 and multinucleation. **a** CBP siRNA abolished the increased TPX2 and Aurora-A phosphorylation caused by COASY knockdown. A549 cells transfected with control, siCOASY or siCBP were released from thymidine-nocodazole block for 20 min and probed for Western blots using indicated antibodies. The phosphorylated Thr 288 of Aurora A indicates activation. **b** CBP knockdown rescued the multinucleation caused by COASY knockdown. Multinucleation was determined by immunofluorescence. **c** C646 abolished the increased TPX2 caused by COASY knockdown. A549 cells with indicated COASY knockdown and/or C646 treatment were synchronized by thymidine-nocodazole block for Western blots. **d** C646 rescued the multinucleation, as determined by immunofluorescence, caused by COASY knockdown.

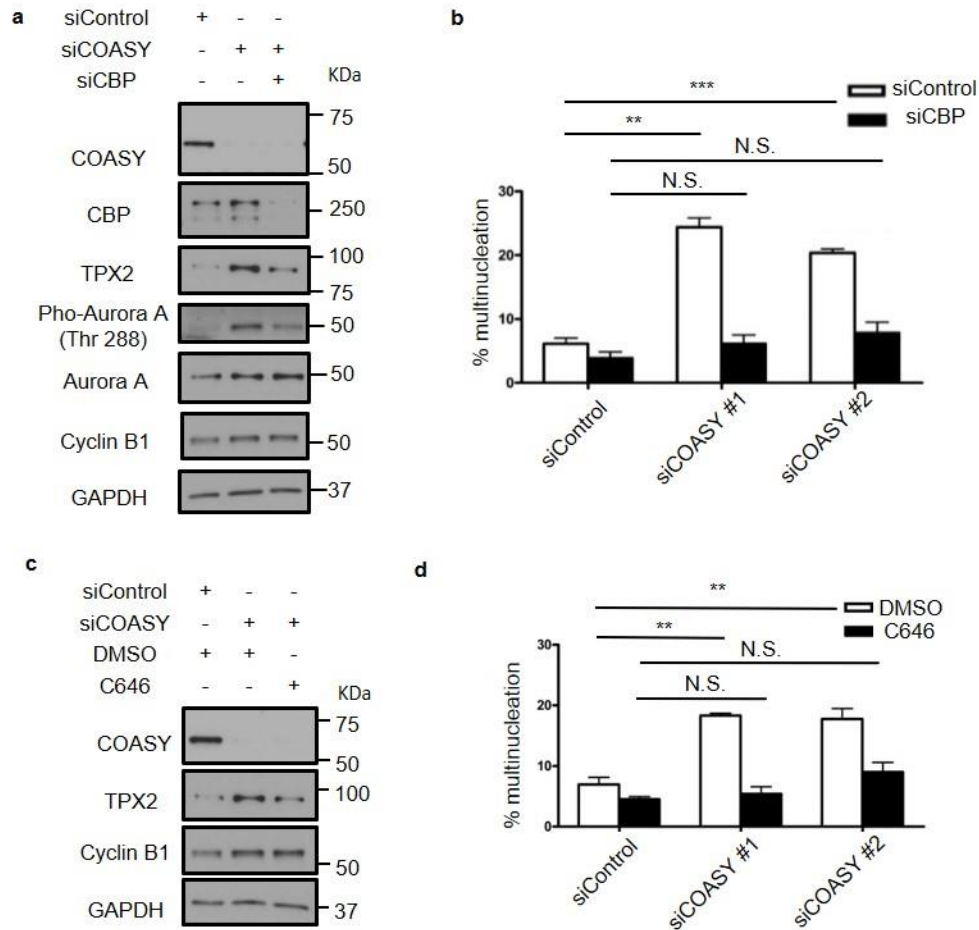


Figure 15 Inhibition of CBP rescued the aberrant upregulation of TPX2 and multinucleation.

We then test whether CBP is a physiological regulator of the TPX2 protein levels during mitosis under normal condition in synchronized A549 cells (Fig. 16a, b). By suppressing CBP expression (by siRNA) or activity (by C646), we found that CBP inhibition markedly blunted the sharp TPX2 increase during early mitosis (Fig. 16a, b). This finding indicates that CBP regulates TPX2 protein levels during normal mitosis.

Figure 16 CBP is a physiological regulator of the TPX2 protein levels. **a** CBP knockdown decreased TPX2 protein level during mitosis. A549 cells transfected with siRNA targeting CBP were synchronized by thymidine-nocodazole block and released in fresh media. The released cells were harvested every 20 min and probed with indicated antibodies. To examine TPX2 protein level in S phase, additional samples were harvested after 24 hours of thymidine block. **b** C646 decreased the induction of TPX2 protein during mitosis. A549 cells were synchronized by thymidine-nocodazole block with or without C646 (5 mM). After 16 hours of nocodazole arrest, the cells were released in fresh media with C646. The samples were then harvested every 10 min after the release for Western blots.

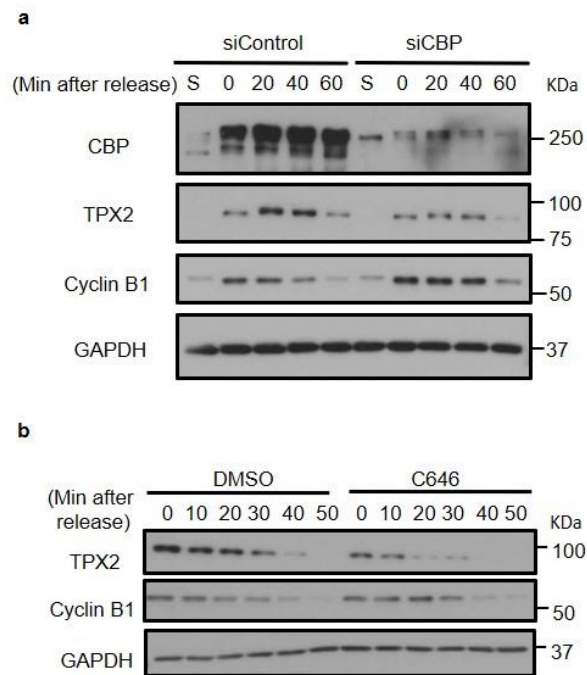
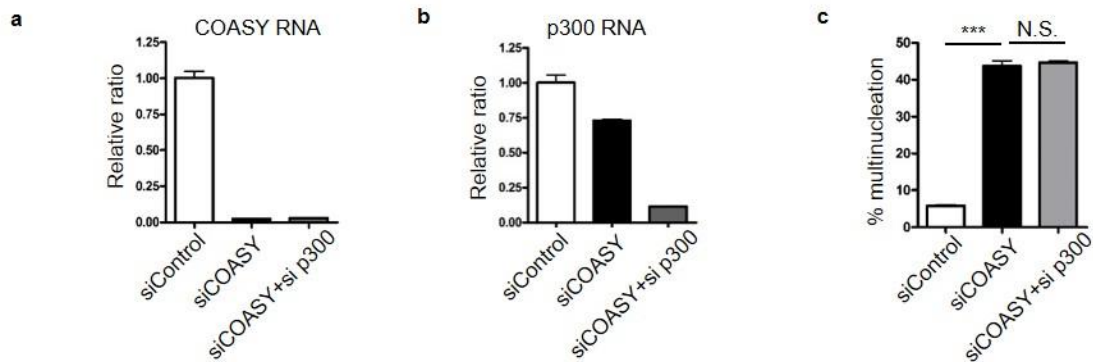


Figure 16 CBP is a physiological regulator of the TPX2 protein levels.

Since CBP and p300 have similar sequences and function (Ogryzko et al., 1996), we further tested whether p300 is also involved in COASY-dependent multinucleation. We knocked down the p300 by targeting its specific sequences together with COASY (Fig. 17a, b), we did not observe a rescue of the multi-nucleation phenotypes (Fig. 17c). This finding indicates that CBP, but not p300, is involved in COASY-dependent mitotic defects.

Figure 17 Validation of knockdown efficiency of COASY (a) and p300 (b) mRNA by real-time PCR. c p300 knockdown did not rescue the multinucleation caused by COASY knockdown.



2.3.5 COASY inhibits CBP-mediated TPX2 acetylation

To further characterize the interacting network among COASY, CBP and TPX2 *in vivo*, we examined their subcellular localizations during mitosis. TPX2 is known to be localized to spindle microtubules during mitosis (Ma et al., 2010), however, the locations

of CBP and COASY during mitosis has not been reported. We expressed a GFP-tagged COASY in A549 cells and examined the subcellular localizations of COASY, TPX2 and CBP in different stages of cell cycle by confocal microscopy (Fig. 18a-c). The stage of cell cycle for each cell was defined by the shape of nuclei (DAPI staining). During interphase, COASY showed a diffuse pattern mainly in nucleus and cytoplasm similar to the pattern of COASY from the Human Protein Atlas (Uhlen et al., 2015). However, the subcellular localization of COASY showed no obvious colocalization with TPX2 or CBP (Fig. 18a, b). Remarkably, during mitosis, COASY-GFP, but not GFP, is recruited to spindle microtubules and co-localized with TPX2 and CBP (Fig. 18a-c). These findings support the idea that TPX2, CBP and COASY interact with each other during mitosis.

Figure. 18 Stage-specific physical association suggest direct interaction among COASY, CBP and TPX2. **a** TPX2 and **b** CBP showed colocalization with COASY in spindle microtubules during mitosis. COASY-GFP expressing A549 cells were stained with TPX2 (**a**) or CBP (**b**) antibody for confocal microscopy. Scale bars, 10 mm. **c** GFP-tagged COASY, but not GFP alone, showed colocalization with tubulin during metaphase.

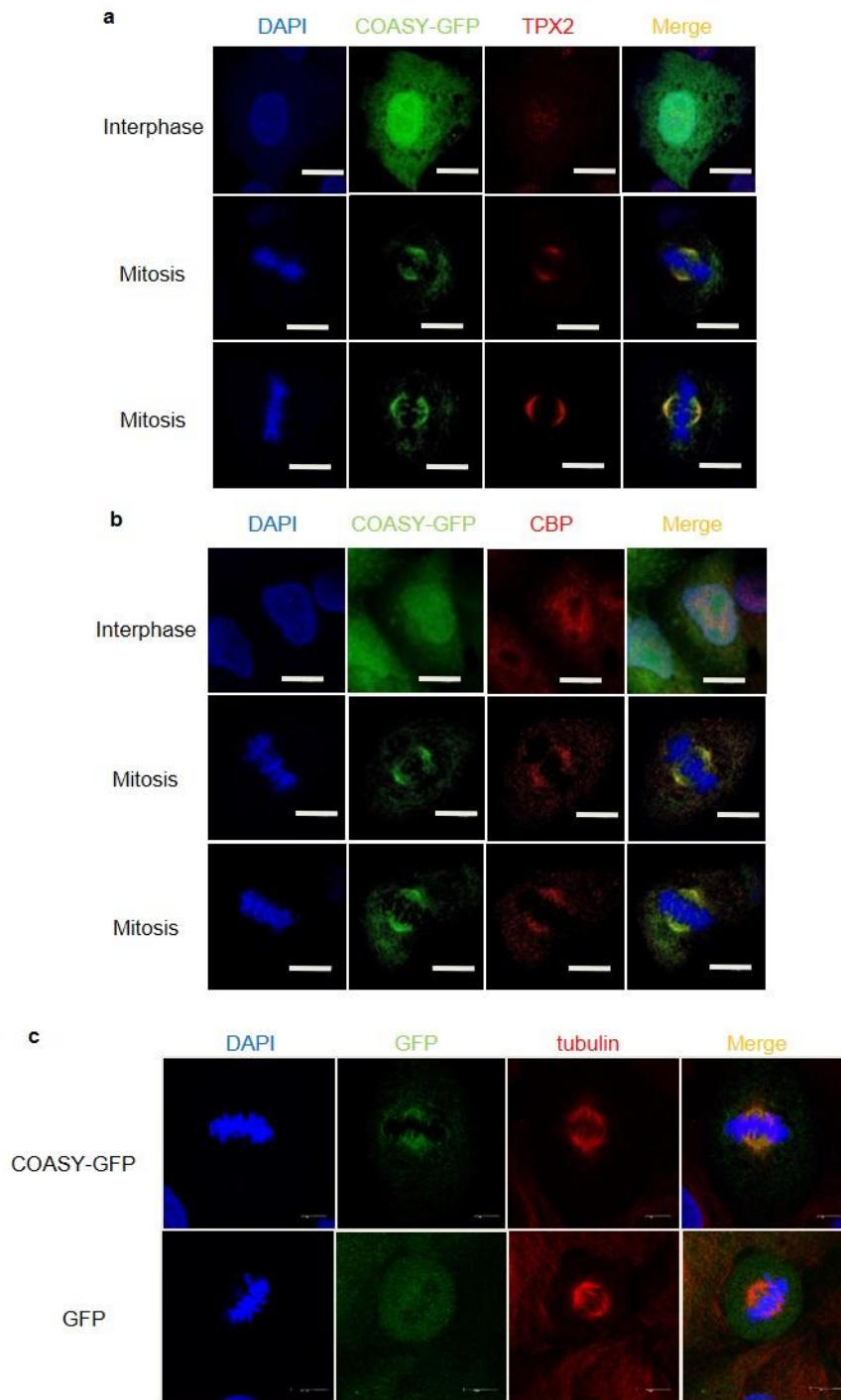


Figure. 18 Stage-specific physical association suggest direct interaction among COASY, CBP and TPX2.

To further examine the physical interactions between COASY, TPX2 and CBP during mitosis, A549 cells synchronized in prometaphase by thymidine-nocodazole block were released into fresh media and harvested at different time points. The endogenous CBP and associated proteins were immunoprecipitated by a CBP antibody followed by Western blots (Fig. 19a). Both COASY and TPX2 showed a stage-specific interaction with CBP, and these interactions largely disappeared by 80 min (Fig. 19a). Reciprocally, the endogenous COASY in mitotically synchronized HEK-293T cells also associated TPX2 and CBP proteins indicated by co-immunoprecipitation (Fig. 19b).

Figure 19 Stage-specific physical association among COASY, CBP and TPX2 **a** TPX2 and COASY physically associate with CBP during mitosis. A549 cells were synchronized by thymidine-nocodazole block and released for the indicated time to enrich cells in different cell cycle stages. An additional sample was harvested after 24 hours of thymidine block for cells enriched in S phase. The CBP was immunoprecipitated, separated by electrophoresis and probed with the TPX2 and COASY antibodies. **b** COASY formed a complex with CBP and TPX2. HEK-293T cells enriched in mitosis were harvested for co-immunoprecipitation of COASY antibody and probed with either CBP or TPX2 antibodies by Western blots.

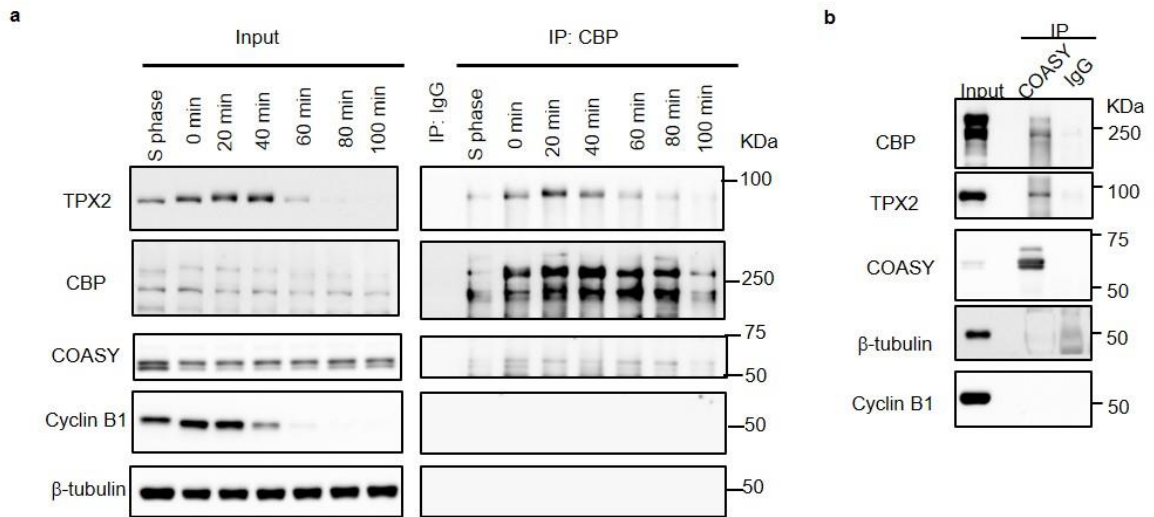


Figure 19 Stage-specific physical association among COASY, CBP and TPX2

Since the physical interaction of CBP and COASY is novel and unexpected, we further validated this interaction of pulling down CBP from HEK293T cells overexpressing Flag-CBP and COASY cDNA. By using mass spectrometry, we confirmed the enrichment of COASY peptides when CBP was immunoprecipitated (Fig. 20a-d). These data strongly suggest that COASY, CBP and TPX2 physically associate with each other in a specific stage of mitosis.

Figure 20 Mass spectrometry confirmed enrichment of COASY peptides when Flag-CBP was pulled down from HEK-293T cells overexpressing Flag-CBP and COASY cDNA. **a**, **b** Extracted Ion Chromatograms for 4 COASY peptides (**a**) and 9 CBP (bait) peptides (**b**) between control and Flag-CBP expressing HEK-293T cells. **c**, **d** Bar Charts signifying the

sum of the 4 COASY peptides (c) increased with pulling down of 9 Flag-CBP peptides (d).

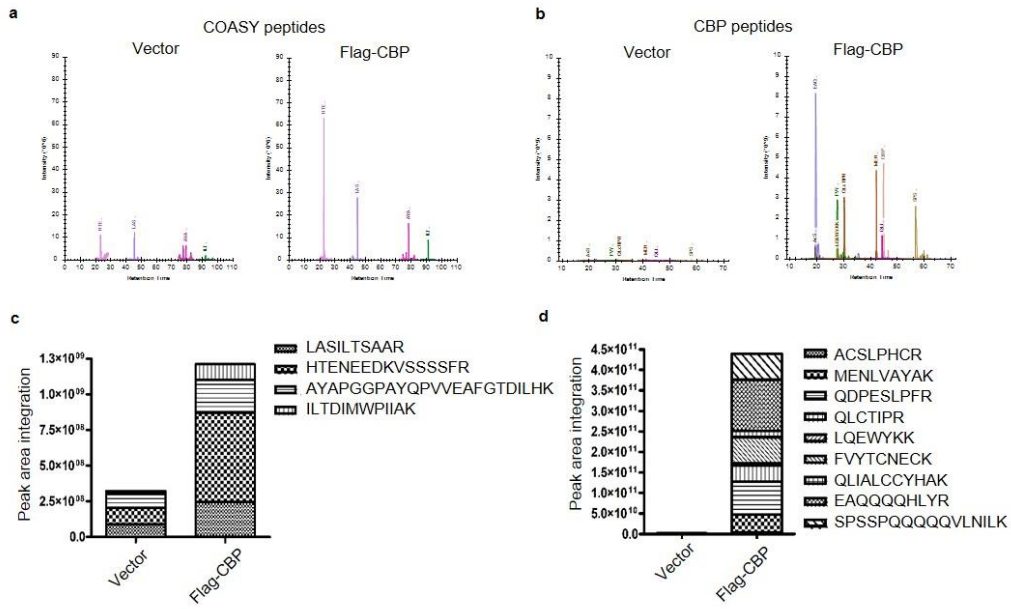


Figure 20 Mass spectrometry confirmed enrichment of COASY peptides when Flag-CBP was pulled down from HEK-293T cells overexpressing Flag-CBP and COASY cDNA.

In principle, COASY could inhibit CBP by direct binding to CBP or by the help of some other unidentified proteins in COASY-CBP-TPX2 protein complex *in vivo*. Therefore, we tested whether COASY could directly inhibit CBP acetyltransferase activity on TPX2 *in vitro*. First, when recombinant CBP (catalytic domain) and TPX2 were incubated with acetyl-CoA, we noted a significant increase in the acetylation of TPX2 (Fig. 21a). When wild type TPX2 was replaced with acetylation-deficient mutant protein, acetylation signal became undetectable (Fig. 21b). Next, we employed the TPX2

acetylation assay to determine the effects of COASY. Importantly, purified recombinant COASY inhibited CBP-mediated TPX2 acetylation in a dose dependent manner (Fig. 21c-e). Together, these data suggest that COASY can directly inhibit CBP-mediated TPX2 acetylation, consistent with the observed CBP hyperacetylation upon COASY knockdown.

Figure 21 COASY inhibited CBP-mediated TPX2 acetylation *in vitro*. **a** CBP acetylated TPX2 *in vitro*. Recombinant full-length TPX2 protein was acetylated by CBP (catalytic domain) human recombinant protein in the presence of acetyl-CoA. Acetylation on TPX2 was determined by Western blots using pan-acetylated lysine antibody. **b** CBP was unable to acetylate acetylation-deficient mutant (3R) of TPX2 *in vitro*. The recombinant catalytic domain of human CBP was incubated with wild type or acetylation-deficient mutant of TPX2 pulled down from HEK-293T cells in the presence of acetyl-CoA. Acetylation on TPX2 was determined by Western blots using pan-acetylated lysine antibody. **c** COASY inhibited CBP-mediated TPX2 acetylation *in vitro*. Bacterially purified COASY or control BSA was added to the CBP activity assay using TPX2 protein as substrate. With increasing amount of COASY, the level of acetylated TPX2 decreased in a dose-dependent manner. **d** Quantification of TPX2 acetylation in the presence of COASY. Acetylated TPX2 level determined by pan-acetylated lysine antibody was quantified by Image J software and normalized to TPX2 protein level.

One-way ANOVA: $p < 0.0001$. Bonferroni post hoc tests, $*p < 0.05$, $***p < 0.001$. $n=4$ independent repeats. Bars show standard error of the mean. **e** Bacterially expressed GST-COASY was purified and resolved by 10% SDS PAGE and silver staining. Human COASY cDNA was subcloned to an GST tagged vector (pGTvL1-SGC) for bacterial expression. Recombinant GST-COASY protein was induced in *E. coli* (BL21) and purified using glutathione agarose.

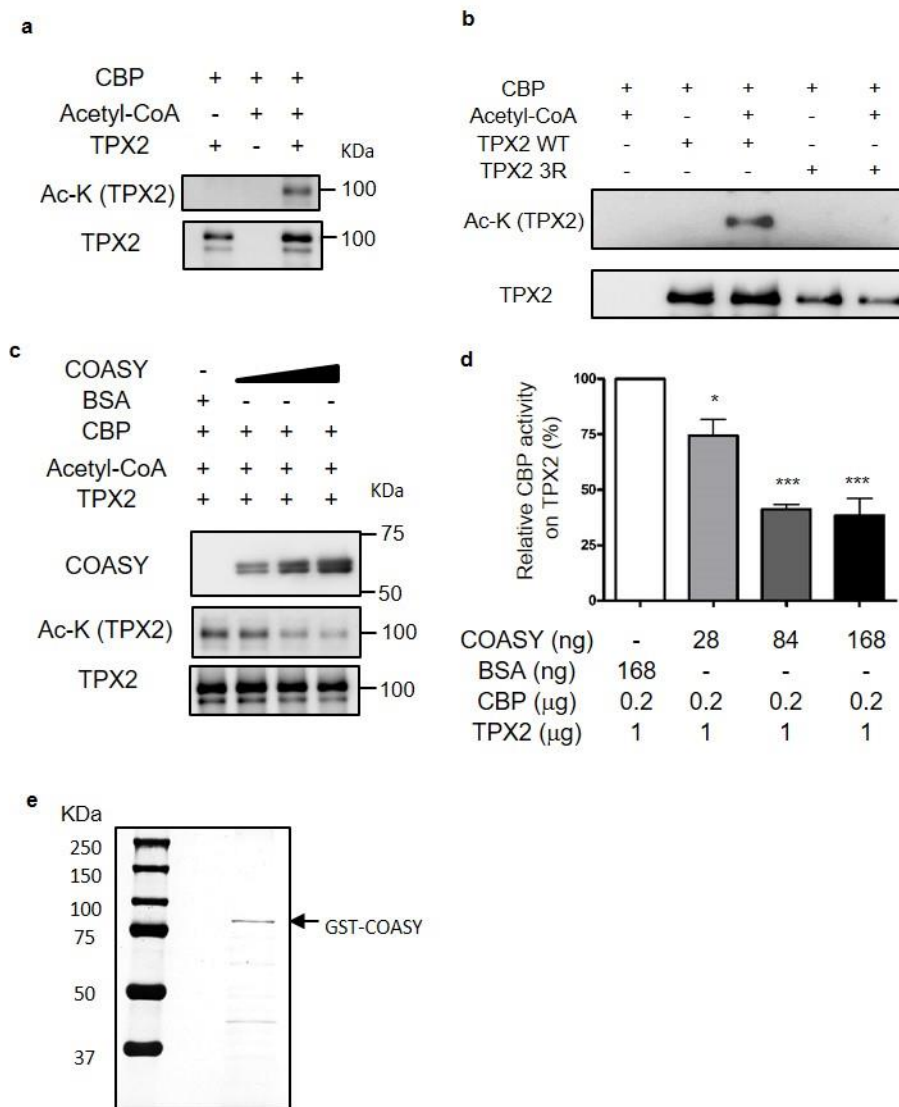


Figure 21 COASY inhibited CBP-mediated TPX2 acetylation *in vitro*.

2.3.6 The PPAT domain regulates TPX2 protein stability

COASY contains two catalytic domains: the Phosphoribosyl Pyrophosphate Amidotransferase (PPAT) domain and the Dephospho-CoA kinase (DPCK) domain (Fig. 22a) (Zhyvoloup et al., 2002). These two domains are responsible for the two sequential enzymatic steps required for the CoA synthesis. In humans, the disease-causing R499C mutation of COASY disrupts the enzymatic activity of DPCK (Dusi et al., 2014). We therefore tested whether this R499C mutation affects the association of COASY with CBP and mitotic abnormalities. We found that the interaction between COASY and CBP was not affected by R499C mutation on COASY (Fig. 22b). Interestingly, we found that COASY with R499C mutation was able to rescue the multinucleation phenotype caused by COASY knockdown comparable to wild type COASY (Fig. 22c, d). These results suggested that the enzymatic activity of DPCK of COASY was not essential for mitotic regulation.

Figure. 22 Both wild and R499C of COASY cDNAs rescued multinucleation. **a** Schematic illustration of domains on COASY. COASY is composed of N terminus regulatory domain and two catalytic domain (PPAT and DPCK). R499C mutant inactivates DPCK. **b** Both wildtype or R499C mutant COASY protein showed strong

interaction with CBP. CBP and COASY cDNAs were cotransfected to HEK-293T cells. The cells were then enriched in mitosis by 16 hours of nocodazole treatment. The samples were harvested for co-immunoprecipitation. **c** Both wild and R499C of COASY cDNAs rescued multinucleation. MDA-MB-231 cells stably expressing control vector (pLKO.1), wildtype or R499C COASY were transfected with COASY siRNA for 72 hours. The multinucleation induced by COASY siRNA can be abolished by both wildtype and R499C COASY. **d** Western blot for validating the expression of indicated proteins in Fig 22c.

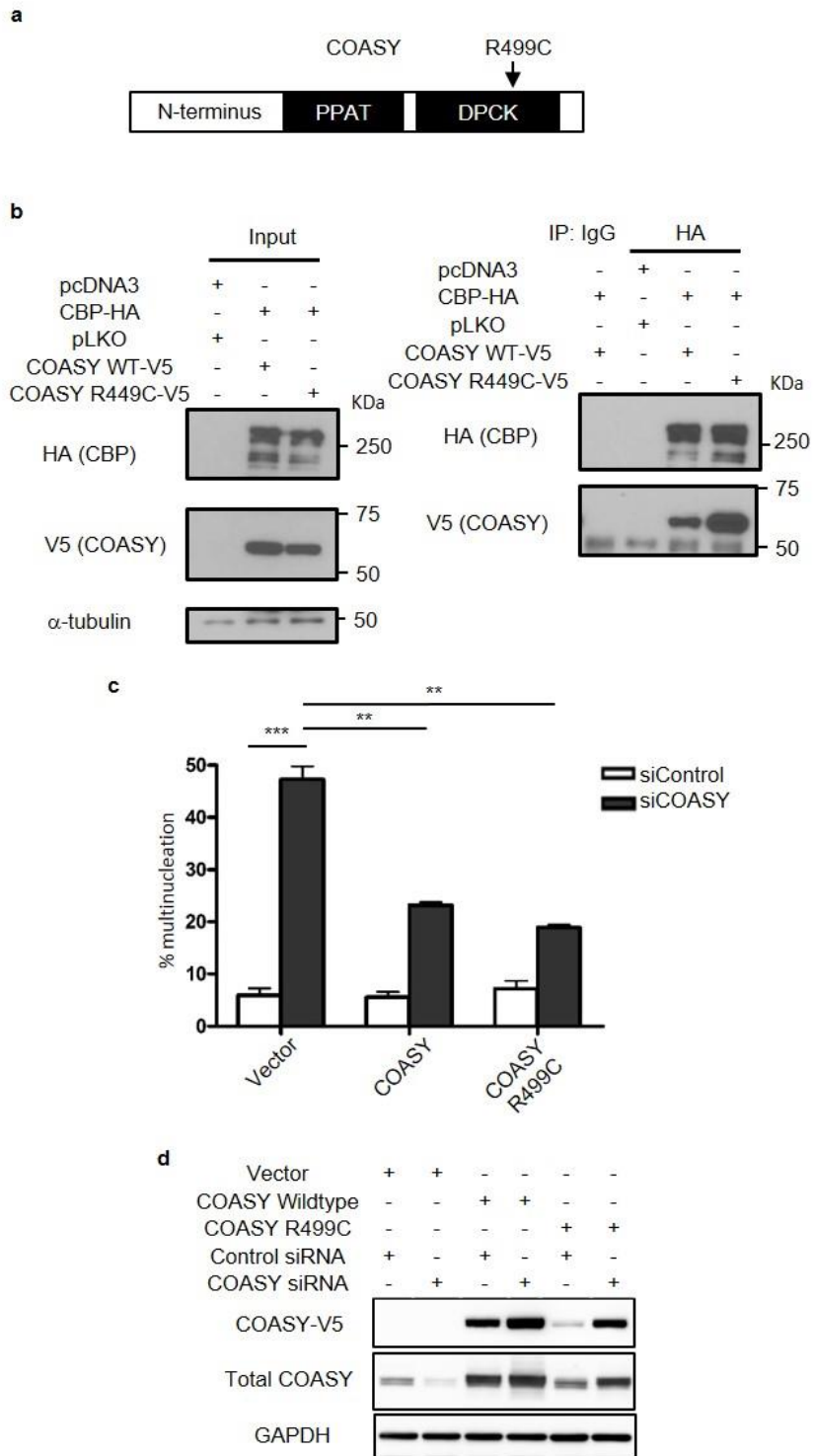


Figure. 22 Both wild and R499C of COASY cDNAs rescued multinucleation.

To further distinguish which domain of COASY contributes to the multinucleation phenotype, we generated V5-tag expression constructs for the three functional domains in COASY protein (N terminus, PPAT and DPCK) and compared their ability to rescue the multinucleation under COASY knockdown (Fig. 23a). While all three constructs result in comparable protein expression based on V5 tag (Fig. 23b, left panel), only the PPAT, but not N-terminal or DPCK, was able to rescue the multinucleation defects induced by COASY knockdown (Fig. 23a). Next, we compared the ability of these domains in their physical interaction with CBP by co-immunoprecipitation assay. We immunoprecipitated HA-CBP and probed with different COASY domains using V5 antibody. Consistent with multinucleation rescue phenotype (Fig. 23a), we found that only PPAT, but not N-terminal and DPCK, strongly interacted with CBP. (Fig. 23b, right panel).

Figure 23 PPAT domain rescued multinucleation and interacted with CBP. **a** Overexpression of PPAT rescued the multinucleation induced by COASY knockdown. * $p < 0.05$, ** $p < 0.01$, two-tailed Student's t-test, $n = 3$ independent repeats. **b** PPAT and CBP showed strong interaction. The cDNA of N-terminus domain, PPAT or DPCK were cotransfected with CBP cDNA to HEK-293T cells. The cells were then enriched in mitosis by nocodazole treatment and harvested for co-immunoprecipitation.

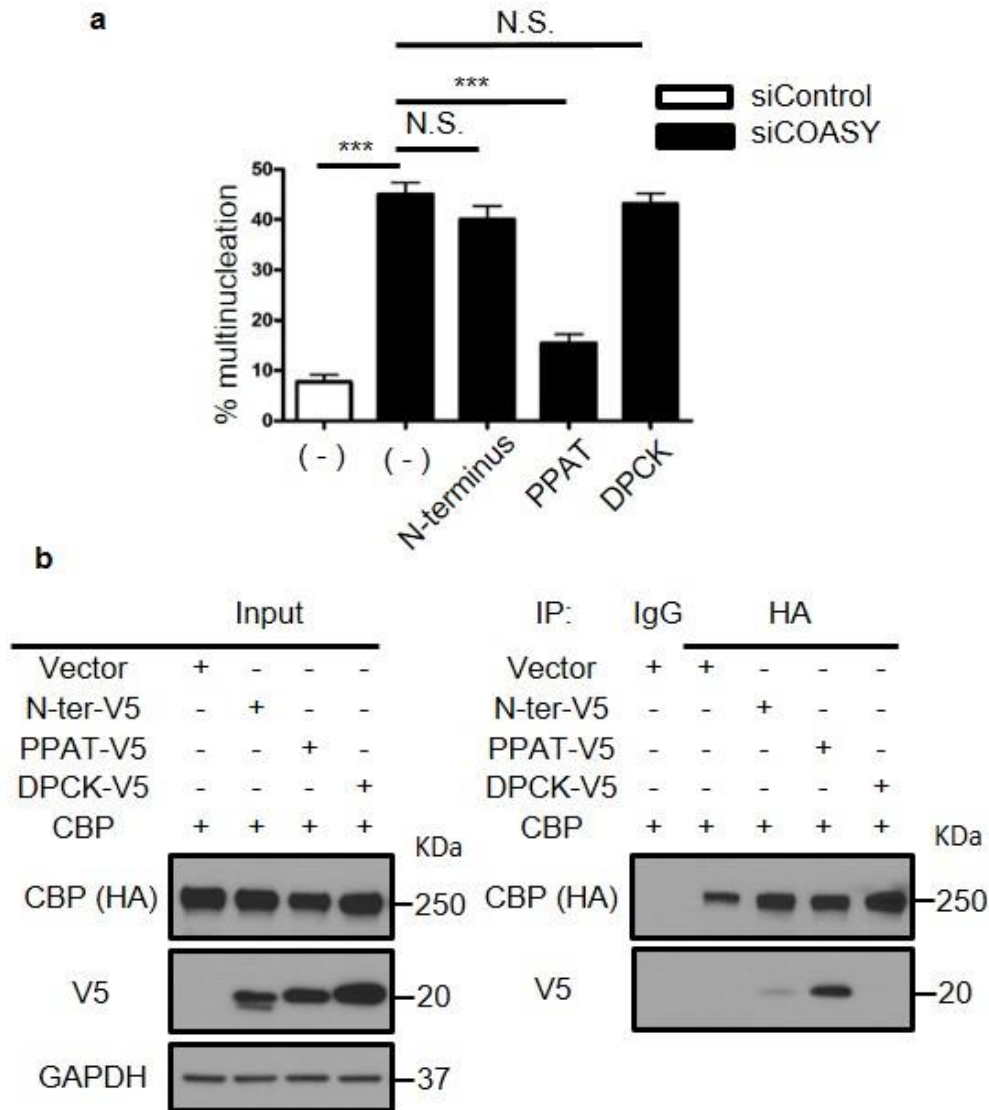


Figure 23 PPAT domain rescued multinucleation and interacted with CBP.

We next examined whether the re-introduction of intact COASY or PPAT, DPCK domain could disrupt CBP-mediated TPX2 protein stabilization previously shown in Fig.13 (Fig. 24a-d). Full-length COASY, PPAT or DPCK domain was cotransfected with V5 tagged TPX2 and CBP cDNA in HEK-293T cells. After 24 hours of incubation, TPX2

expression was translationally inhibited by cycloheximide. The efficiency of CBP-mediated TPX2 protein stabilization was then assessed by monitoring TPX2 degradation. Overexpression of full-length COASY successfully reverse the CBP-dependent TPX2 stabilization (Fig. 24a). Intriguingly, PPAT, but not PDCK domain, was sufficient to disrupt TPX2 stabilization (Fig. 24b, c). Taken together, these data indicate that PPAT domain of COASY associates with CBP and regulates TPX2 protein stabilization to ensure mitotic fidelity.

Figure 24 Both COASY and PPAT, but not DPCK, promote the degradation of TPX2 protein. COASY (a), PPAT (b), DPCK (c) was cotransfected with CBP and V5 tagged TPX2 into unsynchronized HEK-293T cells. After 24 hours, the protein synthesis of the transfected cells were halted with 25 mg/ml cycloheximide and collected at the indicated times for Western blots. The TPX2 protein level at indicated time points was quantified by Image J software and normalized to b-tubulin protein level. Two-way ANOVA: $p < 0.0001$ (a). $p < 0.0001$ (b). N. S. (c) . Bonferroni post hoc tests, $*p < 0.05$, $***p < 0.001$. $n = 3$ independent repeats. Bars show standard error of the mean. **d** V5 tagged PPAT, DPCK and COASY cDNA were expressed with expected size in HEK-293T cells

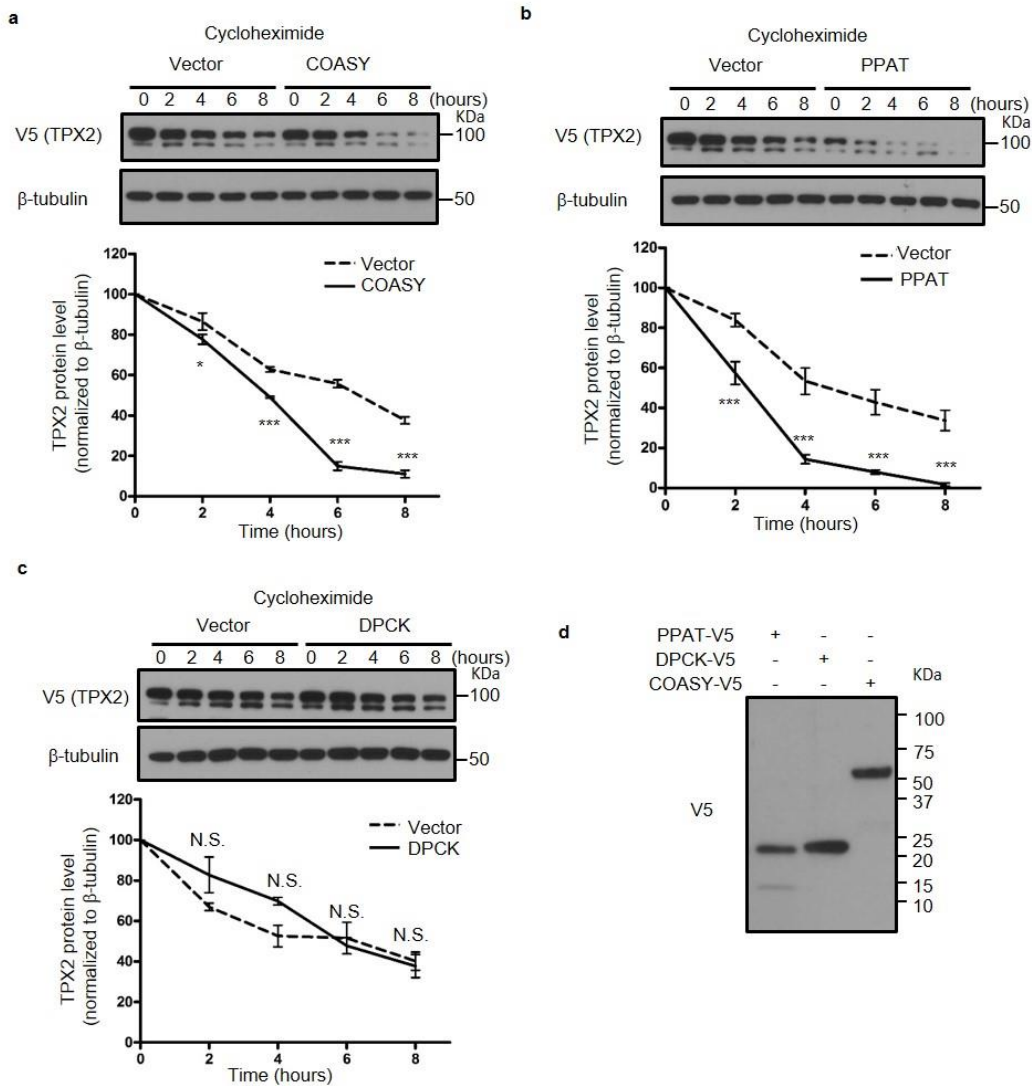


Figure 24 Both COASY and PPAT, but not DPCK, promote the degradation of TPX2 protein.

COASY encodes the last enzyme in the multi-step steps during *de novo* synthesis of CoA from pantothenate acid (Vitamin B5)(Zhyvolou et al., 2002). To further determine the role of CoA synthesis pathway in the multi-nucleation phenotypes observed with COASY knockdown, we used siRNAs to inhibit other upstream enzymes in the CoA

biosynthesis pathway, including Pantothenate Kinases (PANKs) and Phosphopantothenoylcysteine Decarboxylase (PPCDC) (Fig 25a-d). Neither PANKs nor PPCDC siRNAs triggered TPX2 upregulation or similar multi-nucleation phenotypes seen with COASY knockdown (Fig 25e, f). Collectively, the data suggests that COASY regulates CBP activities and mitotic fidelity through a mechanism independent of CoA levels. However, we still cannot completely rule out the relevance of enzymatic activities in the CBP regulation.

Figure 25 Silencing of enzymes upstream of COASY did not lead to TPX2 upregulation and multinucleation **a** A simplified chart of the enzymes involved in CoA biosynthesis that include pantothenate kinase (PANK), phosphopantothenoylcysteine synthetase (PPCS), Phosphopantothenoylcysteine Decarboxylase (PPCDC) and COASY A549 cells were treated pooled siRNAs that targeted COASY, PANKs and PPCDC for 72 hours. **b-d** Real-time PCR was performed to validate the efficient knockdown of PANK1 (**b**), PANK2 (**c**) and PPCDC (**d**) by respective siRNAs. PANK siRNA is a mixture of siRNA that targets both PANK1 and PANK2. **e, f** Inhibition of two upstream enzymes of CoA biosynthesis, PANKs and PPCDC, was unable to induce TPX2 upregulation (**e**) and multinucleation (**f**). N.S. not significant, *** $p < 0.001$, two-tailed Student's t-test, $n=3$ independent repeats. Bars show standard error of the mean.

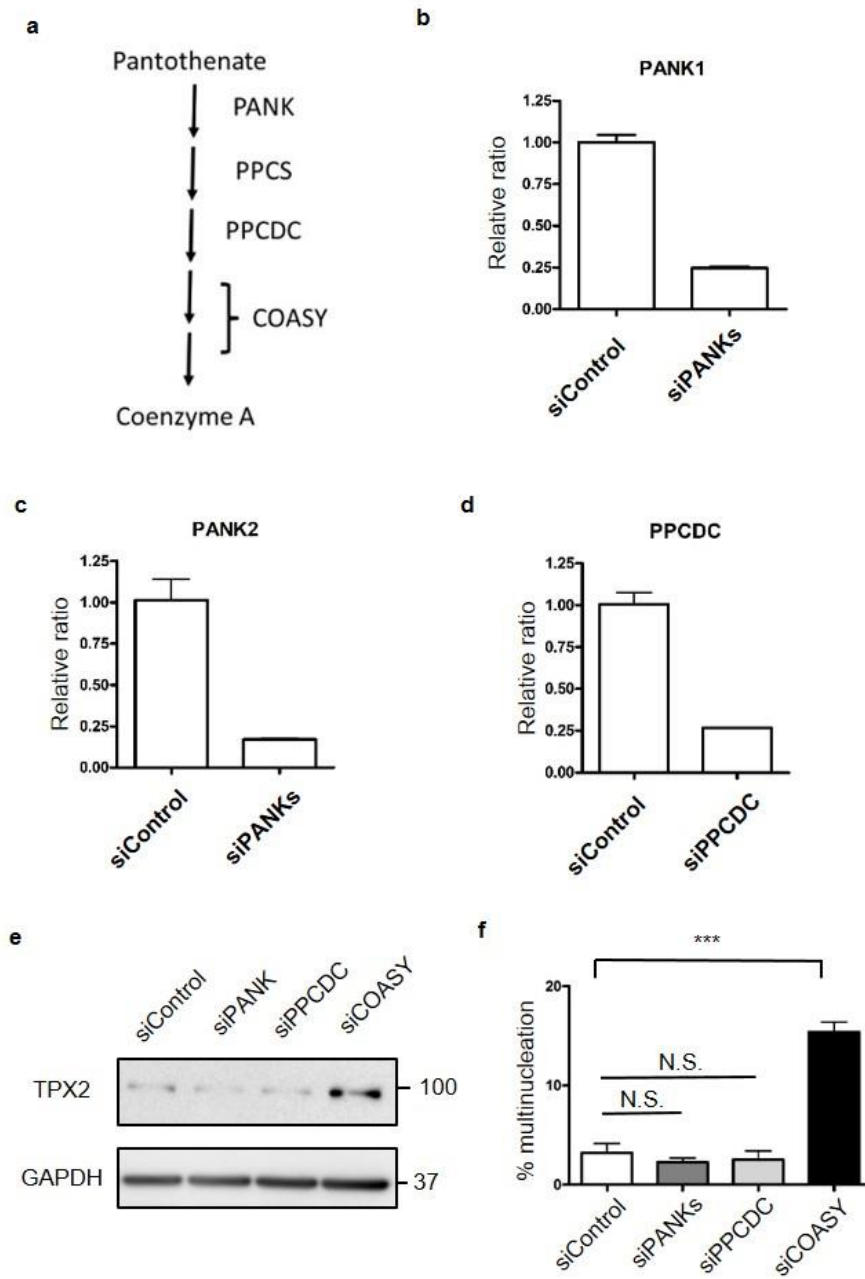


Figure 25 Silencing of enzymes upstream of COASY did not lead to TPX2 upregulation and multinucleation

2.3.7 Low COASY expression is associated with chemo-resistance and poor outcome in tumor expression datasets

Next, we wish to determine the functional and pathological relevance of COASY expression. We have provided evidence that COASY knockdown triggered CBP-mediated TPX2 upregulation and persistent activation of Aurora A. Given that overexpression of Aurora A was reported to confer resistance to chemotherapeutic agent taxol (Anand et al., 2003), we speculated that low COASY expression can lead to taxol resistance. To test this possibility, we transfected control or COASY siRNA in MDA-MB-231 cells and exposed these cells to a dose-titration of taxol. Indeed, we found that COASY siRNA led to significant resistance of MDA-MB-231 cells to taxol (Supplementary Fig. 7a). Next, we examined whether COASY expression in primary tumors was associated with different clinical outcome in breast cancer cohorts using prognostic database PROGgene V2 (Goswami and Nakshatri, 2014). We found that lower level of COASY in primary tumor was associated with poor clinical outcomes in the Enerly and Steinfeld dataset (GSE19783) (Enerly et al., 2011) (Supplementary Fig. 7b). The Loi dataset (GSE6532) (Loi et al., 2007) and Jonsdottir dataset (GSE46563) (Jonsdottir et al., 2014) also revealed that lower expression of COASY was correlated with decreased time to metastases (Supplementary Fig. 7c, d). Together, these data suggest the strong correlation of reduced COASY expression level with taxol resistance and poor clinical outcome of cancer patients.

Figure 26 Low COASY expression is associated with poor outcome

a COASY knockdown rendered MDA-MB-231 cells resistant to treatment of indicated levels of taxol. Relative cell viability was measured by CellTiter-Glo assay (Promega). Two-way ANOVA: $p < 0.0001$. Bonferroni post hoc tests, $***p < 0.001$. $n = 3$ independent repeats. **b-d** Low COASY expression in human tumors is correlated with decreased survival and metastasis. Breast cancer patients were bifurcated into high and low COASY expression groups by the median of COASY expression in the primary breast tumors and their clinical outcomes were compared by Kaplan-Meier analysis in overall survival in the Enerly and Steinfeld dataset (GSE19783) (**b**), metastasis-free survival in the Loi dataset (GSE6532) (**c**), metastasis-free survival in the Jonsdottir dataset (GSE46563) (**d**).

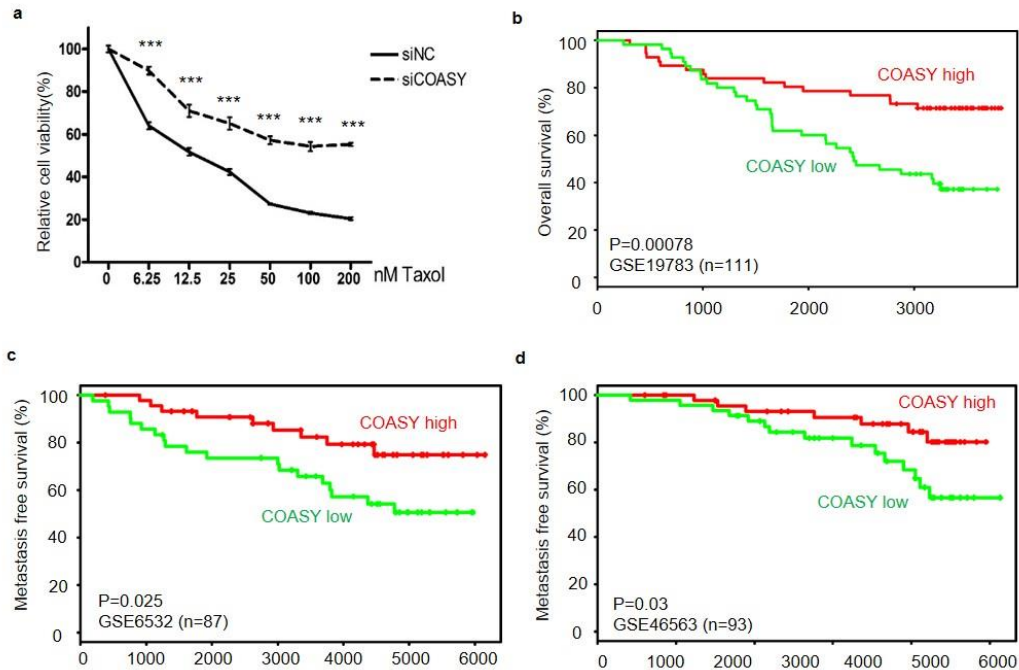


Figure 26 Low COASY expression is associated with poor outcome

Collectively, our results strongly support the stage-specific COASY-CBP association during mitosis regulates CBP-dependent TPX2 protein acetylation and abundance. This novel interaction and regulation ensure the precise modulation of Aurora A kinase and other mitotic components, and eventually result in proper mitotic progression (Fig. 27). In early mitosis, CBP facilitates the TPX2 acetylation to reduce ubiquitination and stabilizes TPX2. At mitotic exit, COASY is relocalized to spindle microtubules and associates with CBP to inhibit acetyl-transferase activities. The stage-specific CBP inactivation destabilizes TPX2 and results in the sharp decline of TPX2 level to allow mitotic exit. Thus, COASY knockdown leads to the CBP overactivation of CBP,

hyper-acetylation and accumulation of TPX2, resulting in the mitotic defects and multi-nucleation.

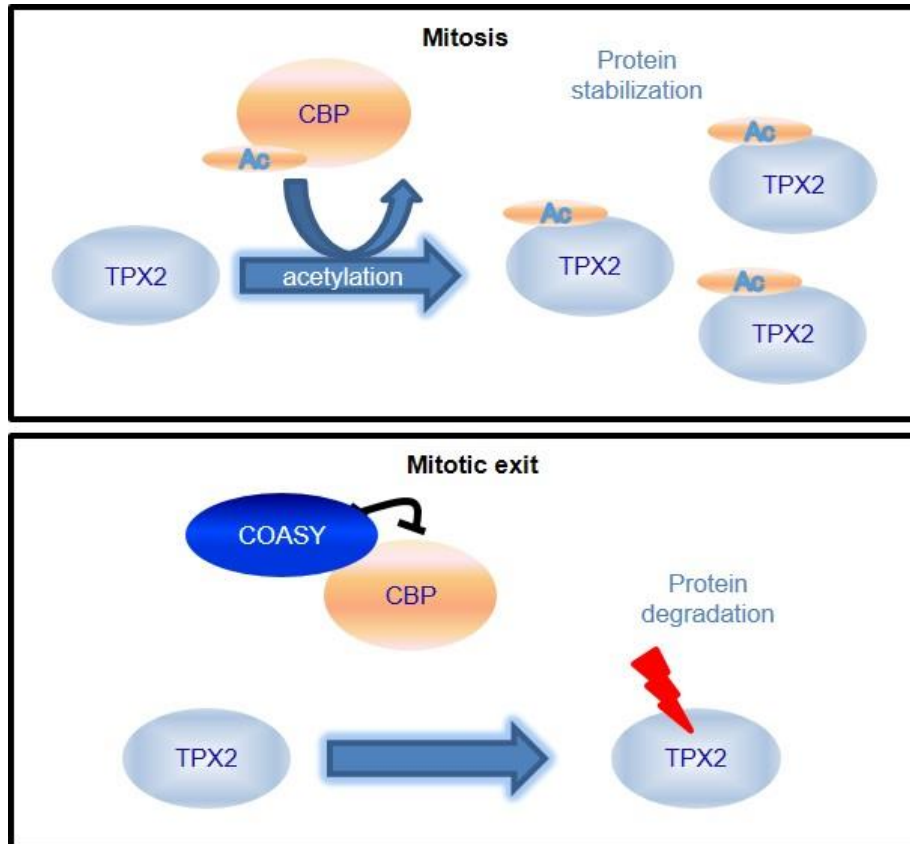


Figure. 27 Schematic illustration of the COASY-CBP-TPX2 model

Together, the experimental data and proposed model provides a conceptual framework of stage-specific COASY-CBP disassociation and association regulates the precise timing of TPX2 accumulation and degradation during mitosis.

3. RIP3 upregulation of the recurrent breast cancers lead to collateral vulnerability

In this chapter, Primary and recurrent breast tumor cell lines were isolated and expanded from Alvarez lab at Duke University. The raw data of microarray between two primary and two recurrent breast tumor cell lines was also provided by Dr. James Alvarez.

3.1 Introduction

In this chapter, we report that recurrent tumor cells, when comparing to primary tumor cells, are extremely sensitive to programmed necrosis triggered by cystine deprivation. Gene expression analysis revealed that RIPK3 expression is dramatically increased in recurrent tumor cells, which contribute to the profound cystine addiction within recurrent tumors. Unexpectedly, RIPK3 overexpression also rendered recurrent tumor cells to grow slower with mitotic defects, suggesting the potential role of RIPK3 in regulating the execution of mitosis. Further investigating is still required to depict the overall mechanism.

3.2 Materials and Methods

3.2.1 Cell culture

Primary and recurrent MTB/TAN tumor cells described previously (Moody et al., 2005) were cultured in Dulbecco's modified Eagle's medium (DMEM; GIBCO-11995) supplemented with 10% fetal bovine serum and 1 × antibiotics (penicillin, 10,000 UI/ml and streptomycin, 10,000 UI/ml). For primary cells, 10 ng/ml EGF, 5 µg/ml insulin, 1 µg/ml hydrocortisone, 5 µg/ml prolactin, 1 µM progesterone and 2 µg/ml doxycycline were added to the media to maintain HER2/neu expression. For recurrent cells, 10 ng/ml EGF and 5 µg/ml insulin were added to the media. Both primary and recurrent cell lines were maintained in a humidified incubator at 37°C and 5% CO₂.

3.2.2 ShRNA and lentivirus infections

RIPK3 shRNA targeting mouse RIPK3 RNA were purchase from Sigma (TRCN0000022536, TRCN0000424625). Lentivirus expressing RIPK3 shRNA was generated by transfecting HEK-293T cells in 6 well plate with a 1: 0.1: 1 ratio of pMDG2: pVSVG: pLKO.1 with TransIT-LT1 transfection reagent (Mirus). After filtering through 0.45 µm of cellulose acetate membrane (VWR, 28145-481), lentivirus (250 ul) were added to a 60mm dish of recurrent cells with polybrene (8ug/ml). After 24 hours of incubation, recurrent cells were further selected with puromycin (5 µg/ml) to increase knockdown efficiency.

3.2.3 Western blots

Primary and recurrent tumor cell lines were harvested and washed once with ice cold PBS. The samples were then resuspended in NP-40 buffer with protease and phosphatase inhibitors and lysed by incubating in at 4°C with constant vortex for 30min, then spun down at 13000 rpm for 10 min at 4°C. Supernatant was transferred to another tube, and protein concentration was measured by BCA protein assay kit (#23225, ThermoFisher). Around 20 ug of protein was loaded on 8% SDS-PAGE gels, transferred to PDVF membrane, blocked with 5% non-fat milk in 1xTBST, incubated with primary antibodies overnight at 4°C. Primary antibodies: RIPK3 (1:1000, sc-374639, Santa Cruz); GAPDH (1:2000, sc-25778, Santa Cruz); Phospho-MLKL (Ser345) (1:1000, #62233, Cell signaling); MLKL(1:1000, #28640, Cell signaling).

3.2.4 Quantitative real-time PCR

RNA from the samples was extracted by the RNeasy Mini Kit (Qiagen) following the manufacturer's protocol. RNA was reverse transcribed to cDNA by random hexamers and SuperScript II (Invitrogen). Quantitative real-time PCR was performed following the manufacturer's protocol by using Power SYBR Green PCR Mix (Applied Biosystems) and StepOnePlus Real-time PCR system (Applied Biosystems). Mouse beta-actin

(reference gene) primers: sense, 5'- GGC TGT ATT CCC CTC CAT CG -3', antisense, 5'- CCA GTT GGT AAC AAT GCC ATG T-3'; Mouse RIPK3 primers: sense, 5'- TCT GTC AAG TTA TGG CCT ACT GG-3', antisense, 5'-GGA ACA CGA CTC CGA ACC C-3'. Real-time PCR were performed in triplicate.

3.2.5 Immunofluorescence microscopy

Recurrent tumor cells were washed once with PBS and fixed in 4% paraformaldehyde for 15 min, followed by permeabilization and blocking with 0.2% Triton X-100 and 2% BSA for 15 min. Primary antibodies were incubated with the cells for 1 hour. Immunofluorescence microscopy were performed using EVOS FL cell imaging system (ThermoFisher) or confocal microscope (SP8, Leica). Antibody: apha-tubulin (1:100, sc-32293, Santa Cruz); Alexa Fluor 594 Phalloidin (1:100, A12381, ThermoFisher).

3.3 Results

3.3.1 Recurrent breast tumor cells are unique addicted to exogenous cystine

To study the phenotypic differences and genetic determinants between the primary and recurrent tumors, two pairs of primary and recurrent tumor cells were isolated and expanded from Alvarez lab. Previously, we have found that the TNBC show strong cystine addiction associated with the process of epithelial mesenchymal

features (Tang et al., 2017). For the murine models of breast cancers, the recurrent cells also have prominent mesenchymal features mediated by EMT regulator SNAIL-1 (Moody et al., 2005). Therefore, we tested whether the recurrent breast tumor cells show stronger cystine addiction than the primary breast tumor cells. After treating 2 primary and 2 recurrent cell lines with Cystine deprivation (2.5 μ M of Cystine) in 6 well plate for 16 hours, the cells were fixed with paraformaldehyde (4%) and stained with crystal violet. We found that the recurrent cells, when compared with primary tumor cells, are profoundly sensitive to cystine deprivation (Fig. 28a). A separate experiment of cystine titration reveals that recurrent cells were largely eliminated under 5 μ M of cystine. In contrast, primary cells can still maintain ~50% viability at this level of cystine (Fig. 28b). Since cell membrane rupture is a feature of cell death, we further measured the level of protease release into the media by CytoTox-fluor assay. Indeed, under normal concentration of cystine (200 μ M), both primary and recurrent cell lines showed low signal for protease release, suggesting low level of cell death. With limited level of cystine (2.5 μ M), we found more protease release in recurrent cells, suggesting more cell rupture and cell death (Fig. 28c), consistent with other viability assays.

Figure 28 Mouse recurrent cells are more sensitive to cystine deprivation. (a) Mouse recurrent cells were more sensitive to cystine deprivation when compared to primary cells. Two primary and two recurrent cell lines were incubated in full media (200 μ M) or

cystine-deprived media (2.5 μ M) for 16 hours. The cells were then fixed with paraformaldehyde (4%) for crystal violet staining. (b) Recurrent cells were largely eliminated with 5 μ M of cystine. Primary and recurrent cells were incubated with decreasing level of cystine for 16 hours. The viability were then proportionally measured by ATP level using Celltiter Glo assay. (c) Cystine deprivation induced more protease release in recurrent cells. Primary and recurrent cells were treated with 2.5 μ M of cystine for 16 hours. The media was then harvested for protease measurement.

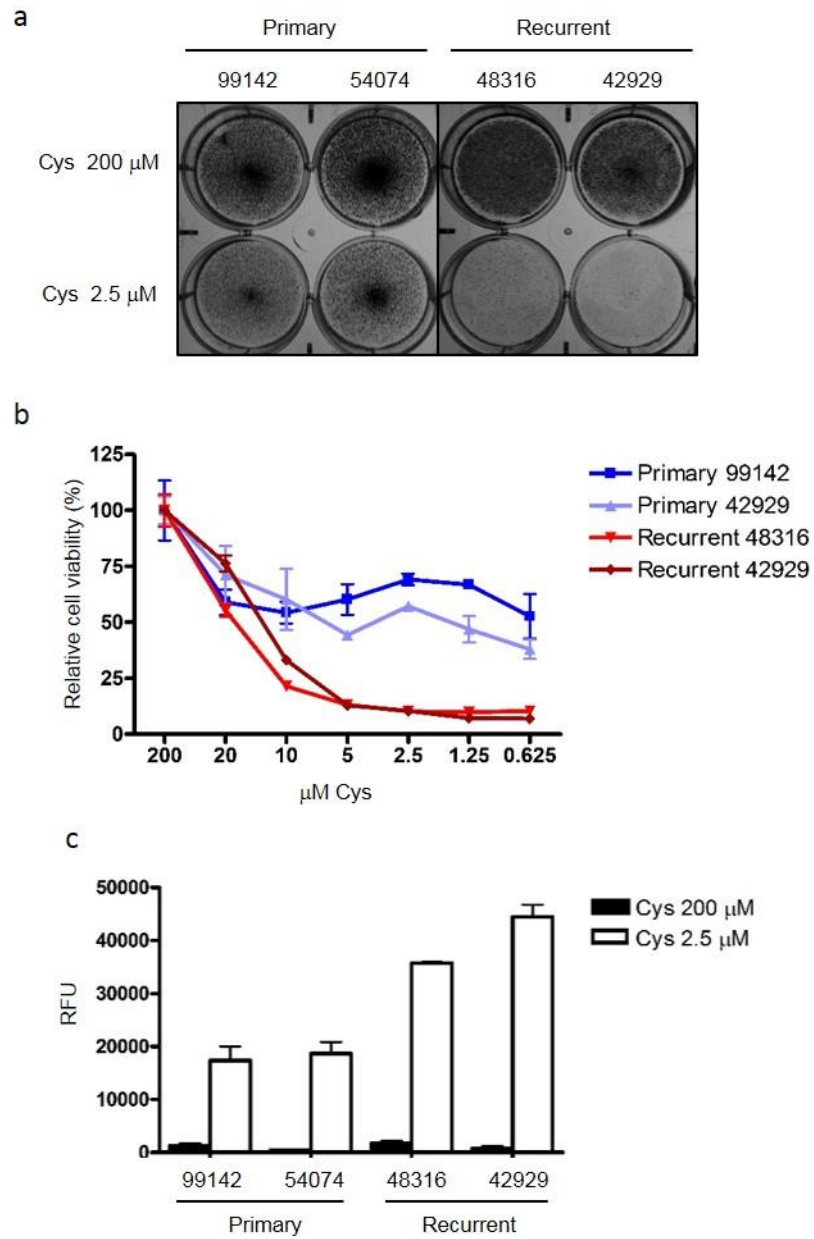


Figure 28 Mouse recurrent cells are more sensitive to Cystine deprivation

In mammalian cells, the outside cystine is uptaken by mammalian cells via the xCT in exchange of the export of glutamate(Lewerenz et al., 2006). The cystine uptake

can be blocked by xCT inhibitors, such as the erastin or sulfasalazine (Dixon et al., 2012; Dolma et al., 2003; Gout et al., 2001). Therefore, we also compared the erastin sensitivities of the 3 primary vs. 3 recurrent breast tumor cells by methods similar to Figure 28. Consistent with Fig 28a, we found recurrent cells, when compared with primary cells, were more sensitive to erastin-induced cell death by crystal violet staining (Fig. 29a). While recurrent tumor cells were largely eliminated between 0.5-1 μ M erastin, the primary cells survived more than 8 μ M of erastin (Fig. 29b). Such recurrent-specific erastin sensitivities are further confirmed by protease release assays (Fig 29c).

Figure 29 Mouse recurrent tumor cells are more sensitive to erastin treatment. (a) Three primary and three recurrent cell lines were incubated in Erastin (1 μ M) or equal amount of DMSO for 18 hours. The cells were then fixed for crystal violet staining. (b) Primary and recurrent cells were treated with increasing indicated doses of erastin for 18 hours and the viability was then then measured by Celltiter Glo assay. (c) Erastin induced more protease release in recurrent cells. Primary and recurrent cells were treated with 1 μ M of Erastin for 16 hours. The media was then harvested for protease measurement.

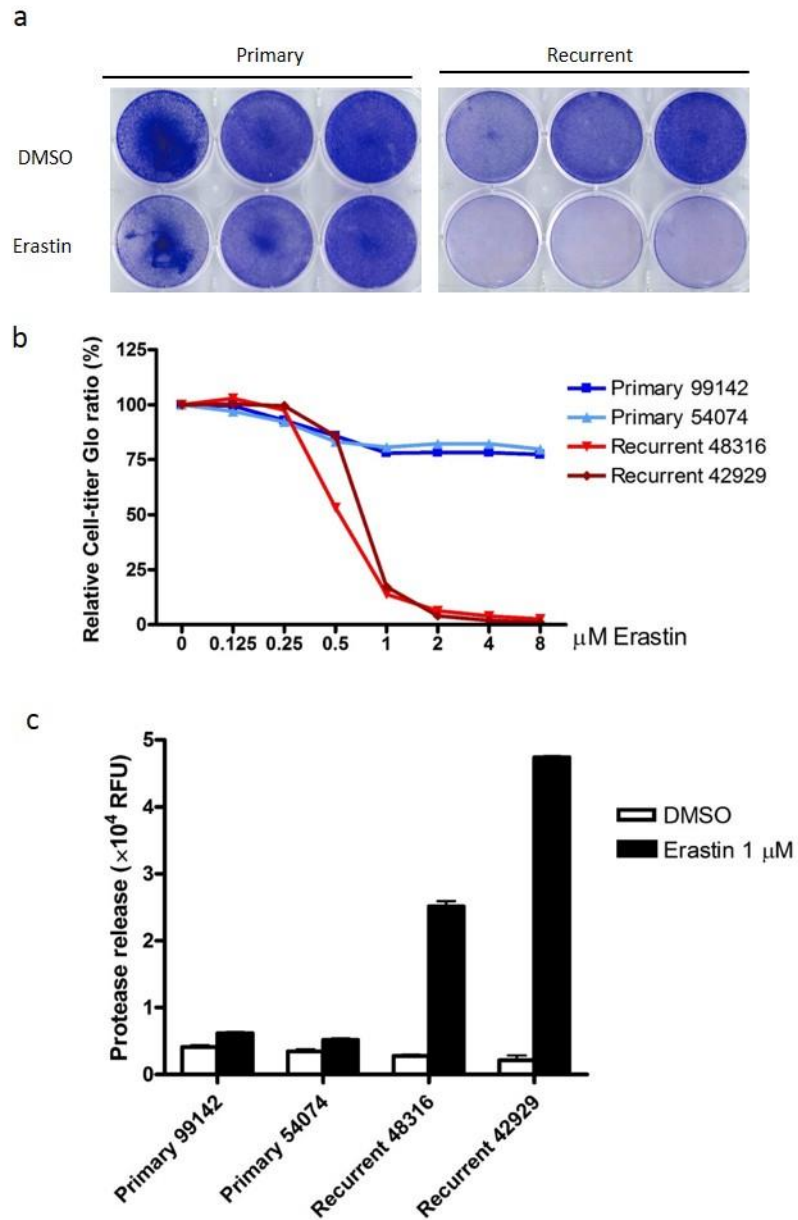


Figure 29 Mouse recurrent cells are more sensitive to Erastin treatment.

Next, we used different inhibitors to define the cell death mechanisms caused by erastin. We found that the apoptosis inhibitor Z-Vad did not rescue the erastin-induced

death. In contrast, both ferrostatin-1 (Skouta et al., 2014) and necrostatin-5 (Wang et al., 2007) robustly rescued the cell death (Fig. 30), indicating the importance of RIPK1-RIPK3 in the cell death.

Figure 30 Erastin-induced cell death was rescued by Nec-5 and Ferrostatin-1. Erastin (2 μ M) were treated at the same time with DMSO, Z-vad (20 μ M), Nec-5 (5 μ M) and Ferrostatin-1 (1 μ M) in recurrent cell lines for 18 hours. The cell viability were then determined by Celltiter Glo assay.

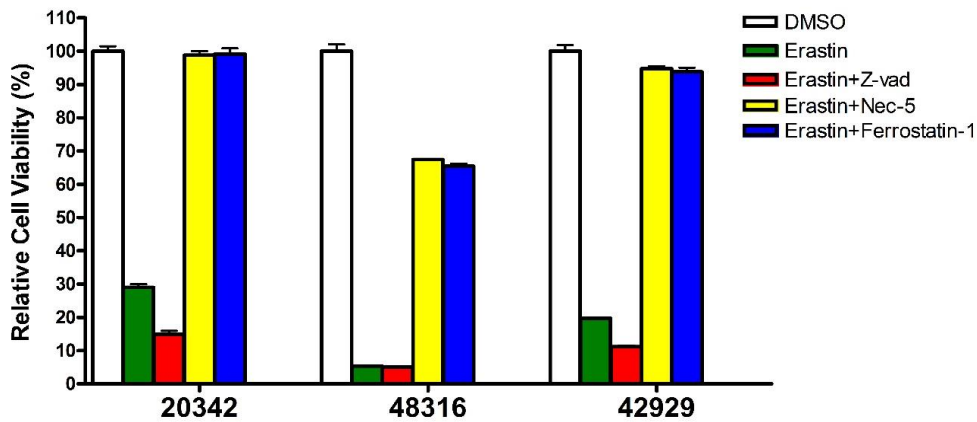


Figure 30 Erastin-induced cell death was rescued by Nec-5 and Ferrostatin-1.

3.3.2 Differential expression of RIPK3 in the recurrent tumor cells and tumors

To identify the expression differences which may account for the recurrence-specific cystine-addiction, we used microarrays to compare the gene expression of

primary and recurrent tumor cells. The gene expression validates the previously reported upregulated expression of Snail-1 (Moody et al., 2005) and repressed PAR-4 (Alvarez et al., 2013) in the recurrent breast tumor cells (Fig 31a). GSEA analysis also shows that the recurrent breast tumors are enriched in the EMT and ROS signaling pathways (Fig 31b). Therefore, these data validate the gene expression differences between the primary and recurrent tumor cells.

Figure 31 Primary and recurrent cell lines are transcriptionally distinct. (a) Heatmap of the transcriptional difference between two primary and two recurrent cell lines. (b) GSEA analysis showed the difference in EMT transition and ROS genesets between primary and recurrent cells.

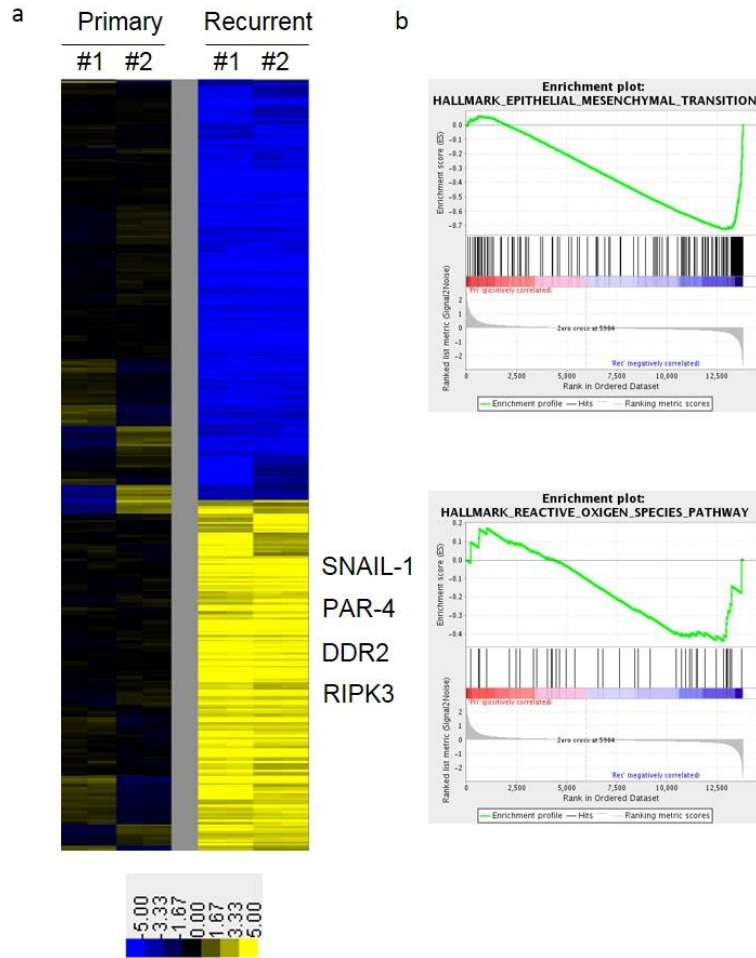


Figure 31 Primary and recurrent cell lines are transcriptionally distinct.

When we examined the expression of genes involved in the cystine-deprived death (Tang et al., 2017; Tang et al., 2016), we noted a consistent and significant over-expression of the RIPK3 in the recurrent tumors cells. In response to the $TNF\alpha$ -induced RIPK1 activation, RIPK3 is activated by RIPK1 to become autophosphorylated, in turn leads to MLKL activation and programmed necrosis. Therefore, RIPK3 over-expression

in the recurrent breast cancer may be of significant interests for the recurrent-specific cystine addiction.

To further investigate RIPK3, we first used real time RT-PCR to validate the exaggerated expression of RIPK3 mRNA in the recurrent tumor cells (Fig 32a). In addition, Western blots reveals that RIPK3 protein is almost entirely absent in the primary cells, but abundantly expressed in the recurrent tumor cells (Fig 32b). Such RIPK3 over-expression is also noted in the panel of mouse recurrent breast tumors, when compared with primary breast tumors (Fig 32c). The absence of RIPK3 protein expression in tumor cells was previously noted and assumed to be death avoid-strategies of tumor cells (Koo et al., 2015) as one of the hallmark of cancers. Therefore, the absence of RIPK3 is consistent with these reports, but the re-expression of RIPK3 in the recurrent tumor cells are quite unexpected.

Figure 32. RIPK3 was highly expressed in recurrent tumor cells. (a) RT-PCR confirmed ~10000 fold of increase in RIPK3 RNA expression in recurrent cells. (b) Western blot showed a robust RIPK3 protein expression in recurrent cell lines. (c) Comparison of RIPK3 RNA expression between 10 primary and 10 recurrent mouse tumor showed an overall increase in recurrent tumors.

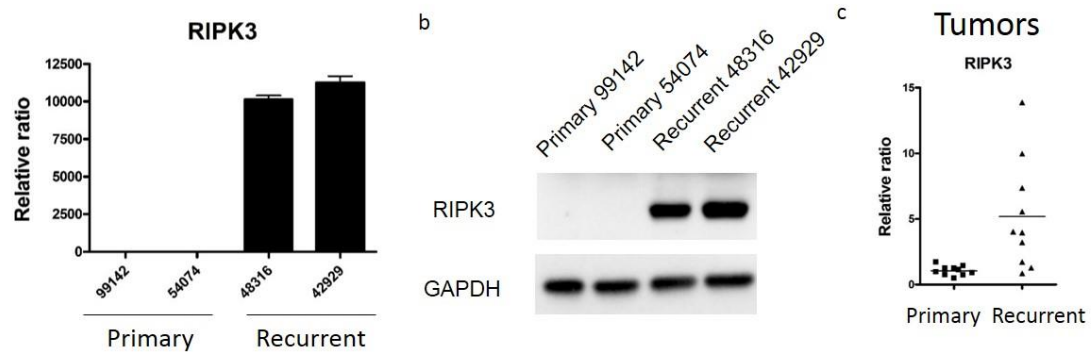


Figure 32. RIPK3 was highly expressed in recurrent tumor cells.

3.3.3 RIPK3 over-expression contribute to the recurrent-specific cystine addiction

Given the previous studies implicating RIPK3-MLKL in the cystine-deprived death(Tang et al., 2016), we speculate that the exaggerated RIPK3 expression may contribute to the cystine addiction of the recurrent tumor cells. First, we found that the silencing of RIPK3 by two shRNAs significantly reduce the cell death triggered by erastin, While erastin (1 μ M) eliminated control recurrent tumor cells to less than 10% cell viability, recurrent tumor cells infected with two different RIPK3 shRNA showed ~70-80% of survival cells (Fig.33a). Similar results were also obtained by crystal violet staining and follow-up quantification (Fig.33b, c). Therefore, the exaggerated RIPK3 expression contributes to the cystine addiction phenotypes of recurrent breast cancers.

Figure 33 RIPK3 over-expression contribute to the recurrent-specific cystine addiction

(a) Silencing of RIPK3 abolished the erastin-induced cell death. Recurrent cells infected with control or two RIPK3 shRNAs were treated with increasing dose of erastin for 16 hours. Cell viability was then measured by Celltiter Glo assay. (b-c) Recurrent cells under control or RIPK3 silencing were treated with 0.5 μ M of erastin for 16 hours before assessing the viability by crystal violet staining (b) and quantification (c).

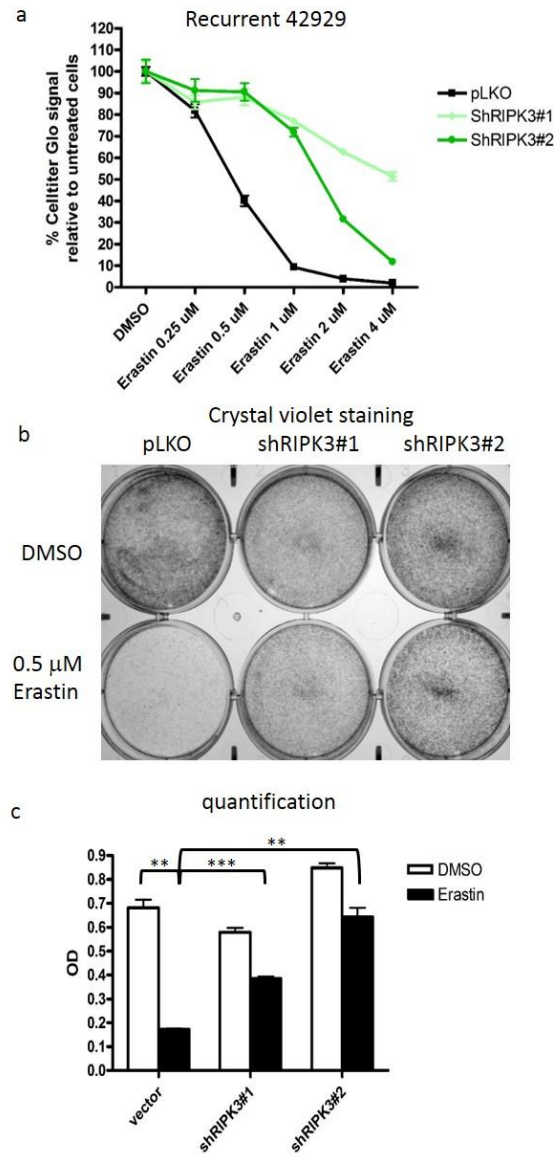


Figure 33 RIPK3 over-expression contribute to the recurrent-specific cystine addiction.

Since the MLKL phosphorylation by RIPK3 leads to the MLKL polymerization necrosis, we inhibited MLKL by necrosulfonamide (NSA) (Sun et al., 2012; Wang et al., 2014) in mouse recurrent cells. , We found NSA was able to rescue the cell death triggered by erastin using either protease release assay (Fig. 34a) or Celltiter Glo assay

(Fig.34b). Therefore, the exaggerated RIPK3 expression and MLKL phosphorylation may determine the sensitivity of mouse recurrent cells to cystine deprivation. Furthermore, we found that the high levels of the RIPK3 in the recurrent cells are associated with the base-line phosphorylation of MLKL (Fig. 34c). The silencing of RIPK3 abolished the MLKL phosphorylation and consistently repressed cystine-deprived death (Fig. 34d). Collectively, the baseline exaggeration of RIPK3 expression leads to the constitutive MLKL phosphorylation and poses the recurrent tumor cells for the cystine-deprived cell death.

Figure 34. MLKL phosphorylation by RIPK3 triggered erastin-induced cell death. (a, b) Inhibiting MLKL by compound inhibitor (NSA, 10 μ M) protected recurrent tumor cells from cell death under erastin treatment (0.5 μ M) when measured by protease release (a) or Celltiter Glo assay (b). (c) The recurrent cells have higher baseline MLKL phosphorylation and posed for cell death. Primary and recurrent cell lines were treated with 2 μ M of Erastin for 12 hours. The cells were then lysed for Western blot with indicated antibodies. (d) RIPK3 silencing abolished MLKL phosphorylation in recurrent tumor cell line. Recurrent cell lines were infected with control vector or two RIPK3 shRNAs for 72 hours. The cells were then lysed for Western blot of indicated proteins.

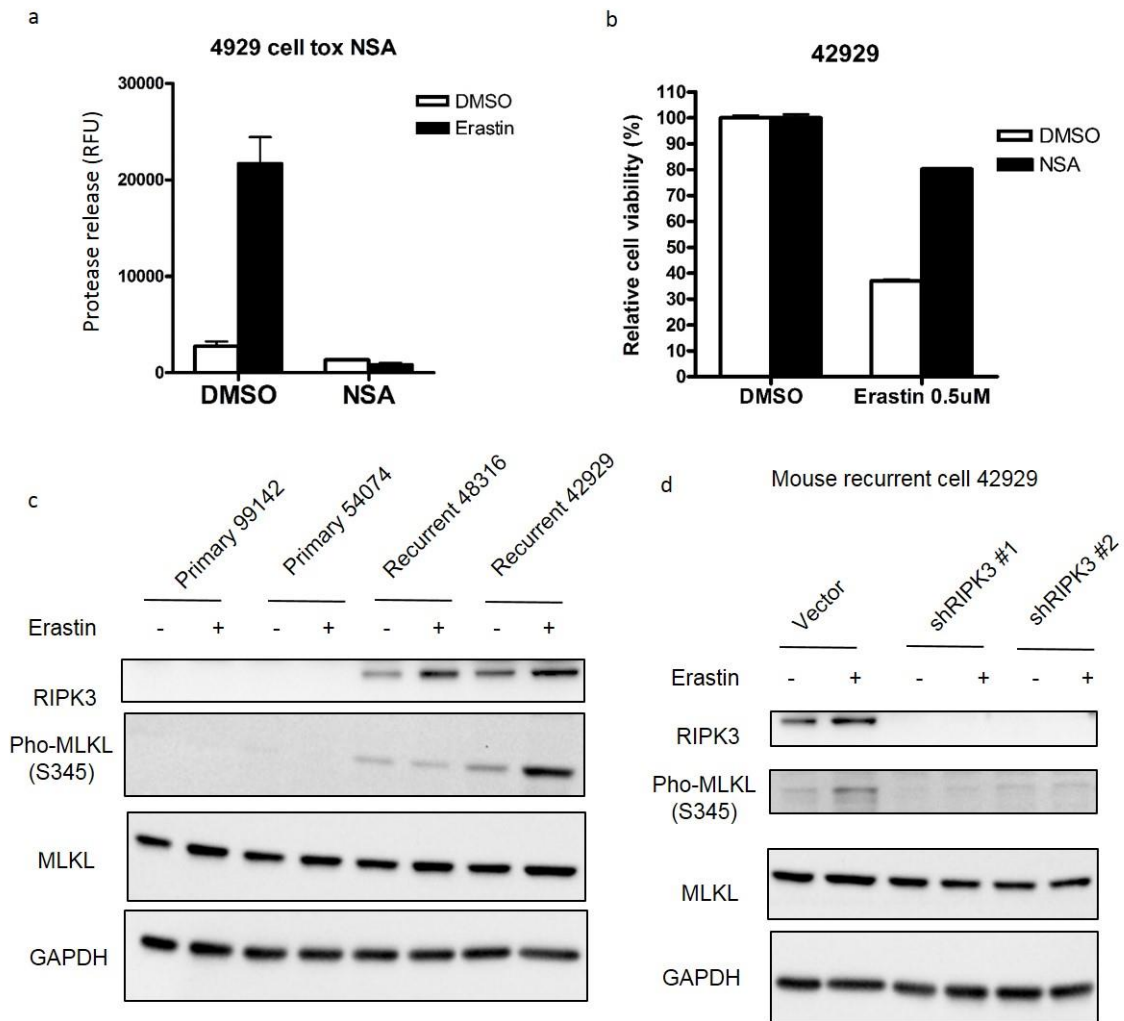


Figure 34. MLKL phosphorylation by RIPK3 triggered erastin-induced cell death.

3.3.4 Functional role of exaggerated RIPK3 in the mitosis of recurrent tumor cells

Given the unexpected exaggerated expression of RIPK3 in the recurrent tumors, we wished to investigate its functional role in recurrent cells. We performed clonogenic assay by plating 500 recurrent tumor cells with or without RIPK3 shRNA. After 10 days

of incubation, we fixed the cells with 4% paraformaldehyde and crystal violet staining (Fig. 35a). We found that RIPK3 knockdown significantly reduced colony formation of the recurrent tumor cells (Fig. 35). In addition, we further examined the effects of RIPK3 knockdown on mitosis using DAPI (nucleus) and Alexa Flour 594 Phalloidin (F-actin) (Fig. 35b). Unexpected, RIPK3 knockdown increased the number of more binucleated recurrent cells (Fig. 35b) as well as chromosome bridges between two daughter cells (Fig. 35c). These data suggests that RIPK3 could be involved in the proper execution of mitosis. However, the mechanisms by which RIPK3 regulates mitosis still require further investigation.

Figure 35. RIPK3 silencing increased mitotic defects in mouse recurrent cells. (a) RIPK3 silencing decreased colony formation. Clonogenic assay was performed by plating 500 recurrent tumor cells to 6 well plates. After 10 days of incubation, cells were fixed with paraformaldehyde (4%) and stained with crystal violet. (b) RIPK3 silencing increased binucleated cells (indicated by arrows). With the sample preparation identical to (a), the cells were stained with DAPI (nucleus) and Alexa Flour 594 Phalloidin (F-actin). The images were taken by immunofluorescence microscopy (EVOS, ThermoFisher). (c) RIPK3 silencing increased the formation of chromosome bridges between two daughter cells. Mouse recurrent tumor cells with/ without RIPK3 silencing were fixed and stained

with DAPI (nucleus), alpha-tubulin and Alexa Fluor 594 Phalloidin (F-actin). The images were then taken by confocal microscopy (Leica SP8).

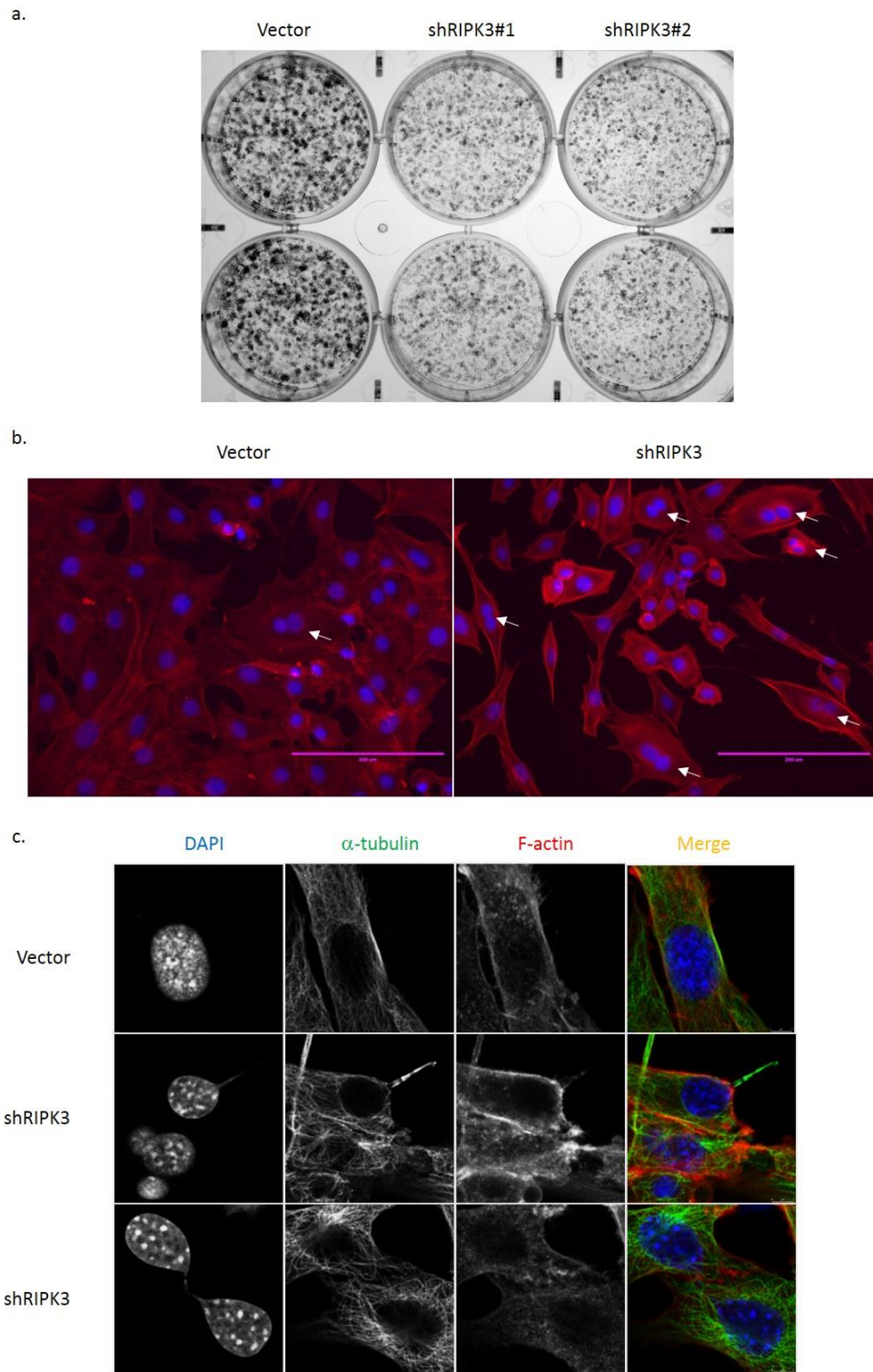


Figure 35. RIPK3 silencing increase mitotic defects in mouse recurrent cells.

4. Discussion and Future directions

Previously, the only known function of COASY is to catalyze phosphorylation of CoA precursor to generate CoA (Zhyvoloup et al., 2002), and most well-known function of RIPK3 is to phosphorylate MLKL (Wang et al., 2014) during the process of necrosis. Given several well-studied kinases, including cyclin dependent kinase 1(CDK1) and CDK2, have been identified to have dozens of protein substrates(Errico et al., 2010), it is not unreasonable to identify novel function and regulatory mechanism of COASY and RIPK3 via non-canonical mechanisms. We therefore provided discussion and proposed future directions with attempt to illuminate this understudied area.

4.1 COASY-CBP-TPX2 ensures faithful mitosis

In mitosis, protein acetylation, compared to protein phosphorylation and ubiquitination, has been an underappreciated layer of regulation. Acetylation on the lysine residues during mitosis have been reported on histones (Kim et al., 2003), cohesion (Terret et al., 2009), and the spindle checkpoint protein BubR1 (Choi et al., 2009). Interestingly, our acetylome analysis upon COASY knockdown revealed a distinct set of hyperacetylated mitotic regulatory proteins, including histone acetyltransferase CBP. Indeed, our data supported a crucial role of over-activation CBP in the dysregulated TPX2 levels and mitotic defect phenotypes caused by COASY knockdown. While CBP is shown to cooperates with APC/C to promote transcription and protein

degradation during mitosis (Turnell et al., 2005), much remains unknown about the regulation and role of the catalytic activities of CBP during mitosis. Our data revealed an unexpected role of CBP, together with COASY, in regulating mitotic progression, at least in part, through orchestrating a tight temporal accumulation and degradation of TPX2 to ensure mitotic fidelity.

The expression of TPX2 is tightly regulated where it promptly accumulates during early mitosis and then undergoes rapid degradation towards mitotic exit (Stewart and Fang, 2005). Our data have revealed a novel regulatory mechanism that the interaction between COASY and CBP cooperatively regulate the initiation and exit of mitotic cycle. During early mitosis, we found that CBP-mediated TPX2 acetylation is important for the TPX2 accumulation. Acetyl-CoA is the essential substrates for CBP-mediated acetylation and the levels of acetate and acetyl-CoA are proposed to serve as energy gauge to allow proliferation (Cai et al., 2011; Comerford et al., 2014). The CBP-mediated TPX2 acetylation and accumulation may be one crucial mechanism by which acetyl-CoA levels are coupled with cellular proliferation. Our results indicate that the sub-cellular localization of COASY is cell cycle-regulated and recruited to spindle microtubules and co-localizes with CBP to regulate its activities toward TPX2. These data indicate that COASY is spatially and temporally regulated to control CBP activities and its downstream target proteins during mitosis. We surmise that, during interphase, COASY is involved in *de novo* CoA synthesis to support the adequate levels of acetyl-

CoA in the cells. However, during mitosis, COASY contributes to the TPX2 degradation essential for mitotic exits by moving to spindle microtubules to associate with CBP and TPX2 to inhibit CBP-mediated TPX2 acetylation. Together, these data suggest a novel mean by which the TPX2 acetylation and levels are regulated by CBP activities and COASY localization during different stages of cell cycle.

During mitosis, nuclear envelope breakdown and chromosome condensation render transcription inactive (Gottesfeld and Forbes, 1997; Johnson and Holland, 1965; Prescott and Bender, 1962; Taylor, 1960). Our findings point out the importance of post-translational modification by COASY-modulated CBP in regulating TPX2 protein and potentially other mitotic proteins found in our acetylome analysis. Since many mitotic and cytokinesis proteins become hyper-acetylated upon COASY knockdown, a broad, coordinated and reversible protein acetylation event may be required during mitosis. Our data strongly suggest a guardian role of COASY for a proper execution of mitosis.

4.2 Inhibition of CoA biosynthesis does not alter global acetylation pattern

Several recent studies suggest that most histone acetyltransferases have similar affinity for CoA and acetyl-CoA. Therefore, CoA can competitively inhibit acetyl-CoA production. Therefore, the acetyl-CoA/CoA ratio, instead of absolute acetyl-CoA levels, may be more relevant determinants of protein acetylation (Galdieri et al., 2014; Pietrocola et al., 2015). In our analysis of COASY-knocked down cells, while both CoA

and acetyl-CoA are lower, the acetyl-CoA/CoA ratio remain unchanged. Consistently, our acetylome analysis revealed that the majority (89%, 955 acetylated /1074 total) of the acetylated peptides were not significantly altered by COASY knockdown. Therefore, COASY knockdown did not lead to global hypo-acetylation. Instead, COASY knockdown altered the acetylation of a specific set of proteins, including CBP and TPX2. These results are consistent with other report that decreasing CoA level in Drosophila or mammalian cells by inhibition of PANK, the upstream enzyme of COASY in CoA biosynthesis pathway, also did not alter the global pattern of protein acetylation(Siudeja et al., 2011). Thus, our results are not inconsistent other studies on the relationship between the level of protein acetylation with cellular CoA and acetyl-CoA abundance.

Instead, our acetylome analysis revealed that COASY knockdown, while reducing cellular CoA and acetyl-CoA, predominantly leads to hyperacetylation of a small subset (9.8%) of total acetylated peptides, including hyperacetylated CBP associated with increased enzymatic activities. We found that COASY controls acetylation, at least in part, by binding and inhibiting acetyltransferase CBP instead of affecting substrate levels. First, the knockdown of COASY, but not other enzymes, in the CoA synthesis pathways, leads to increased TPX2 proteins and multi-nucleation. Second, the enzymatic-deficient mutant of DPCK domain of COASY did not affect the ability to abolish the multi-nucleation phenotypes. Therefore, COASY is likely to regulate CBP through direct interactions instead of affecting substrate levels/availability

for CBP. However, we cannot fully exclude the possible involvement of COASY catalytic activity in regulating CBP, even though the production of CoA per se is not responsible for CBP regulation and multi-nucleation phenotypes. In the future, the structural and functional analysis of COASY will be critical to elucidate the underlying mechanisms of CBP regulation during mitosis.

4.3 Implications of more potential hits in the hyper-acetylated protein network

We have identified the regulatory role of COASY in determining the abundance of TPX2 during mitosis by controlling CBP-mediated acetylation. However, this mechanism could only explain one of the most obvious phenotype of mitotic defects. Acetylome analysis identified many mitotic proteins which have been hyper-acetylated upon COASY knockdown. It is not clear whether the hyper-acetylation of other mitotic protein, beside TPX2, may be involved in other aspects of mitotic dysregulation associated with COASY knockdown. For example, the acetylation cycles of the cohesin complex protein SMC3 at K106 is required for proper sister chromatid cohesion and separation (Beckouet et al., 2010; Zhang et al., 2008). Therefore, the hyperacetylation of SMC3 K106 under COASY knockdown may hinder the de-attachment of kinetochore during mitosis. By comparing the duration of each stage of mitosis between control and COASY knockdown (Fig. 2a), we find that cells under COASY knockdown took 72 min to enter anaphase, while control cells only took 24 min (Fig. 2a). Thus, we can

hypothesize that hyperactive CBP or HBO1 complex under COASY knockdown acetylates SMC3 at K106, which leads to failure of sister chromatid separation. Currently, the only known HAT to acetylate SMC3 for sister chromatid cohesion in human and yeast is Eco1(Zhang et al., 2008). This hypothesis can be tested by knockdown of CBP or HBO1 by siRNA, and monitoring the duration of metaphase by live cell imaging.

Anillin is one of the hyperacetylated proteins under COASY knockdown. Anillin is one of the components of contractile ring localized in the mid-body for the cytokinesis(Piekny and Maddox, 2010). Thus, the hyperacetylation of anillin may reduce the efficiency of cytokinesis that further enhance the mitosis defects associated with COASY knockdown. Since another acetylome analysis also confirmed the increase in anillin acetylation in mitosis(Chuang et al., 2010), it suggests that anillin acetylation may be required for the proper cytokinesis. We can test this hypothesis by knockdown CBP or HBO1 complex and examine whether cytokinesis is affected.

Although additional experiments would be required to assess the impact of these hyperacetylation events, our studies have uncovered a mitotic acetylation network controlled by COASY and CBP. Given CBP acetyltransferase is well studied to be both histone and non-histone acetyltransferase with more than 98 known substrates (Dancy and Cole, 2015), it is reasonable to speculate that COASY could also regulate the acetylation of these CBP mediated acetylated substrates. In addition to CBP, acetylome

analysis also identified COASY knockdown lead to the hyperacetylation of 6 members of another acetyltransferase, HBO1 complex (KAT7, PHF15, PHF16, MEAF6, ING4 and BRPF3). Whether the newly identified acetylation sites on these proteins can determine the acetyltransferase activity of HBO1 under COASY knockdown, requires additional investigation to unveil the underlying regulation network.

4.4 The potential regulatory mechanism of PPAT domain on CBP

Although we have determined the functional domain of COASY in regulating CBP acetyltransferase activity, the molecular mechanism by which the PPAT domain in inhibiting CBP activity can be further addressed. Currently, we hypothesize that the alternative function of COASY PPAT domain is an enzyme which inhibit CBP activity by its AMPylase activity. Using a pan-AMPylated Thr antibody, we found that both purified COASY and CBP are Thr-AMPylated by Western blots. By knockdown or overexpression of COASY in HEK-293T cells, we observed that AMPylated Thr on CBP with COASY expression. In addition, the point mutation in the Thr1427 abolished the AMPylation signals of the CBP. These findings suggest that the PPAT domain of COASY might regulate CBP activity via AMPylation. The definitive confirmation is been investigated by mass spectrometry. When the AMPylated residues are confirmed, *in vitro* AMPylation reactions can be set up with purified PPAT and CBP with point mutants of AMPylation to study the activity and specificity of PPAT domain. These

experiments might provide evidence that CBP activity is regulated by another form of protein modification and potentially the availability of ATP. We are still actively working on several lines of evidence to test this hypothesis and provide the direct mechanisms by which COASY regulated CBP activities.

Next, I want to further discuss about what we have learned from RIPK3 studies and its implications for future directions.

4.5 High RIPK3 expression in recurrent tumor cells determines its sensitivity to programmed necrosis.

Erastin was first identified to be a selective anti-tumor compound targeting human tumor cells with mutations in HRAS, KRAS or BRAF (Yagoda et al., 2007). Follow-up studies indicate that erastin can induce a non-apoptotic form of cell death named ferroptosis (Dixon et al., 2012). Although ferroptosis is considered to be regulated by glutathione peroxidase 4 and independent of RIP1/RIPK3/MLKL-mediated necrosis (Yang et al., 2014), our previous finding has already suggested that low dose of erastin can induce necrosis-mediated cell death (Tang et al., 2016). Consistent with our data, we found that erastin induced cell death in recurrent tumor cells can be rescued by knockdown of RIPK3 or NSA-mediated inhibition of MLKL polymerization (Fig. 33, 34). Furthermore, both Nec-5 and ferrostatin-1 rescued erastin induced cell death (Fig. 30). Therefore, in the primary and recurrent mouse tumor cell lines, these data suggest that

RIPK3 still determines the cell death induced by cystine deprivation or erastin treatment.

4.6 Implication of high RIPK3 expression in recurrent tumor cells

The promoter region of RIPK3 is usually highly methylated in cancer cells, which leads to almost absence of RIPK3 expression (Geserick et al., 2015; Karami-Tehrani et al., 2016; Koo et al., 2015). Since RIPK3 determines necrosis by phosphorylating MLKL (Sun et al., 2012), absence of RIPK3 expression in tumor cells can be considered as adaptation process for tumor cells to evade from signals trigger necrosis. In this study, primary tumor cell indeed showed relatively low RIPK3 expression (Fig. 32). However, after withdrawing of oncogene, the recurrent cell lines showed exaggerating amount of RIPK3 and elevating the basal level of MLKL phosphorylation (Fig.32 and Fig. 34c, d). While tumor recurrence is usually considered incurable, this finding suggest activating RIPK3 mediated necrosis may hold therapeutic potential. However, much remain unknown about the potential advantage of exaggerated RIPK3 for recurrent tumor cells. We found that RIPK3 silencing seems render recurrent cells grow much slower under the stress of low cell density in clonogenic assay (Fig. 35). By confocal microscopy, we found RIPK3 silencing lead to increase of chromosome bridges between two daughter cells after cell division (Fig. 35). These data suggests that high RIPK3 expression may benefit recurrent tumor cells with smooth and productive mitosis under harsh tumor microenvironment. Thus, the collateral vulnerability of RIPK3 mediated necrosis can be

the target by cystine deprivation. These data also points out that RIPK3 may regulate mitosis by a previously undescribed mechanism. However, more investigation is required to establish this hypothesis. Since 3D culture reflect tumor environment better than 2D culture, currently, I am trying to culture the recurrent cell in 3D by Matrigel to understand the advantage of high RIPK3 expression in recurrent tumor cells.

4.7 Potential role of RIPK3 in altering overall expression pattern

Although we have found that RIPK3 expression could be crucial for the proper execution of mitosis in mouse recurrent cells, the detailed mechanism is still needing to be depicted. The most well-known function of RIPK3 is to phosphorylate MLKL and lead to necrosis (Sun et al., 2012). In addition, RIPK3 also regulated the inflammatory genes and play an essential role in the oncogenesis of breast and pancreatic cancer. However, based on the data provided in Fig. 35, we think RIPK3 may have an alternative function in regulating mitosis. RIPK3 has been shown to regulate death domain associated protein (DAXX) by phosphorylation (Lee et al., 2013). DAXX cooperates with α -thalassemia X-linked mental retardation protein (ATRX) to deposit histone H3.3 at heterochromatin to inhibit transcription (Lewis et al., 2010). We therefore hypothesize that RIPK3 may determine transcriptional landscape by regulating DAXX/ATRX-mediated histone H3.3 deposition. We are preparing recurrent tumor cells

with RIPK3 shRNAs for RNA-seq to compare the transcriptional difference and pathways affected by RIPK3 knockdown.

5. Conclusions

The two studies on the non-canonical role of COASY and RIPK3 demonstrate the power of forward genetics to uncover novel genetic elements. Both projects start with the observation of the striking phenotypes associated with COASY and RIPK3. Subsequent mechanistic investigations depict the non-canonical role of two kinases to account for the observed phenotypes. Several interesting questions may result from the non-canonical role of COASY and RIPK3. It would be interesting to further investigate whether and how the canonical roles of these kinases can either enhance or interfere with their respective non-canonical roles. For example, nutrient deprivation is a common feature in the tumor microenvironment (Keenan and Chi, 2015; Lucas et al., 2010; Tang et al., 2017). If the availability of pantothenate (Vitamin B5, the precursor of CoA) can affect the expression level of COASY, pantothenate depletion may reduce COASY expression, in turn, trigger TPX2-Aurora A activation and confer chemo-resistance. Similarly, the translocation of COASY into mitotic spindles to associate with CBP during mitosis may reduce the availability of COASY for the de novo CoA synthesis and reduce the level of CoA, acetyl-CoA and histone acetylation. These hypotheses can be experimentally tested to further elucidate

the regulation of COASY in the CoA synthesis, mitotic progression and nutrient sensing in the future.

Our findings of COASY and RIPK3 may also have therapeutic implications. In terms of COASY-CBP-TPX2 axis, we have found that low COASY expression is associated with poor outcome of patients with breast cancer. Consistently with our findings, many tumors have high levels of Aurora A expression, which contributes to the aneuploidies, chemo-resistance (Anand et al., 2003) and other malignant phenotypes. By the mechanism we found, low COASY expression could promote to CBP hyperactivation, TPX2 overexpression and Aurora A hyperactivation. It is tempting to speculate that pharmacological inhibition of CBP could be used to dampen Aurora A kinase activity in selective tumors. However, since CBP is one of the major acetyltransferases with many other functions, inhibition of CBP could lead to severe side effects. However, chemical compounds which target TPX2 acetylation sites may reduce TPX2 accumulation and Aurora A activation to reduce chemo-resistance. While Aurora A has been tested as therapeutic targets, we envision that further inhibition of TPX2 by small molecule inhibitor may abolish the kinase activity of Aurora A to enhance the efficacy of Aurora A inhibition.

In the RIPK3 study, we have found high RIPK3 expression in recurrent tumor cells. These findings may lead to several possible means to target recurrent breast cancers. First, we can use erastin to target recurrent cells for programmed necrosis. However, erastin shows high toxicities in mice. We are currently testing cysteinase as an alternative strategy to prevent cysteine intake (Cramer et al., 2017) and realize the therapeutic potential. In addition, since we found that RIP3K is also essential for the recurrent breast tumors. RIPK3 inhibitors may also have therapeutic potential to prevent or treat recurrent breast cancers.

The development of small molecules targeting kinases in recent years have provided a large number of effective kinases inhibitors for targeted therapeutics. The majority of these kinase inhibitors were designed to compete with ATP for nucleotide binding site as competitive inhibitors. Depending on the conformation of activation loop on the kinases stabilized by these inhibitors, it may reveal the non-canonical function of kinases. For example, Aurora A is found to stabilize N-Myc by direct binding to prevent N-Myc degradation in neuroblastoma (Otto et al., 2009). This non-enzymatic function of Aurora A is still preserved in the presence of its inhibitor hesperidin, which stabilize the activation loop in the active state. However, when stabilizing in inactive

conformation by MLN8237 or MLN8054, Aurora A-mediated N-Myc degradation is inhibited (Brockmann et al., 2013; Otto et al., 2009). Thus, the development of kinase inhibitors with different strategies may provide us alternative means to investigate the non-canonical function of kinases. Unraveling these non-canonical functions of kinase may reveal novel therapeutic opportunities and help to explain the kinase resistance seen in some tumors.

References

Aggarwal, B.D., and Calvi, B.R. (2004). Chromatin regulates origin activity in *Drosophila* follicle cells. *Nature* 430, 372-376.

Albain, K.S., Allred, D.C., and Clark, G.M. (1994). Breast cancer outcome and predictors of outcome: are there age differentials? *J Natl Cancer Inst Monogr*, 35-42.

Alvarez, J.V., Pan, T.C., Ruth, J., Feng, Y., Zhou, A., Pant, D., Grimley, J.S., Wandless, T.J., Demichele, A., Investigators, I.S.T., *et al.* (2013). Par-4 downregulation promotes breast cancer recurrence by preventing multinucleation following targeted therapy. *Cancer Cell* 24, 30-44.

Anand, S., Penrhyn-Lowe, S., and Venkitaraman, A.R. (2003). AURORA-A amplification overrides the mitotic spindle assembly checkpoint, inducing resistance to Taxol. *Cancer Cell* 3, 51-62.

Avvakumov, N., Lalonde, M.E., Saksouk, N., Paquet, E., Glass, K.C., Landry, A.J., Doyon, Y., Cayrou, C., Robitaille, G.A., Richard, D.E., *et al.* (2012). Conserved molecular interactions within the HBO1 acetyltransferase complexes regulate cell proliferation. *Mol Cell Biol* 32, 689-703.

Bayliss, R., Sardon, T., Vernos, I., and Conti, E. (2003). Structural basis of Aurora-A activation by TPX2 at the mitotic spindle. *Mol Cell* 12, 851-862.

Beckouet, F., Hu, B., Roig, M.B., Sutani, T., Komata, M., Uluocak, P., Katis, V.L., Shirahige, K., and Nasmyth, K. (2010). An Smc3 acetylation cycle is essential for establishment of sister chromatid cohesion. *Mol Cell* 39, 689-699.

Bolanos-Garcia, V.M., and Blundell, T.L. (2011). BUB1 and BUBR1: multifaceted kinases of the cell cycle. *Trends Biochem Sci* 36, 141-150.

Bosveld, F., Rana, A., van der Wouden, P.E., Lemstra, W., Ritsema, M., Kampinga, H.H., and Sibon, O.C. (2008). De novo CoA biosynthesis is required to maintain DNA integrity during development of the *Drosophila* nervous system. *Hum Mol Genet* 17, 2058-2069.

Bowers, E.M., Yan, G., Mukherjee, C., Orry, A., Wang, L., Holbert, M.A., Crump, N.T., Hazzalin, C.A., Liszczak, G., Yuan, H., *et al.* (2010). Virtual ligand screening of the p300/CBP histone acetyltransferase: identification of a selective small molecule inhibitor. *Chem Biol* 17, 471-482.

Boxer, R.B., Jang, J.W., Sintasath, L., and Chodosh, L.A. (2004). Lack of sustained regression of c-MYC-induced mammary adenocarcinomas following brief or prolonged MYC inactivation. *Cancer Cell* 6, 577-586.

Brockmann, M., Poon, E., Berry, T., Carstensen, A., Deubzer, H.E., Rycak, L., Jamin, Y., Thway, K., Robinson, S.P., Roels, F., *et al.* (2013). Small molecule inhibitors of aurora-a induce proteasomal degradation of N-myc in childhood neuroblastoma. *Cancer Cell* 24, 75-89.

Cai, L., Sutter, B.M., Li, B., and Tu, B.P. (2011). Acetyl-CoA induces cell growth and proliferation by promoting the acetylation of histones at growth genes. *Mol Cell* 42, 426-437.

Campeau, E., Ruhl, V.E., Rodier, F., Smith, C.L., Rahmberg, B.L., Fuss, J.O., Campisi, J., Yaswen, P., Cooper, P.K., and Kaufman, P.D. (2009). A versatile viral system for expression and depletion of proteins in mammalian cells. *PLoS One* 4, e6529.

Caron, C., Boyault, C., and Khochbin, S. (2005). Regulatory cross-talk between lysine acetylation and ubiquitination: role in the control of protein stability. *Bioessays* 27, 408-415.

Carrozza, M.J., Utley, R.T., Workman, J.L., and Cote, J. (2003). The diverse functions of histone acetyltransferase complexes. *Trends Genet* 19, 321-329.

Carter, C.L., Allen, C., and Henson, D.E. (1989). Relation of tumor size, lymph node status, and survival in 24,740 breast cancer cases. *Cancer* 63, 181-187.

Cheong, J.W., Jung, H.I., Eom, J.I., Kim, S.J., Jeung, H.K., and Min, Y.H. (2010). Aurora-A kinase inhibition enhances the cytosine arabinoside-induced cell death in leukemia cells through apoptosis and mitotic catastrophe. *Cancer Lett* 297, 171-181.

Chiang, A.C., and Massague, J. (2008). Molecular basis of metastasis. *N Engl J Med* 359, 2814-2823.

Choi, E., Choe, H., Min, J., Choi, J.Y., Kim, J., and Lee, H. (2009). BubR1 acetylation at prometaphase is required for modulating APC/C activity and timing of mitosis. *EMBO J* 28, 2077-2089.

Choudhary, C., Weinert, B.T., Nishida, Y., Verdin, E., and Mann, M. (2014). The growing landscape of lysine acetylation links metabolism and cell signalling. *Nat Rev Mol Cell Biol* 15, 536-550.

Chuang, C., Lin, S.H., Huang, F., Pan, J., Josic, D., and Yu-Lee, L.Y. (2010). Acetylation of RNA processing proteins and cell cycle proteins in mitosis. *J Proteome Res* 9, 4554-4564.

Comerford, S.A., Huang, Z., Du, X., Wang, Y., Cai, L., Witkiewicz, A.K., Walters, H., Tantawy, M.N., Fu, A., Manning, H.C., *et al.* (2014). Acetate dependence of tumors. *Cell* 159, 1591-1602.

Cramer, S.L., Saha, A., Liu, J., Tadi, S., Tiziani, S., Yan, W., Triplett, K., Lamb, C., Alters, S.E., Rowlinson, S., *et al.* (2017). Systemic depletion of L-cyst(e)ine with cyst(e)inase increases reactive oxygen species and suppresses tumor growth. *Nat Med* 23, 120-127.

D'Cruz, C.M., Gunther, E.J., Boxer, R.B., Hartman, J.L., Sintasath, L., Moody, S.E., Cox, J.D., Ha, S.I., Belka, G.K., Golant, A., *et al.* (2001). c-MYC induces mammary tumorigenesis by means of a preferred pathway involving spontaneous Kras2 mutations. *Nat Med* 7, 235-239.

Dancy, B.M., and Cole, P.A. (2015). Protein lysine acetylation by p300/CBP. *Chem Rev* 115, 2419-2452.

Davies, M.N., Kjalarsdottir, L., Thompson, J.W., Dubois, L.G., Stevens, R.D., Ilkayeva, O.R., Brosnan, M.J., Rolph, T.P., Grimsrud, P.A., and Muoio, D.M. (2016). The Acetyl Group Buffering Action of Carnitine Acetyltransferase Offsets Macronutrient-Induced Lysine Acetylation of Mitochondrial Proteins. *Cell Rep* 14, 243-254.

Deardorff, M.A., Bando, M., Nakato, R., Watrin, E., Itoh, T., Minamino, M., Saitoh, K., Komata, M., Katou, Y., Clark, D., *et al.* (2012). HDAC8 mutations in Cornelia de Lange syndrome affect the cohesin acetylation cycle. *Nature* 489, 313-317.

DePamphilis, M.L. (2003). The 'ORC cycle': a novel pathway for regulating eukaryotic DNA replication. *Gene* 310, 1-15.

Dixon, S.J., Lemberg, K.M., Lamprecht, M.R., Skouta, R., Zaitsev, E.M., Gleason, C.E., Patel, D.N., Bauer, A.J., Cantley, A.M., Yang, W.S., *et al.* (2012). Ferroptosis: an iron-dependent form of nonapoptotic cell death. *Cell* 149, 1060-1072.

Dolma, S., Lessnick, S.L., Hahn, W.C., and Stockwell, B.R. (2003). Identification of genotype-selective antitumor agents using synthetic lethal chemical screening in engineered human tumor cells. *Cancer Cell* 3, 285-296.

Doyon, Y., Cayrou, C., Ullah, M., Landry, A.J., Cote, V., Selleck, W., Lane, W.S., Tan, S., Yang, X.J., and Cote, J. (2006). ING tumor suppressor proteins are critical regulators of chromatin acetylation required for genome expression and perpetuation. *Mol Cell* 21, 51-64.

Droge, W. (2005). Oxidative stress and ageing: is ageing a cysteine deficiency syndrome? *Philos Trans R Soc Lond B Biol Sci* 360, 2355-2372.

Dusi, S., Valletta, L., Haack, T.B., Tsuchiya, Y., Venco, P., Pasqualato, S., Goffrini, P., Tigano, M., Demchenko, N., Wieland, T., *et al.* (2014). Exome sequence reveals mutations in CoA synthase as a cause of neurodegeneration with brain iron accumulation. *Am J Hum Genet* 94, 11-22.

Duyndam, M.C., van Dam, H., Smits, P.H., Verlaan, M., van der Eb, A.J., and Zantema, A. (1999). The N-terminal transactivation domain of ATF2 is a target for the co-operative activation of the c-jun promoter by p300 and 12S E1A. *Oncogene* 18, 2311-2321.

Edgar, B.A., and Lehner, C.F. (1996). Developmental control of cell cycle regulators: a fly's perspective. *Science* 274, 1646-1652.

Elston, C.W., and Ellis, I.O. (1991). Pathological prognostic factors in breast cancer. I. The value of histological grade in breast cancer: experience from a large study with long-term follow-up. *Histopathology* 19, 403-410.

Enerly, E., Steinfeld, I., Kleivi, K., Leivonen, S.K., Aure, M.R., Russnes, H.G., Ronneberg, J.A., Johnsen, H., Navon, R., Rodland, E., *et al.* (2011). miRNA-mRNA integrated analysis reveals roles for miRNAs in primary breast tumors. *PLoS One* 6, e16915.

Errico, A., Deshmukh, K., Tanaka, Y., Pozniakovsky, A., and Hunt, T. (2010). Identification of substrates for cyclin dependent kinases. *Adv Enzyme Regul* 50, 375-399.

Esserman, L.J., Moore, D.H., Tsing, P.J., Chu, P.W., Yau, C., Ozanne, E., Chung, R.E., Tandon, V.J., Park, J.W., Baehner, F.L., *et al.* (2011). Biologic markers determine both the risk and the timing of recurrence in breast cancer. *Breast Cancer Res Treat* 129, 607-616.

Eyers, P.A., and Maller, J.L. (2004). Regulation of *Xenopus* Aurora A activation by TPX2. *J Biol Chem* 279, 9008-9015.

Foy, R.L., Song, I.Y., Chitalia, V.C., Cohen, H.T., Saksouk, N., Cayrou, C., Vaziri, C., Cote, J., and Panchenko, M.V. (2008). Role of Jade-1 in the histone acetyltransferase (HAT) HBO1 complex. *J Biol Chem* 283, 28817-28826.

Fu, J., Bian, M., Jiang, Q., and Zhang, C. (2007). Roles of Aurora kinases in mitosis and tumorigenesis. *Mol Cancer Res* 5, 1-10.

Galdieri, L., Zhang, T., Rogerson, D., Lleshi, R., and Vancura, A. (2014). Protein acetylation and acetyl coenzyme a metabolism in budding yeast. *Eukaryot Cell* 13, 1472-1483.

Garcia-Ruiz, C., and Fernandez-Checa, J.C. (2007). Redox regulation of hepatocyte apoptosis. *J Gastroenterol Hepatol* 22 *Suppl* 1, S38-42.

Geserick, P., Wang, J., Schilling, R., Horn, S., Harris, P.A., Bertin, J., Gough, P.J., Feoktistova, M., and Leverkus, M. (2015). Absence of RIPK3 predicts necroptosis resistance in malignant melanoma. *Cell Death Dis* 6, e1884.

Goldhirsch, A., Glick, J.H., Gelber, R.D., Coates, A.S., Thurlimann, B., Senn, H.J., and Panel, m. (2005). Meeting highlights: international expert consensus on the primary therapy of early breast cancer 2005. *Ann Oncol* 16, 1569-1583.

Goswami, C.P., and Nakshatri, H. (2014). PROGgeneV2: enhancements on the existing database. *BMC Cancer* 14, 970.

Gottesfeld, J.M., and Forbes, D.J. (1997). Mitotic repression of the transcriptional machinery. *Trends Biochem Sci* 22, 197-202.

Gout, P.W., Buckley, A.R., Simms, C.R., and Bruchovsky, N. (2001). Sulfasalazine, a potent suppressor of lymphoma growth by inhibition of the x(c)- cystine transporter: a new action for an old drug. *Leukemia* 15, 1633-1640.

Grossman, S.R. (2001). p300/CBP/p53 interaction and regulation of the p53 response. *Eur J Biochem* 268, 2773-2778.

Gunther, E.J., Moody, S.E., Belka, G.K., Hahn, K.T., Innocent, N., Dugan, K.D., Cardiff, R.D., and Chodosh, L.A. (2003). Impact of p53 loss on reversal and recurrence of conditional Wnt-induced tumorigenesis. *Genes Dev* 17, 488-501.

Gupta, G.P., and Massague, J. (2006). Cancer metastasis: building a framework. *Cell* 127, 679-695.

He, S., Wang, L., Miao, L., Wang, T., Du, F., Zhao, L., and Wang, X. (2009). Receptor interacting protein kinase-3 determines cellular necrotic response to TNF-alpha. *Cell* 137, 1100-1111.

Hockendorf, U., Yabal, M., Herold, T., Munkhbaatar, E., Rott, S., Jilg, S., Kauschinger, J., Magnani, G., Reisinger, F., Heuser, M., *et al.* (2016). RIPK3 Restricts Myeloid Leukemogenesis by Promoting Cell Death and Differentiation of Leukemia Initiating Cells. *Cancer Cell* 30, 75-91.

Iizuka, M., Matsui, T., Takisawa, H., and Smith, M.M. (2006). Regulation of replication licensing by acetyltransferase Hbo1. *Mol Cell Biol* 26, 1098-1108.

Iizuka, M., and Stillman, B. (1999). Histone acetyltransferase HBO1 interacts with the ORC1 subunit of the human initiator protein. *J Biol Chem* 274, 23027-23034.

Ito, A., Kawaguchi, Y., Lai, C.H., Kovacs, J.J., Higashimoto, Y., Appella, E., and Yao, T.P. (2002). MDM2-HDAC1-mediated deacetylation of p53 is required for its degradation. *EMBO J* 21, 6236-6245.

Ito, A., Lai, C.H., Zhao, X., Saito, S., Hamilton, M.H., Appella, E., and Yao, T.P. (2001). p300/CBP-mediated p53 acetylation is commonly induced by p53-activating agents and inhibited by MDM2. *EMBO J* 20, 1331-1340.

Iyer, N.G., Ozdag, H., and Caldas, C. (2004). p300/CBP and cancer. *Oncogene* 23, 4225-4231.

Jemal, A., Bray, F., Center, M.M., Ferlay, J., Ward, E., and Forman, D. (2011). Global cancer statistics. *CA Cancer J Clin* 61, 69-90.

Johannessen, C.M., Boehm, J.S., Kim, S.Y., Thomas, S.R., Wardwell, L., Johnson, L.A., Emery, C.M., Stransky, N., Cogdill, A.P., Barretina, J., *et al.* (2010). COT drives resistance to RAF inhibition through MAP kinase pathway reactivation. *Nature* 468, 968-972.

Johnson, T.C., and Holland, J.J. (1965). Ribonucleic acid and protein synthesis in mitotic HeLa cells. *J Cell Biol* 27, 565-574.

Jonsdottir, K., Assmus, J., Slewa, A., Gudlaugsson, E., Skaland, I., Baak, J.P., and Janssen, E.A. (2014). Prognostic value of gene signatures and proliferation in lymph-node-negative breast cancer. *PLoS One* 9, e90642.

Kalkhoven, E. (2004). CBP and p300: HATs for different occasions. *Biochem Pharmacol* 68, 1145-1155.

Karami-Tehrani, F., Malek, A.R., Shahsavari, Z., and Atri, M. (2016). Evaluation of RIP1K and RIP3K expressions in the malignant and benign breast tumors. *Tumour Biol* 37, 8849-8856.

- Karrison, T., Ferguson, D.J., and Meier, P. (2000). RESPONSE: re: dormancy of mammary carcinoma after mastectomy. *J Natl Cancer Inst* 92, 348.
- Keenan, M.M., and Chi, J.T. (2015). Alternative fuels for cancer cells. *Cancer J* 21, 49-55.
- Kim, J.M., Liu, H., Tazaki, M., Nagata, M., and Aoki, F. (2003). Changes in histone acetylation during mouse oocyte meiosis. *J Cell Biol* 162, 37-46.
- Kimbung, S., Loman, N., and Hedenfalk, I. (2015). Clinical and molecular complexity of breast cancer metastases. *Semin Cancer Biol* 35, 85-95.
- Kollias, J., Elston, C.W., Ellis, I.O., Robertson, J.F., and Blamey, R.W. (1997). Early-onset breast cancer--histopathological and prognostic considerations. *Br J Cancer* 75, 1318-1323.
- Koo, G.B., Morgan, M.J., Lee, D.G., Kim, W.J., Yoon, J.H., Koo, J.S., Kim, S.I., Kim, S.J., Son, M.K., Hong, S.S., *et al.* (2015). Methylation-dependent loss of RIP3 expression in cancer represses programmed necrosis in response to chemotherapeutics. *Cell Res* 25, 707-725.
- Krebs, E.G. (1983). Historical perspectives on protein phosphorylation and a classification system for protein kinases. *Philos Trans R Soc Lond B Biol Sci* 302, 3-11.
- Kufer, T.A., Sillje, H.H., Korner, R., Gruss, O.J., Meraldi, P., and Nigg, E.A. (2002a). Human TPX2 is required for targeting Aurora-A kinase to the spindle. *J Cell Biol* 158, 617-623.
- Kufer, T.A., Silljé, H.H.W., Körner, R., Gruss, O.J., Meraldi, P., and Nigg, E.A. (2002b). Human TPX2 is required for targeting Aurora-A kinase to the spindle. *The Journal of Cell Biology* 158, 617-623.
- Kung, J.E., and Jura, N. (2016). Structural Basis for the Non-catalytic Functions of Protein Kinases. *Structure* 24, 7-24.

Lalonde, M.E., Avvakumov, N., Glass, K.C., Joncas, F.H., Saksouk, N., Holliday, M., Paquet, E., Yan, K., Tong, Q., Klein, B.J., *et al.* (2013). Exchange of associated factors directs a switch in HBO1 acetyltransferase histone tail specificity. *Genes Dev* 27, 2009-2024.

Lee, Y.S., Dayma, Y., Park, M.Y., Kim, K.I., Yoo, S.E., and Kim, E. (2013). Daxx is a key downstream component of receptor interacting protein kinase 3 mediating retinal ischemic cell death. *FEBS Lett* 587, 266-271.

Lewerenz, J., Klein, M., and Methner, A. (2006). Cooperative action of glutamate transporters and cystine/glutamate antiporter system Xc⁻ protects from oxidative glutamate toxicity. *J Neurochem* 98, 916-925.

Lewis, P.W., Elsaesser, S.J., Noh, K.M., Stadler, S.C., and Allis, C.D. (2010). Daxx is an H3.3-specific histone chaperone and cooperates with ATRX in replication-independent chromatin assembly at telomeres. *Proc Natl Acad Sci U S A* 107, 14075-14080.

Lin, C.C., Kitagawa, M., Tang, X., Hou, M.H., Wu, J., Qu, D.C., Srinivas, V., Liu, X., Thompson, J.W., Mathey-Prevot, B., *et al.* (2018). CoA synthase regulates mitotic fidelity via CBP-mediated acetylation. *Nat Commun* 9, 1039.

Liu, X., Sadhukhan, S., Sun, S., Wagner, G.R., Hirschey, M.D., Qi, L., Lin, H., and Locasale, J.W. (2015). High-Resolution Metabolomics with Acyl-CoA Profiling Reveals Widespread Remodeling in Response to Diet. *Mol Cell Proteomics* 14, 1489-1500.

Loi, S., Haibe-Kains, B., Desmedt, C., Lallemand, F., Tutt, A.M., Gillet, C., Ellis, P., Harris, A., Bergh, J., Foekens, J.A., *et al.* (2007). Definition of clinically distinct molecular subtypes in estrogen receptor-positive breast carcinomas through genomic grade. *J Clin Oncol* 25, 1239-1246.

Lu, S.C. (2009). Regulation of glutathione synthesis. *Mol Aspects Med* 30, 42-59.

Lucas, J.E., Kung, H.N., and Chi, J.T. (2010). Latent factor analysis to discover pathway-associated putative segmental aneuploidies in human cancers. *PLoS Comput Biol* 6, e1000920.

Luetteke, N.C., Phillips, H.K., Qiu, T.H., Copeland, N.G., Earp, H.S., Jenkins, N.A., and Lee, D.C. (1994). The mouse waved-2 phenotype results from a point mutation in the EGF receptor tyrosine kinase. *Genes Dev* 8, 399-413.

Ma, N., Tulu, U.S., Ferenz, N.P., Fagerstrom, C., Wilde, A., and Wadsworth, P. (2010). Poleward transport of TPX2 in the mammalian mitotic spindle requires dynein, Eg5, and microtubule flux. *Mol Biol Cell* 21, 979-988.

Malumbres, M. (2014). Cyclin-dependent kinases. *Genome Biol* 15, 122.

Malumbres, M., and Barbacid, M. (2009). Cell cycle, CDKs and cancer: a changing paradigm. *Nat Rev Cancer* 9, 153-166.

Mandal, P., Berger, S.B., Pillay, S., Moriwaki, K., Huang, C., Guo, H., Lich, J.D., Finger, J., Kasparcova, V., Votta, B., *et al.* (2014). RIP3 induces apoptosis independent of pronecrotic kinase activity. *Mol Cell* 56, 481-495.

Manning, G., Whyte, D.B., Martinez, R., Hunter, T., and Sudarsanam, S. (2002). The protein kinase complement of the human genome. *Science* 298, 1912-1934.

Miettinen, P.J., Berger, J.E., Meneses, J., Phung, Y., Pedersen, R.A., Werb, Z., and Derynck, R. (1995). Epithelial immaturity and multiorgan failure in mice lacking epidermal growth factor receptor. *Nature* 376, 337-341.

Moody, S.E., Perez, D., Pan, T.C., Sarkisian, C.J., Portocarrero, C.P., Sterner, C.J., Notorfrancesco, K.L., Cardiff, R.D., and Chodosh, L.A. (2005). The transcriptional repressor Snail promotes mammary tumor recurrence. *Cancer Cell* 8, 197-209.

Moody, S.E., Sarkisian, C.J., Hahn, K.T., Gunther, E.J., Pickup, S., Dugan, K.D., Innocent, N., Cardiff, R.D., Schnall, M.D., and Chodosh, L.A. (2002). Conditional activation of Neu in the mammary epithelium of transgenic mice results in reversible pulmonary metastasis. *Cancer Cell* 2, 451-461.

Nakamura, T., Pluskal, T., Nakaseko, Y., and Yanagida, M. (2012). Impaired coenzyme A synthesis in fission yeast causes defective mitosis, quiescence-exit failure, histone hypoacetylation and fragile DNA. *Open Biol* 2, 120117.

Nakayama, K.I., and Nakayama, K. (2006). Ubiquitin ligases: cell-cycle control and cancer. *Nat Rev Cancer* 6, 369-381.

Nam, H.S., and Benezra, R. (2009). High levels of Id1 expression define B1 type adult neural stem cells. *Cell Stem Cell* 5, 515-526.

Neumayer, G., Belzil, C., Gruss, O.J., and Nguyen, M.D. (2014). TPX2: of spindle assembly, DNA damage response, and cancer. *Cell Mol Life Sci* 71, 3027-3047.

Nigg, E.A. (1995). Cyclin-dependent protein kinases: key regulators of the eukaryotic cell cycle. *Bioessays* 17, 471-480.

Ogryzko, V.V., Schiltz, R.L., Russanova, V., Howard, B.H., and Nakatani, Y. (1996). The transcriptional coactivators p300 and CBP are histone acetyltransferases. *Cell* 87, 953-959.

Otto, T., Horn, S., Brockmann, M., Eilers, U., Schuttrumpf, L., Popov, N., Kenney, A.M., Schulte, J.H., Beijersbergen, R., Christiansen, H., *et al.* (2009). Stabilization of N-Myc is a critical function of Aurora A in human neuroblastoma. *Cancer Cell* 15, 67-78.

Peterson, A.C., Russell, J.D., Bailey, D.J., Westphall, M.S., and Coon, J.J. (2012). Parallel reaction monitoring for high resolution and high mass accuracy quantitative, targeted proteomics. *Mol Cell Proteomics* 11, 1475-1488.

Piekny, A.J., and Maddox, A.S. (2010). The myriad roles of Anillin during cytokinesis. *Semin Cell Dev Biol* 21, 881-891.

Pietrocola, F., Galluzzi, L., Bravo-San Pedro, J.M., Madeo, F., and Kroemer, G. (2015). Acetyl coenzyme A: a central metabolite and second messenger. *Cell Metab* 21, 805-821.

Prescott, D.M., and Bender, M.A. (1962). Synthesis of RNA and protein during mitosis in mammalian tissue culture cells. *Exp Cell Res* 26, 260-268.

Puri, P.L., Avantaggiati, M.L., Balsano, C., Sang, N., Graessmann, A., Giordano, A., and Levrero, M. (1997). p300 is required for MyoD-dependent cell cycle arrest and muscle-specific gene transcription. *EMBO J* 16, 369-383.

Rice, J.C., and Allis, C.D. (2001). Histone methylation versus histone acetylation: new insights into epigenetic regulation. *Curr Opin Cell Biol* 13, 263-273.

Roelfsema, J.H., and Peters, D.J. (2007). Rubinstein-Taybi syndrome: clinical and molecular overview. *Expert Rev Mol Med* 9, 1-16.

Roth, S.Y., Denu, J.M., and Allis, C.D. (2001). Histone acetyltransferases. *Annu Rev Biochem* 70, 81-120.

Saksouk, N., Avvakumov, N., Champagne, K.S., Hung, T., Doyon, Y., Cayrou, C., Paquet, E., Ullah, M., Landry, A.J., Cote, V., *et al.* (2009). HBO1 HAT complexes target chromatin throughout gene coding regions via multiple PHD finger interactions with histone H3 tail. *Mol Cell* 33, 257-265.

Siegel, R., Naishadham, D., and Jemal, A. (2013). Cancer statistics, 2013. *CA Cancer J Clin* 63, 11-30.

Siudeja, K., Srinivasan, B., Xu, L., Rana, A., de Jong, J., Nollen, E.A., Jackowski, S., Sanford, L., Hayflick, S., and Sibon, O.C. (2011). Impaired Coenzyme A metabolism affects histone and tubulin acetylation in *Drosophila* and human cell models of pantothenate kinase associated neurodegeneration. *EMBO Mol Med* 3, 755-766.

Sivakumar, S., and Gorbsky, G.J. (2015). Spatiotemporal regulation of the anaphase-promoting complex in mitosis. *Nat Rev Mol Cell Biol* 16, 82-94.

Skouta, R., Dixon, S.J., Wang, J., Dunn, D.E., Orman, M., Shimada, K., Rosenberg, P.A., Lo, D.C., Weinberg, J.M., Linkermann, A., *et al.* (2014). Ferrostatins inhibit oxidative lipid damage and cell death in diverse disease models. *J Am Chem Soc* 136, 4551-4556.

Slamon, D.J., Clark, G.M., Wong, S.G., Levin, W.J., Ullrich, A., and McGuire, W.L. (1987). Human breast cancer: correlation of relapse and survival with amplification of the HER-2/neu oncogene. *Science* 235, 177-182.

Stewart, S., and Fang, G. (2005). Anaphase-promoting complex/cyclosome controls the stability of TPX2 during mitotic exit. *Mol Cell Biol* 25, 10516-10527.

Storchova, Z., and Pellman, D. (2004). From polyploidy to aneuploidy, genome instability and cancer. *Nat Rev Mol Cell Biol* 5, 45-54.

Sun, L., Wang, H., Wang, Z., He, S., Chen, S., Liao, D., Wang, L., Yan, J., Liu, W., Lei, X., *et al.* (2012). Mixed lineage kinase domain-like protein mediates necrosis signaling downstream of RIP3 kinase. *Cell* 148, 213-227.

Szklarczyk, D., Franceschini, A., Wyder, S., Forslund, K., Heller, D., Huerta-Cepas, J., Simonovic, M., Roth, A., Santos, A., Tsafou, K.P., *et al.* (2015). STRING v10: protein-protein interaction networks, integrated over the tree of life. *Nucleic Acids Res* 43, D447-452.

Tanaka, Y., Naruse, I., Hongo, T., Xu, M., Nakahata, T., Maekawa, T., and Ishii, S. (2000). Extensive brain hemorrhage and embryonic lethality in a mouse null mutant of CREB-binding protein. *Mech Dev* 95, 133-145.

Tang, X., Ding, C.K., Wu, J., Sjol, J., Wardell, S., Spasojevic, I., George, D., McDonnell, D.P., Hsu, D.S., Chang, J.T., *et al.* (2017). Cystine addiction of triple-negative breast cancer associated with EMT augmented death signaling. *Oncogene* 36, 4379.

Tang, X., Wu, J., Ding, C.K., Lu, M., Keenan, M.M., Lin, C.C., Lin, C.A., Wang, C.C., George, D., Hsu, D.S., *et al.* (2016). Cystine Deprivation Triggers Programmed Necrosis in VHL-Deficient Renal Cell Carcinomas. *Cancer Res* 76, 1892-1903.

Taylor, J.H. (1960). Nucleic acid synthesis in relation to the cell division cycle. *Ann N Y Acad Sci* 90, 409-421.

Terret, M.E., Sherwood, R., Rahman, S., Qin, J., and Jallepalli, P.V. (2009). Cohesin acetylation speeds the replication fork. *Nature* 462, 231-234.

Thompson, P.R., Wang, D., Wang, L., Fulco, M., Pediconi, N., Zhang, D., An, W., Ge, Q., Roeder, R.G., Wong, J., *et al.* (2004). Regulation of the p300 HAT domain via a novel activation loop. *Nat Struct Mol Biol* 11, 308-315.

Turnell, A.S., Stewart, G.S., Grand, R.J., Rookes, S.M., Martin, A., Yamano, H., Elledge, S.J., and Gallimore, P.H. (2005). The APC/C and CBP/p300 cooperate to regulate transcription and cell-cycle progression. *Nature* 438, 690-695.

Uhlen, M., Fagerberg, L., Hallstrom, B.M., Lindskog, C., Oksvold, P., Mardinoglu, A., Sivertsson, A., Kampf, C., Sjostedt, E., Asplund, A., *et al.* (2015). Proteomics. Tissue-based map of the human proteome. *Science* 347, 1260419.

Vakifahmetoglu, H., Olsson, M., and Zhivotovsky, B. (2008). Death through a tragedy: mitotic catastrophe. *Cell Death Differ* 15, 1153-1162.

van der Heide, L.P., and Smidt, M.P. (2005). Regulation of FoxO activity by CBP/p300-mediated acetylation. *Trends Biochem Sci* 30, 81-86.

Wang, H., Sun, L., Su, L., Rizo, J., Liu, L., Wang, L.F., Wang, F.S., and Wang, X. (2014). Mixed lineage kinase domain-like protein MLKL causes necrotic membrane disruption upon phosphorylation by RIP3. *Mol Cell* 54, 133-146.

Wang, K., Li, J., Degterev, A., Hsu, E., Yuan, J., and Yuan, C. (2007). Structure-activity relationship analysis of a novel necroptosis inhibitor, Necrostatin-5. *Bioorg Med Chem Lett* 17, 1455-1465.

Weissman, A.M. (2001). Themes and variations on ubiquitylation. *Nat Rev Mol Cell Biol* 2, 169-178.

Wittmann, T., Hyman, A., and Desai, A. (2001). The spindle: a dynamic assembly of microtubules and motors. *Nat Cell Biol* 3, E28-34.

Wittmann, T., Wilm, M., Karsenti, E., and Vernos, I. (2000). TPX2, A novel xenopus MAP involved in spindle pole organization. *J Cell Biol* 149, 1405-1418.

Yagoda, N., von Rechenberg, M., Zaganjor, E., Bauer, A.J., Yang, W.S., Fridman, D.J., Wolpaw, A.J., Smukste, I., Peltier, J.M., Boniface, J.J., *et al.* (2007). RAS-RAF-MEK-dependent oxidative cell death involving voltage-dependent anion channels. *Nature* 447, 864-868.

Yang, W.S., SriRamaratnam, R., Welsch, M.E., Shimada, K., Skouta, R., Viswanathan, V.S., Cheah, J.H., Clemons, P.A., Shamji, A.F., Clish, C.B., *et al.* (2014). Regulation of ferroptotic cancer cell death by GPX4. *Cell* 156, 317-331.

Yang, X., Boehm, J.S., Yang, X., Salehi-Ashtiani, K., Hao, T., Shen, Y., Lubonja, R., Thomas, S.R., Alkan, O., Bhimdi, T., *et al.* (2011). A public genome-scale lentiviral expression library of human ORFs. *Nat Methods* 8, 659-661.

Yao, T.P., Oh, S.P., Fuchs, M., Zhou, N.D., Ch'ng, L.E., Newsome, D., Bronson, R.T., Li, E., Livingston, D.M., and Eckner, R. (1998). Gene dosage-dependent embryonic development and proliferation defects in mice lacking the transcriptional integrator p300. *Cell* 93, 361-372.

Yuan, H., Rossetto, D., Mellert, H., Dang, W., Srinivasan, M., Johnson, J., Hodawadekar, S., Ding, E.C., Speicher, K., Abshiru, N., *et al.* (2012). MYST protein acetyltransferase activity requires active site lysine autoacetylation. *EMBO J* 31, 58-70.

Zhang, D.W., Shao, J., Lin, J., Zhang, N., Lu, B.J., Lin, S.C., Dong, M.Q., and Han, J. (2009). RIP3, an energy metabolism regulator that switches TNF-induced cell death from apoptosis to necrosis. *Science* 325, 332-336.

Zhang, J., Shi, X., Li, Y., Kim, B.J., Jia, J., Huang, Z., Yang, T., Fu, X., Jung, S.Y., Wang, Y., *et al.* (2008). Acetylation of Smc3 by Eco1 is required for S phase sister chromatid cohesion in both human and yeast. *Mol Cell* 31, 143-151.

Zhao, X., Sternsdorf, T., Bolger, T.A., Evans, R.M., and Yao, T.P. (2005). Regulation of MEF2 by histone deacetylase 4- and SIRT1 deacetylase-mediated lysine modifications. *Mol Cell Biol* 25, 8456-8464.

Zhyvoloup, A., Nemazanyy, I., Babich, A., Panasyuk, G., Pobigailo, N., Vudmaska, M., Naidenov, V., Kukhareno, O., Palchevskii, S., Savinska, L., *et al.* (2002). Molecular cloning of CoA Synthase. The missing link in CoA biosynthesis. *J Biol Chem* 277, 22107-22110.

Biography

Chao-Chieh Lin was born on December 9, 1982 in Taipei, Taiwan. In 2007, he received his bachelor (B.S.) and master degree (M.S.) in genetics and genomics at National Yang-Ming University in Taiwan. He worked on the molecular mechanism of genetic variations on the susceptibility of uremia. After graduation, He worked at Academia Sinica in Taiwan, focusing on the interaction between ion channels and mouse behavior. After joining UPGG at Duke University in 2011. In Dr. Ashley Chi's lab, he investigated the non-canonical mechanisms of two kinases in the oncogenesis of human cancers.

Lin C.C., Kitagawa M, Tang X, Hou M.S., Wu J., Qu D., Srinivas V., Liu X., Thompson J.W., Mathey-Prevot B., Yao T.P., Lee S.H., and Chi J.T. (2018). CoA Synthase Regulates mitotic fidelity via CBP-mediated acetylation. *Nature Commun* (Accepted)

Tang, X., Wu, J., Ding, C.K., Lu, M., Keenan, M.M., Lin, C.C., Lin, C.A., Wang, C.C., George, D., Hsu, D.S., and Chi J.T. (2016). Cystine Deprivation Triggers Programmed Necrosis in VHL-Deficient Renal Cell Carcinomas. *Cancer Res* 76, 1892-1903.

Bhattacharyya, J., Bellucci, J.J., Weitzhandler, I., McDaniel, J.R., Spasojevic, I., Li, X., Lin, C.C., Chi, J.T., and Chilkoti, A. (2015). A paclitaxel-loaded recombinant polypeptide nanoparticle outperforms Abraxane in multiple murine cancer models. *Nat Commun* 6, 7939.

Tang, X., Lin, C.C., Spasojevic, I., Iversen, E.S., Chi, J.T., and Marks, J.R. (2014). A joint analysis of metabolomics and genetics of breast cancer. *Breast Cancer Res* 16, 415.

Cheng, C.F., Kuo, T.B., Chen, W.N., Lin, C.C., and Chen, C.C. (2014). Abnormal cardiac autonomic regulation in mice lacking ASIC3. *Biomed Res Int* 2014, 709159.

Cheng, C.F., Chen, I.L., Cheng, M.H., Lian, W.S., Lin, C.C., Kuo, T.B., and Chen, C.C. (2011). Acid-sensing ion channel 3, but not capsaicin receptor TRPV1, plays a protective role in isoproterenol-induced myocardial ischemia in mice. *Circ J* 75, 174-178.

M., Keenan, Lin, C.C and Chi, J.-T.A. (2014). A Genomic Analysis of Cellular Responses and Adaptions to Extracellular Acidosis (New York: Springer).

Hong Taiwan Scholar, Taiwan 2011-2013

Travel Grants for Visits to Duke-NUS Medical School, Singapore 2016